Spatial variability of leachate flow and distribution in a landfill stabilized by leachate recirculation

M.S.A. Feenstra

TU Delft

SPATIAL VARIABILITY OF LEACHATE FLOW AND DISTRIBUTION IN A LANDFILL STABILIZED BY LEACHATE RECIRCULATION

by

Merel Sybrigje Anneke FEENSTRA

in partial fulfillment of the requirements for the degree of

Master of Science in
Applied Earth Sciences

at the Delft University of Technology,
to be defended publicly on Thursday November 24, 2022 at 14:00.

Student number:	5183057	
Project duration:	November 22, 2021	November 24, 2022
Thesis committee:	Dr. J. Gebert (Chair)	TU Delft Geo-Engineering
	Prof. dr. ir. T. J. Heimovaara	TU Delft Geo-Engineering
	Dr. T. A. Bogaard	TU Delft Water Management
	Dr. T. C. Rees-White	University of Southampton Engineering

An electronic version of this thesis is available at `http://repository.tudelft.nl/`.

Cover image is a picture of well A5 (white casing) and piezometer nest 5 (blue casings) on top of landfill De Kragge.

TU Delft CURE attero energiek met milieu

SUMMARY

Recirculation and infiltration of leachate in landfills are performed to accelerate the process of stabilizing organic matter in waste. At landfill De Kragge (Bergen op Zoom, the Netherlands), leachate recirculation and infiltration measures started in March 2018. This research aims to provide insight related to leachate flow throughout the landfill. Knowledge about the leachate flow is essential for evaluating the success of the stabilization measures. In this research, uniform and point borehole dilution tests were conducted to investigate the horizontal and vertical flow velocities. In addition, measured leachate levels throughout the landfill were analyzed.

The leachate levels indicated perched leachate zones: above the basal drainage system and below the injection drains at the top. Leachate injected through the infiltration drains cannot efficiently infiltrate the waste body, and the effects of the infiltration events were not picked up in the wells and piezometers throughout the landfill, implying little hydraulic connectivity.

The results of the dilution tests indicated horizontal and vertical flow within the landfill. Vertical velocities measured in the wells were estimated to be considerably higher (77 - 225 m/d) than the average horizontal velocities (0.02 - 1.0 m/d). The wells provide a path for vertical flow. Apart from the highest horizontal velocities measured in deeper sections of the landfill (15-18 m below ground level), velocities varied without a clear relation to landfill depth, indicating preferential flow paths. Uniform dilution tests performed with the infiltration drains turned off suggested that leachate infiltration does not increase the horizontal velocities. This research suggests that waste stabilization through recirculation is not optimal at De Kragge.

Due to an overall lack of understanding about the well and filter pack installation and the high spatial heterogeneity of the waste, the calculated velocities are uncertain. Further research into possible error sources (e.g., the borehole correction factor) is recommended. Additional tracer tests, including tests on the neighboring compartment without stabilization measures, are recommended to further assess the effectiveness of the recirculation system.

PREFACE

You are reading the final installment of my master's thesis which has been written to fulfill the graduation requirements of the master Geo-Engineering at the faculty of Civil Engineering and Geosciences at Delft University of Technology. This research has been concluded in light of the CURE project and I would like to express my gratitude to everyone involved. With this research, I hope to have provided a bit more insight into the black box issue of the landfill.

First, I would like to thank Julia Gebert for introducing me to the topic and providing me with great guidance during this research. At the beginning of this master, I would have never believed someone if they told me I was going to perform research at a landfill, but I'm happy I was able to find a project that included fieldwork. I would also like to thank my other supervisors, Timo Heimovaara, Thom Bogaard, and Tristan Rees-White for their feedback and involvement during the previous months. In particular, I would like to express my appreciation to Tristan Rees-White and Richard Beaven from the University of Southampton for helping me out with the dilution tests and offering me to stay at their cottage in Bergen op Zoom, saving me from hour-long commutes on several occasions. I would like to thank Roland Klasen for driving out to De Kragge and helping me with the pumping of the wells. From Attero I would like to thank Twan Kanen for providing background knowledge on the measures at the site, and the on-site personnel (Frank Simons, Marco van den Burg, and Marcel de Baat) at De Kragge, for helping me out, and for their company during lunch breaks. I want to express gratitude to my friends, who always supported me and made my student time unforgettable. Lastly, I want to sincerely thank my family for their support, on multiple fronts. I could not have done it without you.

Merel Feenstra
Amsterdam, November 2022

NOMENCLATURE

Abbreviations

ANNAMOX	Anaerobic ammonium oxidation
AU	Arbitrary Units
CL	Cable length
CTD	Conductivity, temperature, depth
CURE	Coupled multi-process research for reducing landfill emissions
ERT	Electrical resistivity tomography
ETV	Emission test value
GL	Ground level
HDPE	High-density polyethylene
ID	Identification
iDS	Dutch sustainable landfill management project
KNMI	Royal Netherlands Meteorological Institute
LFG	Landfill gas
LL	Leachate level
mBTC	Meters below top casing
NAP	Amsterdam Ordnance Datum
NTU	Nephelometric Turbidity Units
OD	Outer diameter
P	Piezometer

ppb	Parts per billion
RIS	Recirculation infiltration system
RWT	Rhodamine water tracer
SBDT	Single borehole dilution test
TOC	Top of casing
UoS	University of Southampton
VMS	Vadoze-zone Monitoring System^{TM} (Sensoil)
WB	Water balance

Chemical formulas

$CH_2O_xN_y$	General formula biomass
H_2O	Water
H^+	Hydrogen ion
HCO_3^-	Bicarbonate
N_2	Nitrogen gas
NH_4^+	Ammonium
NO_2^-	Nitrite
NO_3^-	Nitrate
O_2	Oxygen

Greek symbols

α	Borehole correction factor	[-]
μ	Dynamic viscosity	$[L^{-1}MT^{-1}]$
ν	Flow velocity	$[LT^{-1}]$
ρ	Mass density	$[L^{-3}M]$

Latin symbols

A	(Cross-sectional) Area	[L^2]
C	Concentration	[ML^{-1}]
g	Gravitational constant	[LT^{-2}]
H	Height	[L]
h	Head	[L]
i	Hydraulic gradient	[-]
K	Hydraulic conductivity	[LT^{-1}]
k	Intrinsic permeability	[L^2]
m	Slope	[-]
n_e	Effective porosity	[-]
p	Pressure	[$L^{-1}MT^{-2}$]
Q	Discharge	[L^{3-1}]
q	Specific discharge	[LT^{-1}]
r	Radius	[L]
R_c	Rainfall	[L^3]
t	Time	[T]
W	Volume	[L^3]
x	Initial concentration	[AU]
z	Depth	[L]

CONTENTS

List of Figures

List of Tables

1

INTRODUCTION

Each year, around 60 million tons of waste is produced in The Netherlands. From this Waste, around 2 million tons cannot be reused or recycled (Werkgroep Afvalregistratie, 2021). The non-reusable and non-recyclable Waste mainly consist of soil and soil decontamination residues, commercial and industrial Waste, and residues after sorting and separating. This Waste is deposited into landfills. Sanitary landfills have an impermeable bottom seal and are completely sealed with a top cover, consisting of an impermeable surface seal and a cover soil to limit rainwater infiltration as much as possible (VROM, 1993, 1991). A drainage system above the bottom liner controls the water level inside the landfill and captures the produced leachate.

Waste is stabilized by the degradation of organic matter. Anaerobic conditions and lack of water and leachate transport due to the before mentioned barrier systems delay the stabilization process within a conventional landfill. Therefore, the emission potential of the landfill remains high, and a leak or failure of the barrier systems can cause severe damage to the environment (e.g., BNNVARA 2018; Omroep Gelderland 2018; Brabants Dagblad 2022). The landfill, including the barrier systems, and the groundwater surrounding the site, require eternal after-care and monitoring for possible environmental threats.

1.1. SUSTAINABLE LANDFILLING

The Dutch Sustainable Landfill Management project (iDS) has been operating since 2010 with its primary goal to reduce eternal after-care efforts and costs by enhancing biological stabilization of the waste body through aeration or recirculation of leachate into the landfill (Vereniging Afvalbedrijven, 2015). Experiments are carried out on three existing landfills in the Netherlands: Braambergen (Flevoland), Wieringermeer (Noord-Holland), and De Kragge II (Noord-Braband). Emission Test Values (ETVs) are calculated for each landfill to determine whether contaminants (such as chloride and

ammonia) in the leachate have reached an acceptable level, after which the landfill can be released from after-care. The iDS project aims to determine whether the concentrations of target contaminants can be reduced below the ETV by implementing the previously mentioned stabilization strategies.

The project "Coupled Multiprocess Research for Reducing Landfill Emissions" (CURE) is closely involved with the iDS project. The CURE project aims to conduct fundamental scientific research on the relationship between the conversion of organic matter in the waste body and the emission of contaminants. The project seeks to couple the biogeochemical reactivity and transport processes within the landfill, resulting in a strategy that minimizes contaminants from landfills and contaminated sites into the environment (Gebert et al., 2020).

1.1.1. METHODS TO REDUCE THE EMISSION POTENTIAL

Measures taken to reduce the emission potential by stabilization of the landfill include aeration and leachate recirculation. The choice between aeration or leachate recirculation is based on the amount of spontaneous biological degradation of organic matter in the waste package, which can be estimated from the realized landfill gas extraction. A feasibility study concluded that the degradation at Wieringermeer is more advanced than the degradation at De Kragge. At Braambergen, the waste is dominated by inorganic materials (van Vossen et al., 2009). Therefore, Braambergen and Wieringermeer are suitable for aeration, whereas De Kragge is first subjected to leachate recirculation and thus the focus of this research.

Recirculation of leachate can be implemented under anaerobic and aerobic conditions. The added liquids stimulate bacteria to break down the organic matter present in the waste, creating a bioreactor landfill. At De Kragge, recirculation of leachate is performed anaerobically. In an anaerobic bioreactor landfill, leachate and added water is recirculated into the landfill to obtain optimal moisture levels (Ma et al., 2021). Waste stabilization occurs under anaerobic conditions, initiating the production of landfill gas (LFG) at a higher rate and an earlier stage in the life of the bioreactor landfill compared to a traditional landfill. The LFG is captured by the gas collection system and treated with a flare to prevent greenhouse gas emissions. LFG production (including methane production) within the landfill is reduced in the long term. In addition, the leaking of contaminants (e.g., metals and chloride) into the groundwater is reduced as these are

removed. In an aerobic bioreactor landfill, there is leachate recirculation, and additionally, air is injected to stimulate aerobic activity.

1.1.2. UNKNOWNS REGARDING THE EFFECTIVENESS OF IN-SITU WASTE STABILIZATION

The effectiveness of the stabilization measures remains uncertain due to the challenge of identifying which part of the landfill is effectively flushed or aerated, resulting from the heterogeneous structure of a landfill. Characteristics of a landfill and leachate flow, such as barrier layers, preferential flow, and channeling to wells, are illustrated in a conceptual model presented in Figure 1.1. The anisotropic behavior of the waste body is increased due to landfilling and waste compaction by applying vertical pressure; this results in the horizontal orientation of impermeable barrier layers (e.g., plastics). The horizontal layering results in smaller vertical permeability compared to horizontal permeability. Therefore, leachate flow mainly occurs horizontally and not throughout the whole landfill. The horizontal flow paths are intersected by vertical channels and fissures, differences in landfill settlement, and the construction of vertically oriented elements (Fellner & Brunner, 2010).

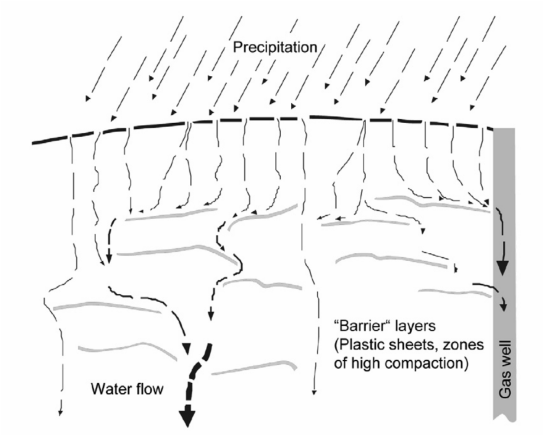

Figure 1.1: Conceptual model of leachate flow within a landfill. The structure of the waste body leads to the funneling of leachate flow towards the base of the landfill. At De Kragge, there is the additional infiltration of leachate by the recirculation system. Figure by Fellner & Brunner (2010).

Regarding De Kragge, there is little knowledge about the hydraulics and flow velocities within the waste body. Drilling conducted in light of new piezometers and wells in 2020

revealed that at some locations, the waste was saturated from the top, while the upper 6 meters of waste were dry at other locations. The drilling conducted for installing another well revealed that the upper 12 meters of the landfill were saturated, whereas the waste was dry below this depth. The drilling indicated spatial heterogeneity in the presence of leachate and that there are saturated zones above unsaturated zones and vice versa. In addition, the drilling work revealed that the waste at the base was more compact compared to the top of the landfill. Several authors report fully saturated zones above dry zones and perched leachate tables (Fellner & Brunner, 2010; Di Bella et al., 2012; Trapani et al., 2015).

Tracer tests can provide insight regarding the movement and velocity of groundwater and potential contaminants (Ward et al., 1998). In the early 2000s, tracer test experiments started on waste samples to study preferential flow paths. Later on, tracer tests were performed on field-scale landfills. A Single Borehole Dilution Test (SBDT) uses a known amount of tracer injected into the saturated zone of a well equipped with a slotted screen. The decrease in tracer concentration due to the lateral flow of water over time is monitored inside the borehole (Freeze & Cherry, 1979).

SBDTs performed in landfills are scarce. Lloyd et al. (1979) performed SBDTs to investigate the permeability of landfill materials, such as domestic waste. However, they only used one sampling point per well, assuming that flow over the entire saturated section of a well is uniform. Rollinson et al. (2010) performed a total of 32 dilution tests on landfill wells on three UK sites, concluding that SBDTs are an excellent resource for determining Darcy flow velocities within landfills. In addition, the advantage of performing an SBDT over using a flowmeter is the ability to quantify lower velocities (Pitrak et al., 2007; West & Odling, 2007). When SBDTs are performed on numerous wells or piezometers spread out over the landfill and at different depths, the dilution tests will provide insight into leachate flow within the waste body.

1.2. RESEARCH OUTLINE

1.2.1. PROBLEM STATEMENT

Stabilizing the waste body by leachate recirculation and water infiltration can only be successful when a significant part of the waste body is flushed. An understanding of leachate flow paths within the waste body is essential because there is a large degree of variability in the hydraulic conductivity of the waste (de Jong, 2021). It is known that the heterogeneous and anisotropic characteristics of a landfill can lead to preferential flow paths (short-circuiting) (e.g., Rosqvist et al. 2005, 2014; W. J. Zhang & Yuan 2019; Blight et al. 1992; Bendz et al. 1997; Oonk et al. 2013). If the leachate cannot reach a large part of the waste body, the emission potential of these hard-to-reach areas will remain too high to release the landfill from monitoring and after-care. With changes in flow pattern (e.g., consolidation caused by the degradation of organic matter), new parts of the landfill are exposed to leachate flow, resulting in a change of leachate quality which may not meet the ETVs (Rosqvist et al., 2005).

1.2.2. AIM

This research aims to obtain quantitative information on the vertical and lateral movement of leachate inside an anisotropic waste body. A better understanding of leachate flow will result in a better assessment of the effectiveness of the recirculation measures regarding the stabilization of waste.

1.2.3. RESEARCH QUESTIONS

This research focuses on the following main research question: How does leachate flow vary spatially throughout the waste body of De Kragge landfill?

In addition, the following sub-questions will be addressed in order to answer the main research question:

- How fast does the leachate infiltrate through the recirculation infiltration system?
  - Can the leachate levels be linked to the infiltration and each other?
- What are the Darcy flow velocities?
  - Is there any variation with depth?
  - Can zones of preferential flow be distinguished from zones with negligible flow?
  - Does the recirculation infiltration system influence the flow velocity?

1.2.4. HYPOTHESES

Following the conceptual model presented in Figure 1.1 and the observations at the test site, several hypotheses were formulated. The results of the uniform dilution tests are expected to indicate zones with negligible flow velocities and zones with significantly higher flow velocities without a relationship between location and depth due to the anisotropic nature of the waste. If the wells act as a preferential flow path for vertical flow, measured vertical velocities will be higher than the measured horizontal velocities. Additionally, it is hypothesized that the recirculation and infiltration of leachate lead to higher flow velocities as the measures increase the volume of leachate in the waste body.

1.2.5. RESEARCH APPROACH

- A spatial and temporal assessment of the measured leachate levels across the infiltration drains and throughout the waste body created an overview of the connection between leachate levels and infiltration. In addition, the leachate levels in the basal drainage system were investigated. This leachate level analysis was coupled with a first estimation of the water balance of the landfill to investigate leachate flow.
- Uniform borehole dilution tests were carried out to retrieve information on the lateral movement of the leachate. The decline of tracer concentration was measured in the well screen in 0.25 m increments or at a certain depth. From the dilution tests, Darcy velocities were calculated.
- Point dilution tests were carried out to estimate the vertical flow velocity within the wells.

1.3. READING GUIDE

Chapter 2 contains background information about the landfill site and the waste body. Theoretical background information on relevant concepts and literature follows in Chapter 3. Chapter 4 elaborates on the methodology of the numerical analysis, the field experiments, and the materials needed. The results and discussion follow in Chapter 5 and Chapter 6. Lastly, Chapter 7 follows with the conclusions and recommendations.

2

SITE DESCRIPTION OF DE KRAGGE

This chapter presents the specifics of the test site, followed by the composition of the waste body. The leachate recirculation and infiltration system are explained in detail, and the location and details of the monitoring wells and piezometers at De Kragge are described.

2.1. SPECIFICS OF DE KRAGGE II

Landfill De Kragge II (hereafter De Kragge) is located in the southwest of the Netherlands in Bergen op Zoom (Noord-Brabant). Around 2.5 million tons of waste were processed at De Kragge in its operational period from 1993-2008. The total surface area of the landfill is approximately 16 ha. The landfill is subdivided into four compartments (Fig. 2.1). Each compartment has a liner at the bottom, consisting of 2 mm HDPE (High-density polyethylene), with gravel and drainage sand on top of the liner. The basal leachate drains are located in the drainage sand, and 2-meter high dikes lined with foil divide the landfill compartments (Fig. 2.2). The dikes prevent lateral flow from compartment 3, where the leachate recirculation pilot is performed, to compartments 2 and 4. The drainage of leachate is separated as each compartment has its own basal drains (Vereniging Afvalbedrijven, 2015).

Compartment 3 has a total surface area of around 5.6 ha. The maximum height of the landfill is approximately 20 m (on average, 17 m). The compartment is covered with a sandy soil layer of 0.5-1 m, preventing odor and debris from blowing around. The cover is not impermeable, unlike the cover of compartments 1 and 2, which is permanent and impermeable (Appendix A, Fig. A.1). The cover of compartment 3 allows for the infiltration of rainwater. The focus of the pilot at De Kragge is on anaerobic treatment of the waste body, as there is still a significant amount of biodegradable organic material. Stabilization is first performed by infiltration of leachate, with the possibility of switching to a period of aerobic treatment after infiltration of leachate to enable further

decomposition of organic matter (van Vossen et al., 2009). Thus far, the operators have not installed aeration systems.

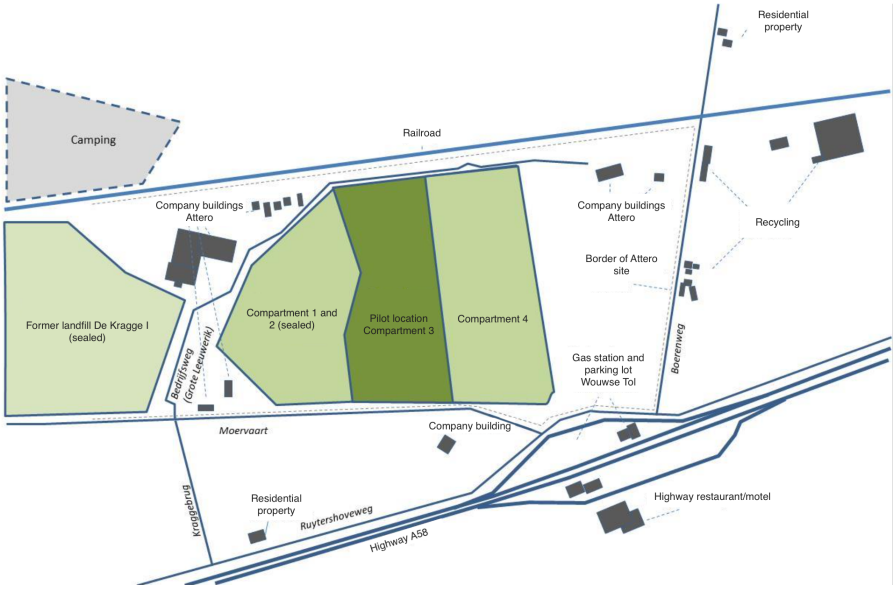

Figure 2.1: Aerial overview of landfill De Kragge II, indicating the division in different compartments (1 to 4). Former landfill De Kragge I is located on the left side. Figure adapted from Kanen & Kedzia-Kowalski (2021).

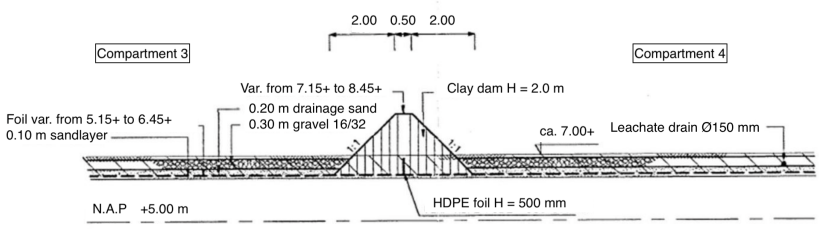

Figure 2.2: Cross section of the bottom liner and separation dike between compartments, illustrated are compartments 3 and 4. Figure adapted from Kedzia-Kowalski (2021).

2.2. WASTE ORIGIN

The total volume of waste in compartment 3 is estimated to be 990,880 tons. This waste mainly consists of household waste (29.15%), construction and demolition waste (21.36%), and commercial or industrial waste (21.25%) (Vereniging Afvalbedrijven,

2015). The waste composition is dominated by domestic waste, resulting in a high amount of biodegradable organic matter.

Table 2.1: Origin of the waste in compartment 3 of landfill De Kragge (Vereniging Afvalbedrijven, 2015).

Waste origin	**Amount [tons]**
Soil and soil decontamination residues	8,974
Construction and demolition waste	213,601
Commercial and industrial waste	212,480
Shredder waste	63
Street cleaning waste	0
Bulky household waste	126,598
Sludge and composting waste	146,737
Household waste	291,427

2.3. LEACHATE RECIRCULATION AND INFILTRATION SYSTEM

Stabilization at De Kragge is carried out with a Recirculation-Infiltration-System (RIS). The RIS recirculates leachate and clean water through the waste body (Meza, 2021). The system includes 14 parallel ditches installed across the top of the landfill, in which infiltration drains are embedded into gravel. The infiltration drains are perforated pipes that allow for the injection of leachate and clean water (labeled 0 to 7A and 1 to 6B, Fig. 5.12). The ditches are located approximately 0.5 - 0.9 m below the landfill surface. The gravel box is covered by geotextile (Fig. 2.3).

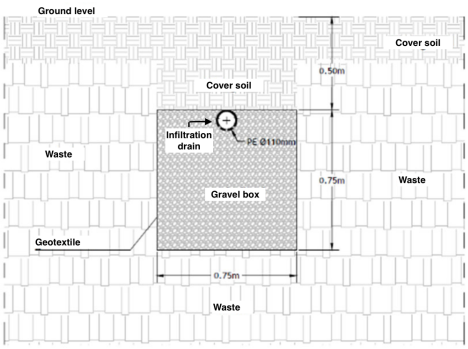

Figure 2.3: Cross-section of the recirculation and infiltration system, indicating the components (Kanen & Kedzia-Kowalski, 2021). The actual dimensions may differ from this design.

Each day, it is determined by the landfill operators how much the total volume of infiltrated leachate and water will be and how long the valve between two drains (e.g., 1A and 1B) opens. The total volume depends, among other things, on the measured leachate level in the basal drains. The aim is to keep the level in the basal drains a maximum of 2 meters above the leachate level sensor in the collection pit, located at the northeast corner of the landfill (Fig. A.2). This is to prevent lateral flow over the separation dike between the compartments. It is not possible to determine exactly how the infiltration is distributed between two matching drains. After injection by the infiltration drains, the leachate has about 7-8 hours to infiltrate the waste body before the drain is injected again. Operations in this way have happened since 7/7/2021. Before, the drains were filled every hour to maximum capacity.

Compartment 3 has 12 base drain access points on the north and south sides of the compartment. The base of the landfill is on a northward slope, causing leachate to flow toward the collection point on the north side of the landfill. From the collection point (buffer), the leachate is directed to the wastewater treatment plant (Fig. 2.4). A large volume of the leachate (90%) is sent to the Anammox (anaerobic ammonium oxidation) reactor where ammonium is converted to nitrogen gas (Kanen & Kedzia-Kowalski, 2021). From the Anammox reactor, leachate recirculates into the infiltration system or is discharged into the sewer to remove chloride in the leachate. To effectively remove chloride from the waste body, it is necessary to discharge ca. 500 mm of sanitized leachate to the sewer per year (Van Turnhout et al., n.d.). The remaining volume of leachate from the buffer (10%) flows to the nitritation reactor where ammonium is converted to nitrite.

Clean groundwater and rainwater are added to the nitritation and Anammox reactor effluent to reach a sufficient volume for recirculation. The aim is to infiltrate 300 - 1200 mm/y, which causes the total volume of injected water and leachate to be about 2-5 times the natural precipitation surplus (estimated at 300 mm/y). The leachate and additional water are distributed over the infiltration pipes and infiltrated into the waste body by gravity, starting the recirculation process over (Van Turnhout et al., n.d.).

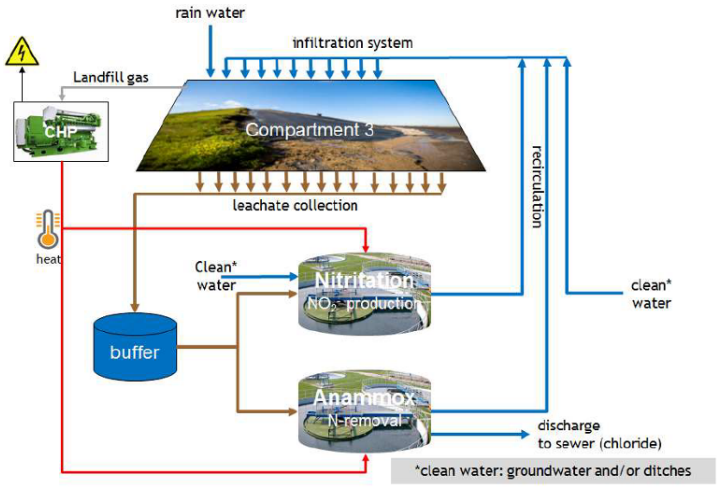

Figure 2.4: Schematic overview of the recirculation system and treatment plant at De Kragge (Kanen & Kedzia-Kowalski, 2021). CHP = Combined Heat and Power system, used to heat the leachate using waste heat.

2.4. MONITORING WELLS AND PIEZOMETERS

The wells labeled with an 'A' were installed in 2020. The wells labeled A2.1, A2.2, A8.1, and A8.2 are equipped with a LevelLog system (VRM) that measures the leachate level at the top of the well (Fig. 2.5). In addition, 15 leachate level measuring points are installed across RIS drains 0.1 - 7A.1 (Fig. 2.5). The LevelLog is an instrument that measures the distance between the top of the tube and the water level inside the well using sonar technology. The A wells have a 2 m slotted screen and an outer diameter of 110 or 63 mm depending on their depth (Table 2.2).

The Z wells, piezometer nests 5, 6, and 7, and the single piezometer 8.18 were installed in January 2022 (design in Appendix B). Wells Z1 and Z2 have an outer diameter of 110 mm and a slotted screen of 10 and 12 m, respectively (Table 2.2). A gravel layer surrounds the slotted screen, followed by a sandy gravel layer and a bentonite seal up to the ground level (Fig. B.1). The piezometers have an outer diameter of 50 mm and a slotted screen of 2 m. The piezometers have a sandy gravel layer around the screen, as the slots are smaller than the slots of the Z wells. Again, bentonite up to ground level seals the borehole (Fig. B.2). The depth of the piezometers ranges from approximately 6 to 19 m below ground level. These wells and piezometers are eligible for dilution tests because they are equipped with a slotted screen and have a diameter of at least 50 mm to fit the measuring equipment (Table 2.2).

Figure 2.5: Schematic overview of the infiltration trenches and wells and piezometers in compartment 3 of De Kragge. RIS = Recirculation-infiltration-system, UoS = University of Southampton, WL = water level, LevelLog = automatic leachate level measuring device.

Table 2.2: Overview of wells and piezometers eligible for a borehole dilution test.

Well reference	**Depth of well**		**Screen**	**Diameter**
	(m-GL)	(m+NAP)	(m)	(m OD)
Z1	18.34	9.71	10	0.110
P5.7	6.89	21.06	2	0.050
P5.10	9.55	18.44	2	0.050
P5.13	12.98	15.01	2	0.050
P5.15	15.27	12.74	2	0.050
P5.18	17.71	10.28	2	0.050
P6.5	5.02	23.78	2	0.050
P6.8	7.68	21.09	2	0.050
P6.11	10.45	18.30	2	0.050
P6.14	14.41	14.40	2	0.050
P6.17	17.45	11.43	2	0.050
P7.6	5.49	23.27	2	0.050
P7.9	9.46	19.32	2	0.050
P7.12	12.33	16.50	2	0.050
P7.15	15.26	13.55	2	0.050
P7.18	18.11	10.71	2	0.050
Z2	18.00	10.91	12	0.110
P8.18	16.83	11.56	2	0.050
A1.1	8.72	10.69	2	0.063
A2.1	19.02	9.89	2	0.110
A2.2	16.15	12.71	2	0.063
A3.1	18.98	9.16	2	0.110
A3.2	15.54	12.66	2	0.063
A4	18.30	10.10	10	0.110
A5	8.35	10.13	2	0.063
A8.1	15.34	10.22	2	0.110
A8.2	12.68	12.90	2	0.063

3

BACKGROUND INFORMATION ON LANDFILL HYDROLOGY AND TRACER TESTS

This chapter first provides an overview of the theoretical background on water and leachate flow within a landfill. After, a short overview of tracer tests performed on landfills is given, followed by previous research conducted at landfill De Kragge, which provides a first indication of the hydraulics and leachate distribution at the site.

3.1. LANDFILL HYDROLOGY

3.1.1. HYDRAULIC CONDUCTIVITY

The hydraulic conductivity is a measure of the ability of fluid transmission through a saturated porous medium (in the case of a landfill, this is waste). It depends both on the medium and fluid properties. Darcy's law defines the hydraulic conductivity for a uniform flow passing through a porous medium and can be used to estimate the water flow rate (Darcy, 1856). Hydraulic conductivity is the linear relationship between discharge and hydraulic gradient.

The total discharge is given by:

$$Q = -K * A * \frac{\delta h}{\delta z} \tag{3.1}$$

Where Q is the total discharge [L^3T^{-1}], K the hydraulic conductivity [LT^{-1}], A is the cross-sectional area (perpendicular to the direction of flow) [L^2], h the head [L], and z the depth ordinate [L]. $\frac{\delta h}{\delta z}$ is also known as the hydraulic gradient, i [-], which is change in head per unit of lateral distance along the flow direction. The negative sign in Eq.

(3.1) indicates that fluid flows towards a decreasing hydraulic head.

Darcy's law can be rewritten in terms of the specific discharge (also known as the Darcy flux):

$$q = -K * \frac{\delta h}{\delta z} \tag{3.2}$$

Here, q is the specific discharge [LT^{-1}].

The specific discharge is not the actual velocity of the fluid; this is the flow velocity. The flow velocity, also known as the average linear velocity, v [LT^{-1}], is related to the specific discharge by the effective porosity n_e [-]:

$$v = \frac{q}{n_e} = -\frac{K}{n_e}\frac{\delta h}{\delta l} \tag{3.3}$$

When the hydraulic conductivity is the same for every flow direction, the medium is isotropic. The medium is anisotropic when the hydraulic conductivity varies with the direction of flow (i.e., $K_h \neq K_v$).

3.1.2. INTRINSIC PERMEABILITY

Intrinsic permeability is only a measure of the porous medium, indicating how easily the medium allows for fluid transmission. Unlike hydraulic conductivity, intrinsic permeability is independent of the properties of the fluid. Eqs. (3.1) and (3.2) can be rewritten to present the relationship between hydraulic conductivity and intrinsic permeability:

$$k = \frac{K * \mu}{\rho * g} \tag{3.4}$$

Where k is the intrinsic permeability [L^2], g the gravitational constant [LT^{-2}], μ the dynamic viscosity of the fluid [$ML^{-1}T^{-1}$], and ρ the liquid density [ML^{-3}].

3.1.3. LEACHATE TRANSPORT

Several transport mechanisms cause transport of water . In a landfill, leachate flow is controlled by advection and dispersion through preferential flow paths (mobile zones), and diffusion and slower advection through the less mobile zones (Statom et al., 2006).

3.1.3.1. ADVECTION

The bulk movement of solutes with water and leachate flow is called advection (Fetter, 2001). Pressure gradients induce advection, where water flows from high to low pressure. An adequate advection rate in the permeable (mobile zones) is required to remove contaminants. A sufficient diffusion rate is required to move water and solutes from less permeable (stagnant or immobile zones) to the mobile zones.

3.1.3.2. DIFFUSION

Diffusion of solutes results from a difference in concentration gradients. Water or leachate moves from zones with high concentration to zones with lower concentration. Diffusion is generally negligible but becomes more critical when advection is slow (due to low porosity and a shallow hydraulic gradient). The solute may move with a higher velocity than the actual fluid. Due to diffusion, the solute can move even when the hydraulic gradient is zero (Fetter, 2001).

3.1.3.3. MECHANICAL DISPERSION

The fluid moves through the pores at different velocities. Mechanical dispersion is a combination of the frictional forces from the pores, the porosity of the medium itself, and the various lengths of the flow paths (Fetter, 2001). A faster flow can result from a more direct flow path or bigger pores, and a slower flow path can be caused by flow closer to pore boundaries which causes more friction. The solute dissolves and decreases in concentration due to diffusion.

3.2. TRACER TESTS ON LANDFILLS

Field experiments and laboratory experiments during the late 1990s have reported that the structure of waste results in mobile zones (macropores) that surround immobile zones (micropores) with negligible advective flow (Rosqvist et al., 1997; Blight et al., 1992; Bendz et al., 1997). A dual-porosity system describes contaminant transport in a landfill (Rosqvist & Destouni, 2000; Woodman et al., 2014).

In Landgraaf (the Netherlands), a landfill pilot was performed to enhance the stabilization of the waste. The test cell had a surface area of 3500 m^2 and was 8 m deep (Oonk et al., 2013). The waste was premixed and homogenized, and recirculation of leachate and aeration was conducted. A tracer test revealed that part of the waste was held in immobile blocks (at least 20-50 cm). The immobile blocks were largely excluded

from flow occurring in the surrounding higher mobile blocks through preferential flow paths.

Doublet tracer tests were conducted on a field scale by Woodman et al. (2017) to observe horizontal solute transport in an MSW landfill with a saturated zone of 17 m. The estimated timescale of diffusion between mobile and immobile blocks was between one and eight years, and the mobile porosity was 0.02. Rees-White et al. (2021) performed single-well injection-withdrawal tests. Results suggested diffusion times between 0.2 and 276 days and a mobile porosity of 0.02 - 0.14. Such values for the mobile porosity are indicative of a highly preferential dual-porosity flow system.

3.3. PREVIOUS RESEARCH AT LANDFILL DE KRAGGE II

Vermeijden (2018) attempted to model the water dynamics of De Kragge. At that time, the leachate recirculation system had not been installed. Vermeijden (2018) simulated a model with three layers: a recultivation layer, followed by a waste layer, and a storage layer. The infiltration into the waste layer from the recultivation layer was calculated using rainfall, evaporation, and water storage. The model of the drainage layer calculated the balance of inflow, leachate outflow, lateral flow, and storage, which resulted in a volume of water and leachate leaving the landfill. Vermeijden (2018) concluded that the lateral flow between the compartments was between 5 to 25 m^3/d. In addition, the model pointed out that water that enters the landfill from the cover layer flows quickly to the drainage layer. Pointing to limited water storage and flow in the recultivation layer.

Ren (2021) performed Electrical Resistivity Tomography (ERT) measurements intending to clarify the variation in leachate levels measured throughout the landfill in wells and piezometers. Five ERT lines were installed at De Kragge to obtain a continuous spatial pattern of the leachate distribution in the landfill. The ERT measurements indicated that the top leachate table showed significant gradient variations. In addition, saturated bulks of waste were pictured above dry bulks, as well as the reverse. The measurements indicated low-permeability waste barriers that hinder the free diffusion of leachate. The results of Ren (2021) suggest local ponding of stagnant leachate. It was not possible to explain the leachate levels observed in the wells using the obtained ERT data, as the leachate levels in the wells represent the local pressure head at the base of the screened filter of the well.

4

METHODOLOGY

This chapter first presents the methodology used for the numerical study of the leachate levels and the estimated water balance. Following is the methodology of the dilution tests and the subsequent analysis of the obtained concentration measurements. The methodology development is described since the work conducted for this research was the first time such tests were performed at De Kragge. Therefore, there was little knowledge about the execution and most suitable methodology. The data analysis sections present two methods to calculate the horizontal Darcy velocity and one to calculate the vertical velocity.

4.1. LEACHATE LEVELS

Leachate levels have been measured across the RIS drains, the waste body, and the basal drains. It is important to note that these three leachate levels will be analyzed separately as they represent different sections of the landfill. As part of regular monitoring by the landfill operator, the leachate level in the drainage system of compartments 3 and 4 is measured by a sensor installed at the base of the leachate collection pits at the north end of the landfill (Fig. A.2 for the location of the collection pit in compartment 3). Conductivity, Temperature, and Depth (CTD) pressure gauges (CTD-Diver®, Van Essen Instruments) were installed across RIS infiltration drains 2B (four), 3A (six) and ERT wells 7, 8, 9, 10, and 12 at the beginning of June 2021 (Fig. 4.1). Data are available until the end of October 2021.

The CTD-Divers® installed across the infiltration drains (Fig. 2.3) were placed in slotted filter pipe with a diameter of 0.32 m, except for the pipe of point 3A.1, which had a diameter of 0.63 m. The depths of the piezometers and the measuring device were not identical. The depth of the piezometers differs up to 0.6 m across drain 2B and up to 2.3 m across drain 3A (Table 4.1). The piezometers are located about 0.5 m from the drain. An extensive table with the top of the piezometer, ground level, infiltration drain, and

gravel box depths can be found in Appendix C, Table C.1.

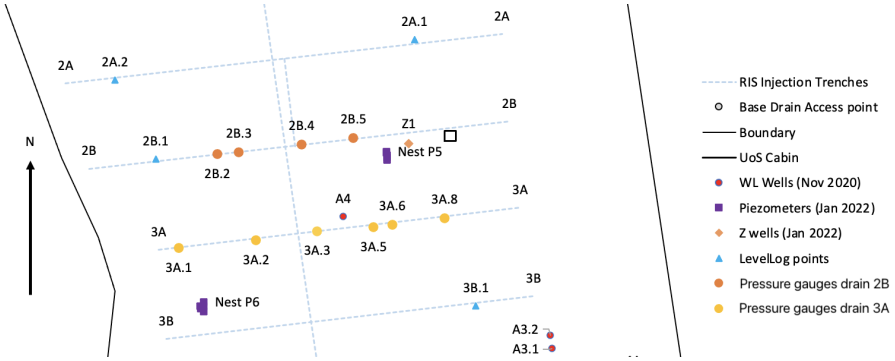

Figure 4.1: Location of CTD (conductivity, time, depth) pressure gauges placed in infiltration drains 2B and 3A. RIS = Recirculation-infiltration-system, UoS = University of Southampton, LevelLog = automatic leachate level measuring device.

Table 4.1: Depths of the installed CTD-Divers® (conductivity, time, and depth) and base of the piezometers across drains 2B and 3A.

Depth (m+NAP)	2B.2	2B.3	2B.4	2B.5	3A.1	3A.2	3A.4	3A.5	3A.6	3A.8
CTD-Diver®	24.6	25.2	24.8	25.0	27.3	26.1	27.0	25.5	24.9	26.5
Base piezometer	24.3	24.4	24.9	24.8	27.0	25.9	26.2	25.4	24.7	26.0

Following the installation of new piezometers in January 2022, CTD-Divers® were installed in piezometers 5.10, 5.13, 6.8, 6.11, 7.9, and 7.12. Data are available from January 2022 to the end of April 2022. The cable length of the CTD-Divers® is about 10 meters, so it was impossible to install them in piezometers where the leachate level was below 10 mBTC (meter below top of casing) as the CTD-Diver® would then only measure the atmospheric pressure. The cable length was noted whenever a CTD-Diver® was installed in a piezometer. The length was used to calculate the leachate column. The program Diver-Office (Van Essen Instruments) was used to download the stored data.

The CTD-Diver ® measures the pressure of the leachate column (LC) above the instrument and the atmospheric pressure (p_{Diver}) (Van Essen Instruments B.V., 2022). Meteorological data (atmospheric pressure and precipitation data) were downloaded from the closest KNMI weather station in Woensdrecht (p_{Baro}), which is located about 6

km from landfill De Kragge. The atmospheric data is used to perform a barometric correction of the CTD-Diver ® data. The piezometer CTD-Diver® data were further calibrated using manual measurements of the leachate levels that were taken when performing the dilution tests. The device stored a measurement every 5 minutes.

$$LC = 9806.65 * \frac{p_{Diver} - p_{Baro}}{\rho * g} \tag{4.1}$$

Where p is the pressure [$L^{-1}MT^{-2}$], and ρ the density of water [$L^{-3}M$].

The leachate level (LL) relative to a vertical datum (Amsterdam Ordnance Datum, NAP) can be calculated by:

$$LL = TOC - CL + LC \tag{4.2}$$

Here, TOC is the top of the casing [L] in m+NAP, and CL is the cable length [L].

4.2. WATER BALANCE

Data collected from 01-01-2018 to 01-02-2022 were used for the water balance model. Meteorological data were downloaded from the KNMI-weather station Gilze-Rijen, as this station had a more comprehensive data set than the station in Woensdrecht. The Gilze-Rijen weather station is located about 43 km from the weather station in Woensdrecht, and 42 km from landfill De Kragge. The cumulative outflow from cells 2, 3, and 4 were measured on-site.

The water balance (WB) was estimated using:

$$WB = R_c - pEv_c - Q_{out_c} + Q_{in_c} \tag{4.3}$$

Here, R_c and pEv_c are the daily cumulative rainfall and potential evaporation multiplied by the surface area of the relative compartment. Q_{in_c} and Q_{out_c} are the cumulative total flow to the infiltration system and the measured cumulative total flow from the drainage system, respectively (all in [L^3]). The different fluxes are pictured in Figure 4.2.

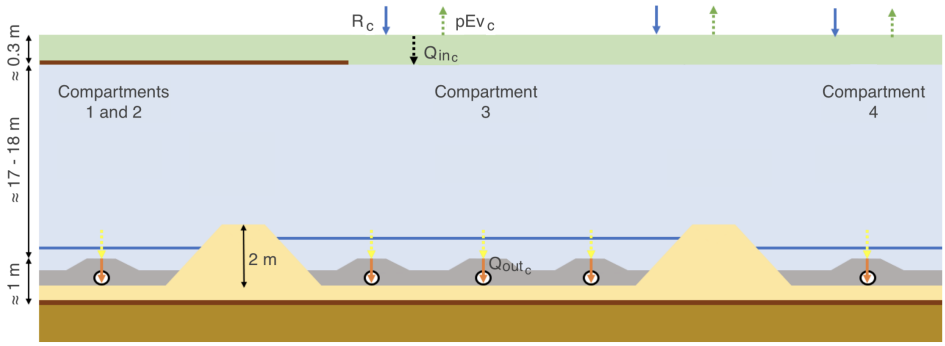

Figure 4.2: Schematization of the water and leachate fluxes at landfill De Kragge. The blue arrow is the cumulative precipitation (R_c), the green arrow is the cumulative evaporation (pEv_c), and the black arrow is the cumulative infiltration by the recirculation-infiltration system (Q_{in_c}). The orange arrow is the cumulative outflow through the drainage system, measured in the collection pit (Q_{out_c}). Additionally, the figure shows the separation dikes and that compartments 1 and 2 are sealed. Figure adapted from Vermeijden (2018).

4.3. UNIFORM DILUTION TEST

This section explains the methodology for the uniform Single Borehole Dilution Tests. As this was the first time that SBDTs were performed on this landfill, it took a few tries to get to a suitable methodology that resulted in the most uniform tracer concentration over the saturated depth of the well or piezometer. Therefore, the development of the methodology will be described first, followed by the most suitable methodology. A submersible fluorometer (Cyclops-7F^{TM} Fluorescence Sensor, TURNER Designs) was used to measure RWT (Rhodamine water tracer) concentrations. The probe has a diameter of 2.23 cm and a length of 14.48 cm. A data logger (CR10X Data Logger, Campbell Scientific) was connected to the fluorometer to read and store the measurements. Whenever the fluorometer was kept inside the well or piezometer to take logged measurements, PC400 (Campbell Scientific) was used as data logger support software to program the data logger and to download the measurements stored on the data logger onto a laptop.

4.3.1. DEVELOPMENT OF METHODOLOGY

On 10-02-2022, a first SBDT for this project was performed on well Z1. The method used resulted in immeasurable tracer concentrations. The injection of RWT was performed as described in section 4.3.3, and a concentration-depth profile was measured right after the tracer injection. Although not uniformly distributed, the readings were between 500 and 900 Arbitrary Units (AU) (Appendix D.1). Executed

differently was that after the first measurement, a small submersible pump was lowered down the well until about 10 cm above the base. The pump was turned on to mix the injected tracer and leachate in the well by moving the pump up and down 5 times. After mixing with the pump, the RWT concentration readings were between 22 and 150 AU, resulting in concentrations lower than the background RWT values.

The wells in which dilution tests were performed are relatively new (installed in January 2022), so residual sediment from the drilling and installation of the well casings might have been present in the wells. After mixing the tracer and leachate inside the well using the pump, the suspended sediment, in combination with the dark leachate, resulted in a reduction of the fluorescence signal, making it so that tracer was not detected even though it was present inside the well. Therefore, the pump was not used in succeeding tests, the new piezometers were purged first, and samples were collected to calibrate the fluorometer. Purging could not be performed on the two new Z wells due to potential clogging of the used pump.

4.3.1.1. PURGING

Purging was performed on all newly installed piezometers with sufficient leachate levels (piezometers 5.7, 6.5, and 6.8 did not) and were still intact (piezometer 6.18 had foam coming out of the top). The methodology can be found in Appendix D.2. For piezometer 7.15, sediment was still present in the last filled bucket after about 40 L (Fig. 4.3). Therefore, sediment is highly likely to remain in the piezometer even after the purging attempts. In addition, pieces of plastic came out attached to the inertial pump for several piezometers.

Figure 4.3: Left and middle picture: pieces of plastic attached to the dip-meter and inertial pump. Right picture: ± 1 cm of sediment (clay/silt) that came out while purging 7.15 (volume of the bucket is about 10 L).

4.3.1.2. CALIBRATION

After purging, calibration of the RWT fluorometer was carried out on a sample of 400 mL native leachate collected from the respective piezometer after the piezometer had been purged. The calibration was performed the day after, so the leachate was at air temperature, about 14.7 °C. Calibration was performed on piezometers 5.10, 5.13, 5.15, 5.18, and 8.18, and well Z1. Steps performed for the calibration are explained in Appendix D.3 as well as the calibration curves.

The output from the fluorometer is linear up to a concentration of 625 - 1000 AU, depending on the piezometer or well. Following the calibration curves, the target concentration was initially set to 750 ppb to stay within the linear range. However, RWT concentration-time graphs from the first week of SBDTs showed that reaching this concentration in the screened section of the piezometer or well was not possible with the injected tracer that corresponds to an initial target concentration of 750 ppb. Therefore, the target concentration was increased. For some piezometers or wells, the measured RWT concentration (in AU) got out of the linear range and into the polynomial range (5.10-1,2,3; 5.13-2,3; 5.18-2,3; 6,11; 6.14; 7.9-1; 7.12-1; 7.15; 7.18; Z2; A5).

There are many governing factors (section 4.3.2.1) which may influence the fluorescence intensity. These parameters were not controlled during the calibration process. For example, natural background fluorescence was different for most piezometers: well Z2 had an average background fluorescence of 15.6 AU, whereas piezometer 7.9 had an average background fluorescence of 56.1 AU. Additionally, the background fluorescence generally increased going down the well or piezometer.

It would be complicated to get an exact calibration curve for each piezometer and well. Calibration would require a lot of time and resources to measure the different parameters. It was decided not to convert the AU output to ppb or mg/L using the polynomial formula. The formula is likely incorrect and not applicable to the untested piezometer and wells. The performed calibration was used as guidance; when possible, only values below 800 - 900 AU were used in further calculations to stay within the linear range, thus discarding the need for converting AU to ppb.

4.3.1.3. TRACER MIXING

Tests 5.18-1 and 5.15-1 were performed using a cone attached above the weight with a diameter of 0.045 m, without any cutouts. Test 5.13-1 was performed using one extra

cone attached below the weight, also without cutouts (Fig. 4.4). The cone was attached to help promote the mixing of tracer and leachate in the well or piezometer. For test 5.13-1, the hosepipe was pulled up in 0.25 m sections after the tracer was poured in, waiting about 30 seconds. This method did not lead to a more uniformly distributed initial tracer concentration. Therefore, this method was not adopted for further SBDTs.

Figure 4.4: Two cones attached to the end of the hosepipe, used for dilution test 5.13-1.

Figure 4.5: One cone with added cutouts attached to the end of the hosepipe.

All three tests did not significantly increase the RWT concentration, and for test 5.13-1, it led to a lowered RWT concentration for the first few measurements. The used cones were most likely too big; the cones had a diameter of 0.045 m, while the inner diameter of the piezometer was 0.048 m which does not leave much space for leachate to flow around the cone. Moving up and down the cone can lead to fresh leachate being pulled into the piezometer by suction, flushing out, and remixing the tracer inside the piezometer. Furthermore, possible suspended and settled sediment may have been carried up throughout the leachate column by this movement, decreasing the intensity of the RWT signal. Keeping this in mind, for the subsequent SBDTs, the cone was made smaller and only attached on top of the weight, with added cutouts (Fig. 4.5). For both well Z1 and Z2, a cone with a diameter of 0.08 m was used, with added cutouts and

attached above the weight as pictured in Figure 4.5.

4.3.2. PREPARATION OF THE TRACER SOLUTION

4.3.2.1. TRACER SELECTION

Selecting a suitable tracer depends on the background concentration and the reactive nature of the leachate to the tracer. For tracer tests on landfills, fluorescent dyes are preferred as a tracer. Saline tracers are not as suitable in landfills because leachate has a high background electrical conductivity (Ogata et al., 2016; Fan et al., 2006). Therefore, large volumes of salt are required, which causes problems with density. For this project, RWT was selected to use as a tracer. RWT was developed especially for water tracing by the company DUPONT.

RWT has been used for uniform SBDTs (e.g., Libby & Robbins 2014) and for tracer testing in landfills (e.g., Woodman et al. 2017; Marius et al. 2010). RWT is noted to be stable regarding light and has a low dependency of fluorescence on pH values. Furthermore, RWT is easy to prepare as it is readily available to purchase in a 20% solution that can be diluted to the desired concentration (methodology to prepare a 1 ppt stock solution in Appendix E.1). Several factors can affect the fluorescence intensity picked up by the Rhodamine detection probe (Cyclops-7F). These include temperature, turbidity, sorptivity, natural background fluorescence, pH value, and salinity.

Fluorescence is inversely related to the temperature: an increasing temperature decreases the fluorescence intensity (Käss, 1998). At De Kragge, the temperature of the leachate varied depending on location (on average, around 20 °C). Data measurements of CTD-Divers® show that over several days, the temperature is stable.

Turbidity results from suspended or dissolved particles in the leachate, which scatter light and cause a cloudy appearance. The turbidity can cause a signal in the fluorometer by refraction, causing a false-positive result (Käss, 1998). The newly installed piezometers at De Kragge were purged to remove suspended sediment in the piezometers. However, after purging, it was evident that there was still sediment and possibly other fractions inside the piezometers. In addition, the landfill contains organic material, which causes the light to dark brown color of the leachate, increasing turbidity. Turbidity values in landfill leachate are reported to be high and variable. For example, Ishak et al. (2016) reports a value of 155 NTU (Nephelometric Turbidity Units) on leachate samples from a sanitary landfill in Malaysia. Raghab et al. (2013) measured

values of 1400 NTU in a solid waste landfill in Alexandria. Values reported by Lei et al. (2007) fall within the same order as the study by Raghab et al. (2013) with values of 1625 NTU.

All transported substances in water (leachate) will interact with the solid state, varying in intensity. Sorption during transport through the waste mass (e.g., onto organic matter) can result in retarding the movement of the tracer through the waste (Ward et al., 1998).

The natural background fluorescence is determined by several factors; dissolved organic carbon is the most affecting. Suspended sediment in the leachate can also increase the apparent background fluorescence (Ward et al., 1998). At De Kragge, the background fluorescence of RWT was between 10 and 75 AU measured using a Cyclops 7F fluorometer (Turner Designs), depending on location and usually increasing towards the base of the piezometer.

The intensity of fluorescence is dependent on the pH value. For RWT, the intensity is 1.0 (on a scale of 0 - 1) between a pH-values of about 5 - 9. Beyond these values, the intensity decreases. In 2021, the average pH value of the leachate of compartment 3 at De Kragge was 7.70, which falls within the before-mentioned range.

In addition, an increasing salinity decreases the intensity of the RWT fluorescence (Ward et al., 1998).

4.3.2.2. CALCULATING VOLUME OF STOCK SOLUTION NEEDED

The volume of stock solution (methodology in Appendix E.1) required to reach a specific target concentration within the well or piezometer was calculated according to the following steps.

- The leachate level in the well was measured using a dip-meter.
- The volume of stock solution needed to reach a certain concentration of RWT was calculated by multiplying the volume of the well (in L) by the target concentration, where 1000 ppb equals 1 mg/L.
- The volume of the injection hose was calculated, with the length being the saturated depth of the piezometer.
- The volume of stock solution needed was subtracted from the volume of the

injection hose to get the amount of leachate to which the stock solution should be diluted before injection.

Although the target concentration was increased after the first SBDT (from 750 to 1000 ppb), the initial concentration measurements in the screen section did not have RWT concentrations of 1000 ppb (test 5.13-1, 5.15-1, 5.18-1, and Z1). Therefore, the diameter of the screened section used for calculating the required volume of stock solution to be added was increased to 0.105 m for the piezometers and 0.150 m for the Z wells (instead of the inner diameter of the casings: 0.48 and 0.106 m, respectively.

4.3.3. INJECTION OF THE TRACER

The RWT-leachate solution was injected into the piezometers and wells using a hosepipe. Three hosepipe lengths were used for the tests performed during this project; 11, 14, and 20 meters. Since none of the piezometers and wells had the same depth, it was not possible to modify a hosepipe for each piezometer, as this would have led to wasted material.

- A hosepipe was selected, and a weight and cone were attached to the end of the hosepipe. The weight was necessary for the hosepipe to lower down the leachate column.
- The cover cap was removed from the well, and the hosepipe was lowered into the well until the end reached the well base. The hosepipe was lifted a few cm and was kept in place with a horizontal piece of wood taped to the top of the hosepipe (Fig. 4.6).
- Tracer was poured into the hosepipe at a slow and steady pace using a funnel (Fig. 4.7). A few moments after the tracer was added, the hosepipe was removed to ensure all of the tracer went down the hosepipe. The hosepipe was removed steadily to release the tracer evenly into the surrounding leachate.
- The hosepipe was inserted into the well or piezometer again and moved up and down to promote mixing.

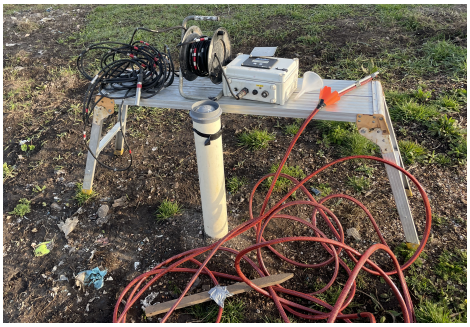

Figure 4.6: Set-up for a uniform dilution test. From left to right on the bench: Cyclops-7F sensor attached to a 22 m rod, which is attached to the data logger. A funnel to pour in the tracer and the hosepipe with a cone and weight attached.

Figure 4.7: Adding the tracer to the hosepipe through a funnel.

4.3.4. MONITORING OF THE TRACER CONCENTRATION

The following steps were performed to monitor the RWT tracer concentration after injection of the tracer into the well or piezometer.

- A concentration log over the entire saturated depth was taken directly after the initial application of the tracer by lowering the fluorometer (connected to the data logger) into the well, being careful not to disturb the mixture.
- For fully-screened wells, the full depth of the slotted section was measured in 0.25 m increments.
- For piezometers that have a 2 m slotted section, the measurements were taken at 0.25 m increments in the slotted section and usually at 1 m increments in the blind section.
- Logged measurements at a set horizon were performed either overnight or during the day. When an overnight measurement was performed, the data logger was connected to an external battery to ensure the internal battery would not run out. The battery and data logger was put inside a plastic box to protect them. The rod with the data logger was secured to the piezometer with tape (Fig. E.1, Appendix E.2).
- The manual measurements were repeated roughly every 30 minutes, depending on the rate of the decline in RWT concentration. The measurements were usually

continued until 0-10% of the initial tracer concentration was left.

- For logged measurements, whenever the data logger was shut off or removed from its power source, all data stored on the data logger was removed. In the case of an overnight logged measurement, the data logger needed to be connected to a laptop after the rod connecting the fluorometer was detached from it. By connecting the data logger to a laptop with the data logger support software, the data on the data logger was transferred to the laptop. The software was used to program the measuring intervals of the data logger. The data logger was set at either 1- or 5-minute intervals for overnight logged measurements.

Fahrmeier et al. (2021) illustrate three typical tracer concentration dilution patterns after a uniform SBDT. In the figure, the curve of t_1 shows the aimed uniform starting concentration after injection, t_2, t_3, and t_4 are measurements taken at a later stage after the initial injection when lateral water flow dilutes the tracer concentration. Figure 4.8A shows a higher velocity section at the top of the well and a lower velocity section at the base of the well; this is indicated by a lower tracer concentration at the top. Figure 4.8B shows two sections with a higher flow velocity, alternating with sections of lower flow. Lastly, Figure 4.8C shows vertical movement, with an inflow horizon at the top of the well and an outflow horizon at the base of the well.

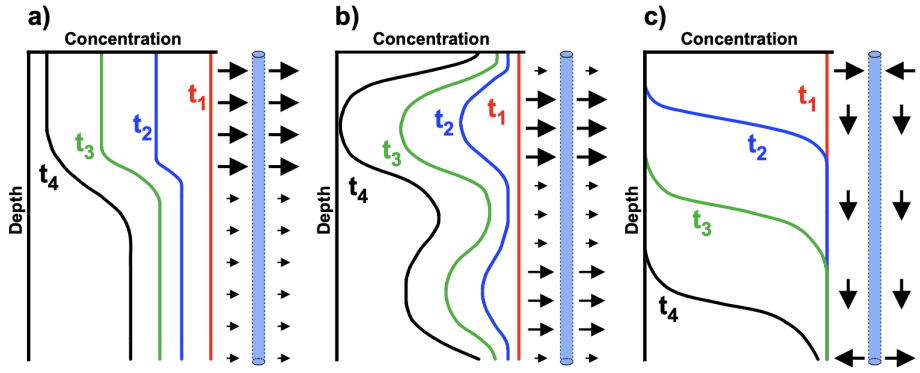

Figure 4.8: Figure a) shows a higher flow at the top of the borehole and a lower flow towards the bottom, indicated by a faster decrease of tracer at the top compared to the bottom. b) shows two sections with higher flow, alternating with sections of lower flow. Figure c) shows vertical flow, with an inflow horizon at the top and an outflow horizon at the bottom. Figure by Fahrmeier et al. (2021).

4.3.5. DATA ANALYSIS

Assuming that the tracer is only diluted by horizontal leachate flow in the well, the tracer is non-reactive and injected instantaneously at t = 0: at time t > 0, the tracer

concentration in the well (C) decreases according to Eq. (4.4) (Freeze & Cherry, 1979):

$$\frac{dC}{dt} = -\frac{Av_aC}{W} \tag{4.4}$$

Where, A is the cross-sectional area [L^2], W is the volume of the well segment [L^3], v_a is the apparent filtration velocity [LT^{-1}]. Rearranging Eq. (4.4) gives:

$$\frac{dC}{C} = -\frac{Av_a dt}{W} \tag{4.5}$$

Integrating Eq. (4.5) upon t = t_0 and C = C_1, gives:

$$ln\left(\frac{C_i}{C_1}\right) = -\left(\frac{2v_a}{\pi r}\right)t_i \tag{4.6}$$

Here, C_i is the tracer concentration [ML^{-1}] at a time t_i [T] after application of the tracer, C_1 is the tracer concentration immediately after tracer application [ML^{-1}], and r is the radius of the well [L].

Eq. (4.6) indicates that the ratio of $ln(C_i)$ exhibits a linear trend to the initial concentration $ln(C_1)$ with time t_i. Plotting the natural log of the obtained RWT concentration data for regression analysis should yield a linear trend line if the RWT concentration follows an exponential decay (Fig. 4.9 and 4.10). Deviation from linearity indicates additional flow processes. The slope of this regression line, m [-], is proportional to the horizontal flow velocity:

$$m = -\left(\frac{2v_a}{\pi r}\right) \tag{4.7}$$

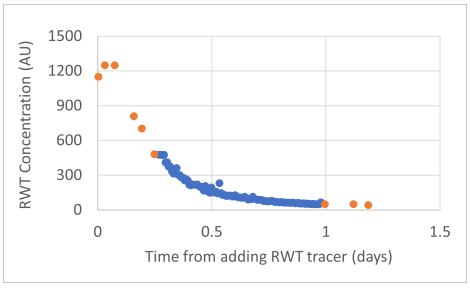

Figure 4.9: Exponential decay of the tracer concentration over time. Orange is manual data; blue is overnight logged data. Piezometer 5.13 at 11.71 m-GL (16.28 m+NAP).

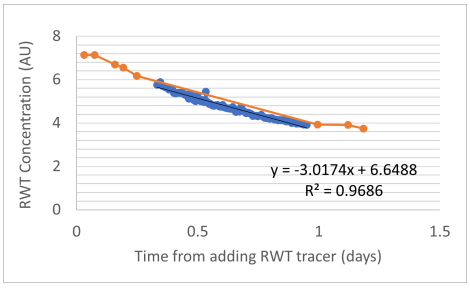

Figure 4.10: Example of the log-linear relationship between the tracer fluorescence and time. Orange is manual data; blue is overnight logged data. Piezometer 5.13 at 11.71 m-GL (16.28 m+NAP).

Rearranging of Eq. (4.7) leads to Eq. (4.8) (Piccinini et al., 2016):

$$v_a = -\left(\frac{m\pi r}{2}\right) \tag{4.8}$$

The filtration velocity [LT^{-1}], also the Darcy velocity, can be calculated from the apparent filtration velocity using Eq. (4.9). Drost et al. (1968) suggest that the apparent filtration velocity consists of the filtration velocity (v_f) combined with a borehole correction factor (α, [-]). The borehole correction factor compensates for the flow field distortion caused by the well (Fig. 4.11). The presence of the well distorts the velocity towards a higher velocity inside the borehole than throughout the rest of the aquifer (Pitrak et al., 2007; Englert, 2003). Furthermore, the presence of a filter pack causes more distortion to the flow lines than a well without a filter pack (Fig. 4.11).

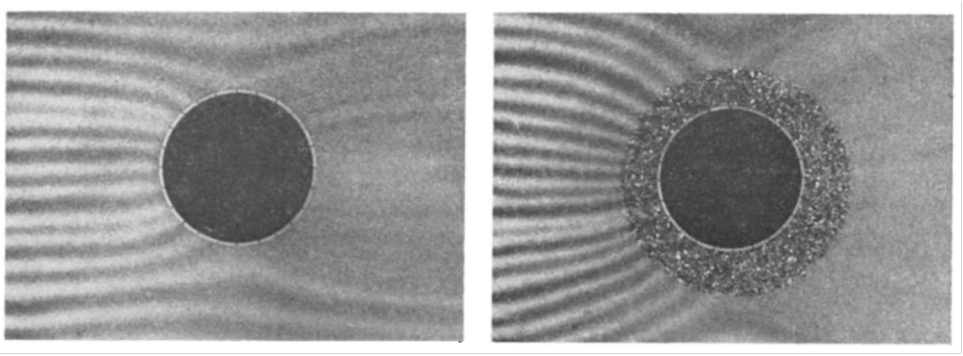

Figure 4.11: Experiments using dye tracers showing the distortion that a well screen causes to the groundwater flow (Drost et al., 1968). The left figure shows the flow lines in the vicinity of a well screen without a filter pack, and the right figure shows the flow lines in the vicinity of a well screen with a filter pack.

The apparent velocity additionally includes the apparent flow velocities due to density convection (v_k), vertical flow in the well screen (v_s), the mixing device (v_m), and molecular diffusion of the tracer (v_d), all in [LT^{-1}]:

$$v_a = \alpha * v_f + v_k + v_s + v_m + v_d \tag{4.9}$$

The effect of molecular diffusion (v_d) is dependent on the tracer concentration, which decreases over time. The overall effect on the data will therefore be non-linear. The same applies to the effects of density convection (v_k). The effects of possible vertical currents (v_s) in an open borehole can be ignored (Gomo, 2020). For a screened well under natural head conditions, the effects of v_s reflect the influence of the lateral flow, which replenishes the well through the screened part causing dilution of the tracer

concentration. The tracer injection and measuring method cannot result in a constant dilution rate. Thus, the impact of additional manual mixing (v_m) on the tracer dilution rate cannot be linear (Gomo, 2020). Therefore, the only component in the equation for the apparent velocity (Eq. 4.9) that produces a constant, linear dilution rate is the Darcy velocity. A strong linear correlation between the log of the concentration (log(C)) and dilution time (t) in Eq. (4.6) indicates that horizontal groundwater flow is the dominant factor that controls the dilution rate.

Eq. (4.9) can be reduced to Eq. (4.10) (Piccinini et al., 2016):

$$v_f = -\frac{m\pi r}{2\alpha} = \frac{v_a}{\alpha} \tag{4.10}$$

The value of the borehole correction factor, α, is dependent upon several variables: the hydraulic conductivity of the aquifer (K_3), the gravel filter (K_2), and the well screen (K_1); the inside radius of the screen (r_1), the outside radius of the screen (r_2), and radius of the borehole (r_3) [L], Eq. (4.11) (Fig. 4.12).

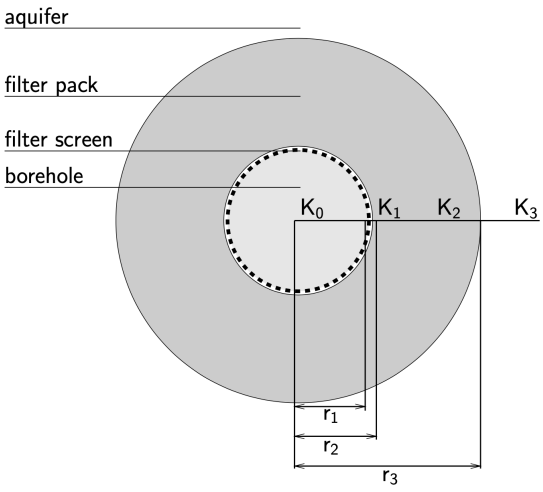

Figure 4.12: Schematized diagram of a horizontal borehole cross-section with a well screen, filter pack, and the surrounding aquifer. K_3, K_2, and K_1 are the hydraulic conductivities of the aquifer, the gravel filter, and the well screen, respectively; r_1, r_2, and r_3 are the inside radius of the screen, the outside radius of the screen, and the radius of the borehole, respectively. Figure by Englert (2003).

$$\alpha = \frac{8}{\left(1+\frac{K_3}{K_2}\right)\left\{1+\left(\frac{r_1}{r_2}\right)+\frac{K_2}{K_1}\left[1-\left(\frac{r_1}{r_2}\right)^2\right]\right\}+\left(1-\frac{K_3}{K_2}\right)\left\{\left(\frac{r_1}{r_3}\right)^2+\left(\frac{r_2}{r_3}\right)^2+\frac{K_2}{K_1}\left[\left(\frac{r_1}{r_3}\right)^2-\left(\frac{r_2}{r_3}\right)^2\right]\right\}} \tag{4.11}$$

Eq. (4.11) can be simplified whenever there is no filter pack installed, or whenever the filter pack is the same as the the aquifer: $r_2 = r_3$ and $K_2 = K_3$.

$$\alpha = \frac{4}{\left[1+\left(\frac{r_1}{r_2}\right)^2\right]+\frac{K_2}{K_1}\left[1-\left(\frac{r_1}{r_2}\right)^2\right]} \tag{4.12}$$

When the construction only consists of a well: $r_1 = r_2 = r_3$ and $K_1 = K_2 = K_3$, Eq. (4.11) can be simplified to:

$$\alpha = 2 \tag{4.13}$$

It is generally accepted to use a borehole correction factor of 2 for a well in a homogeneous aquifer that is in good hydraulic connectivity with the aquifer, or if the value cannot be calculated directly (Drost et al., 1968; Pitrak et al., 2007; Piccinini et al., 2016; Fahrmeier et al., 2021). Considering a horizontal cross-section, a value of 2 for the borehole correction factor indicates that a flow channel with a width of twice the well diameter converges through the screen of the well (Nordqvist et al., 2008). The value of the correction factor decreases when the drilling of the well results in a zone of lower hydraulic conductivity in the vicinity of the well. A zone of higher hydraulic conductivity results in an increased correction factor (Nordqvist et al., 2008). A borehole correction factor of 2 was used in the initial velocity calculations due to a lack of knowledge about the surrounding waste and installation of the filter pack. Sensitivity and possible error in the calculated Darcy velocity is examined in section 6.2.1.2.

4.4. POINT DILUTION TEST

A less common method of performing a dilution test is a point emplacement. A tracer slug is injected at a specific horizon, which can be useful to identify vertical flow, as the tracer plume will move up or down the borehole in the presence of vertical flow (Tate et al., 1970). Point dilution tests were performed using two different techniques: the point and constant depth techniques. Injection of the tracer was carried out similarly and will be explained first, followed by the monitoring method for both techniques and the data analysis.

4.4.1. INJECTION AND MONITORING OF THE TRACER CONCENTRATION

The tracer was injected into the well or piezometer using the same method; monitoring differed for the chasing and constant depth techniques.

- Before injection of the tracer, the data logger was connected to a laptop with the data logger support software and set to store a measurement every minute. The rod with the fluorometer was attached to the data logger. The fluorometer was lowered into the well or piezometer before injection of the tracer.
- For the 'chasing technique', the fluorometer was attached about 2 m below the leachate table. The fluorometer was attached at a chosen horizon for the 'constant depth technique'.
- The stock solution and leachate required were calculated using the same method as for the uniform dilution tests, but the target concentration was set to 1500 ppb. A diameter of 0.150 m for the Z wells and 0.105 m for the piezometers was used.
- The aim of the point dilution tests was to only inject tracer into the upper 0.50 m of the leachate column. Therefore, the hosepipe with the weight attached was lowered into the well or piezometer up to 0.50 m below the leachate table.
- Tracer was poured into the hosepipe through a funnel and removed from the well at a slow and steady pace. After, the hosepipe was inserted and removed another time for 0.50 m to promote horizontal mixing.

For the chasing technique:

- The starting output was noted down.
- Every time the fluorometer detected tracer for the first time; the fluorometer was lowered down another meter until the lowest measurable point of the well or piezometer was reached (about 0.25 - 0.50 m above the base).

For the constant depth technique:

- The fluorometer was either left overnight or for a few hours at a chosen depth.

When the test was finished, the data was downloaded from the data logger using a laptop.

4.4.2. DATA ANALYSIS

For the tests using the constant depth technique, the velocity was calculated from the first arrival of the tracer plume using the breakthrough curve. For the chasing technique, the vertical flow velocity was calculated by:

$$v_v = \Delta H / \Delta t \tag{4.14}$$

Where ΔH is the distance between two points of 'first tracer arrival' [L], and Δt the time between these measurements [T] (Fig. 4.13).

When calculating the horizontal flow velocity for wells when there is evidence of vertical flow within the well, the general computation by Freeze & Cherry (1979) is not valid as the method assumes that there is only horizontal flow inside the well. The method can result in significant errors in calculating the horizontal flow velocity. Y. Zhang et al. (2020) propose a model that includes both vertical and horizontal flow (Fig. 4.14).

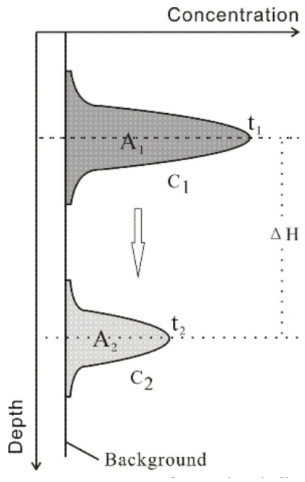

Figure 4.13: Concentration-depth diagram illustrating the movement of a tracer slug at two moments. Figure by Y. Zhang et al. (2020).

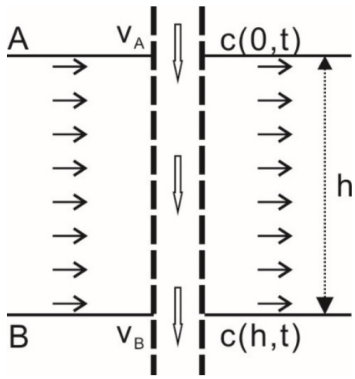

Figure 4.14: Model including vertical and horizontal flow inside a borehole. Figure by Y. Zhang et al. (2020).

The horizontal velocity was calculated by:

$$v_f = \frac{\pi r}{2\alpha\Delta t} * ln\frac{A_1}{A_2} \tag{4.15}$$

Here, A_1 and A_2 [L^2] are the integrated areas underneath the concentration-depth curve at times t_1 and t_2 [T] (Fig. 4.13). An assumption made by this method is that vertical flow does not dilute the tracer. This method only results in an average horizontal velocity over the selected depth interval.

5

RESULTS

In this chapter, the results of the measured leachate levels throughout De Kragge are presented, divided into leachate levels across the infiltration drains (top of the landfill), throughout the waste body (middle of the landfill), and in the basal drains (bottom of the landfill). The results of the uniform and point dilution tests follow. Table 5.1 illustrates an overview of the performed tests and the available data per piezometer and well.

Table 5.1: Overview of performed measurements and available data per piezometer or well.

ID	Leachate level measurements			Uniform dilution test		Point dilution test	
	Manual	CTD-Diver® (continuous data)	LevelLog (continuous data)	Tracer decline over slotted screen (manual)	Tracer decline at constant depth (logged)	Tracer breakthrough curve (*not complete)	Vertical movement of tracer (catching technique)
P5.7		x					
P5.10	x	x		x	x		
P5.13	x	x		x	x	x*	
P5.15	x			x			
P5.18	x			x			
P6.5		x					
P6.8	x	x					
P6.11	x	x		x	x		
P6.14	x			x			
P6.17							
P7.6		x					
P7.9	x	x		x	x		
P7.12	x	x		x	x		
P7.15	x			x			
P7.18	x			x			
P8.18	x			x			
Z1	x			x		x	x
Z2	x			x		x*	x
A5	x		x	x			
A1.1	x		x	x			
RIS drain 2B		x	x				
RIS drain 3A		x	x				
Collection drain comp. 3 and 4		x					

5.1. LEACHATE LEVELS THROUGHOUT THE LANDFILL

The leachate levels were measured at several depths throughout the landfill: in the infiltration drains close to the surface, throughout the waste body, and in the basal drainage system. The cumulative flows were used to estimate the water balance.

5.1.1. LEACHATE LEVELS MEASURED IN THE INFILTRATION DRAINS

The piezometers across the RIS drains reach different depths (Table 4.1). The leachate level data collected from the pressure gauges (CTD-Divers®) indicate two different periods regarding measured leachate levels: before and after change of infiltration scheme in July (Fig. 5.1 and 5.2). In June, when infiltration was continuous, RIS drain 3A appeared to behave more as one unit and with less noise than drain 2B. Leachate levels measured at point 3A.6 began to differentiate from mid-June; minimum and maximum leachate tables differed up to one meter, while at other points, the difference was 0.20 m maximum (Fig. 5.1). From the 6th of July, the infiltration changed to 20-30 minutes of infiltration per drain at approximately 8-hour intervals. The minimum and maximum leachate levels from drain 3A (except 3A.6 and 3A.8) appear more even than the levels in drain 2B. From mid-September, maximum leachate levels start to rise. For drain 2B, this is most prominent in points 2B.2 (± 25 cm) and 2B.4 (± 20 cm) (Fig. 5.2). This rise was not as visible in the leachate levels measured in drain 3A.

Figure 5.1: Leachate levels measured across infiltration drain 3A.

Figure 5.2: Leachate levels measured across infiltration drain 2B.

However, as shown in Figures 5.2 and 5.1, both the minimum and maximum leachate levels along the length of the drain do not line up. The piezometers where the CTD-Divers® were installed intersect the gravel around the infiltration drain (Fig. 2.3). Whenever the drain is infiltrated, it is expected that the gravel acts as one communicating vessel and that the leachate levels across the infiltration drain are even. It should be noted that the depths of the installed piezometers across the drain are not uniform (Table 4.1). For the piezometers across drain 3A, there is a difference up to 2.29 m; for drain 2B, the difference is 0.57 m. Likewise, the leachate levels measured across drain 2B differed less. For drain 3A, the deepest piezometer (3A.1) and the most shallow piezometer (3A.6) showed the lowest and highest minimum level, respectively. However, this did not apply to the maximum level or the levels across drain 2B, where 2B.2 is the deepest piezometer, and 2B.4 is the most shallow one. There is no clear connection between the depth of the piezometer and the measured leachate level.

The raw data of the leachate levels were normalized by calculating the difference between maximum leachate levels across the drain compared to point 2B.2 for drain 2B and 3A.1 for drain 3A using the first infiltration event on October 12th. The difference between the maximum levels compared to points 2B.2 and 3A.1 led to a 'delta' for every data point. This delta was subtracted or added to every measurement to shift the entire graph up or down, creating uniform maximum levels across the drain. Figures 5.3 and 5.4 zoom in on four days in October, and Figures F.7 and F.6 show normalized data from

mid-September to mid-October.

Points 3A1, 3A.2, 3A.3, and 3A.6 showed sharp peaks for the maximum leachate levels, whereas points 3A.5 and 3A.8 had broader bases as peaks and more or less the same minimum leachate value (Fig. 5.3). The leachate levels did not increase simultaneously across the drain but differed up to 10 minutes (measurement interval was 5 minutes). Apart from point 3A.6, the leachate level generally receded to the minimum before a new infiltration event. Smaller peaks before an infiltration event were visible, except for point 3A.5.

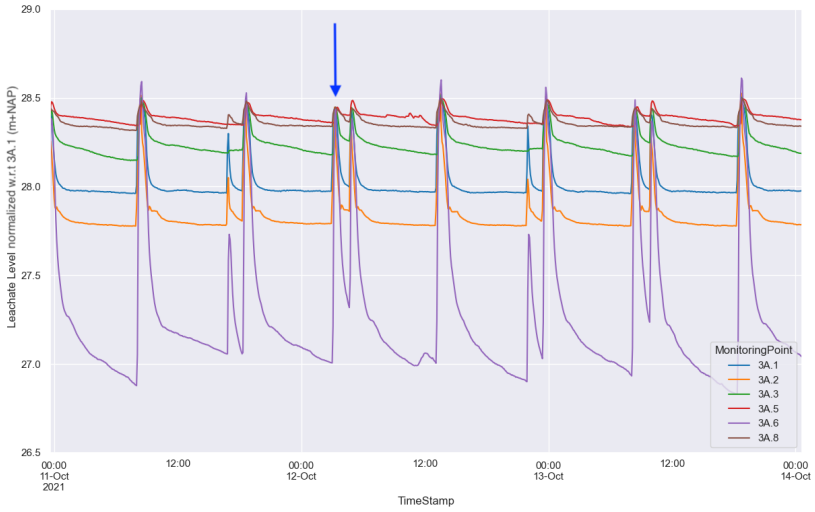

Figure 5.3: Leachate level measurements from 11 to 14 October 2021 for infiltration drain 3A, normalized with respect to point 3A.1 (the infiltration event with the arrow).

The leachate levels for all four points across drain 2B started to increase simultaneously (Fig. 5.4). The maximum leachate levels did not show sharp peaks; instead, all points showed a broader peak. After peak leachate levels, the levels declined more slowly than across drain 3A, and they did not reach back to the minimum levels before another infiltration event. There appear to be additional infiltration events after the main event. These events were most prominent in the levels for points 2B.2 and 2B.4.

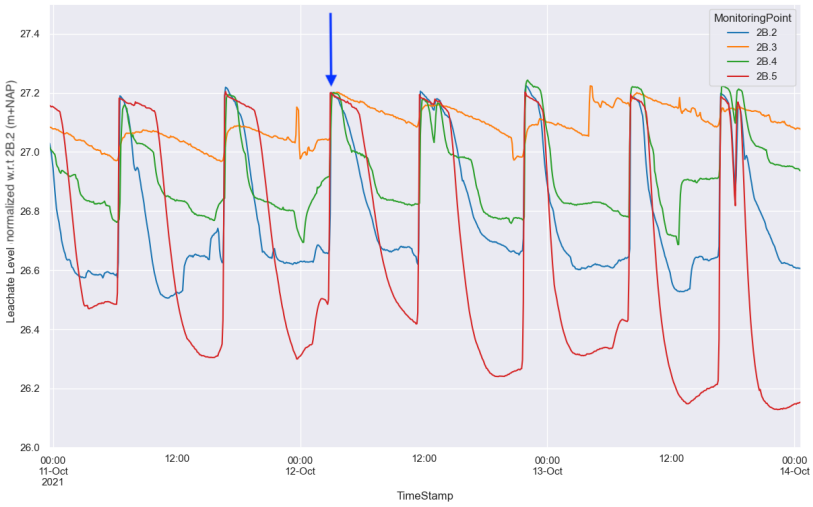

Figure 5.4: Leachate level measurements from 11 to 14 October 2021 for infiltration drain 2B, normalized with respect to point 2B.2 (the infiltration event with the arrow).

5.1.2. LEACHATE LEVELS MEASURED IN THE WASTE BODY

The leachate levels measured in the piezometers (nests 5 - 8) are not necessarily the actual leachate level in the waste body but rather represent the pressure head at the depth of the screen. A higher pressure leads to a greater elevation of the leachate level inside the piezometer. If there are different pressures in a set of nested piezometers, the leachate flows from high to low pressure. Downward vertical flow is indicated by the deepest piezometer having the lowest leachate level. If the end of the slotted casing of a piezometer intercepts a perched leachate table, the leachate in the casing will rise above the originally saturated zone.

The head difference measured per piezometer over 12 hours was 0.10 to 0.15 m, but generally less (Fig. 5.5). Leachate levels in different piezometers followed the same trends (regarding peaks and declines). The difference between the peaks and declines in leachate level was more prominent in the deeper piezometers (P5.13, P6.12, and P7.12) than in the shallow piezometers (P5.10, P7.9). Manual leachate measurements taken with a dip-meter showed the same trends; the measurements can be found in Appendix F (Figure F.3). The 15- and 18-meter deep piezometers could not be equipped with CTD-Divers®, and it is thus not possible to state whether this trend continues

down with depth. Leachate levels showed a downward gradient, with lower leachate levels in deeper piezometers. Leachate levels measured in the piezometers of nest 6 appeared to be higher than the levels in piezometers from nests 5 and 7. Measured leachate levels in the piezometers across the landfill show a spatial difference of up to 3 m.

Leachate levels measured in gas wells remained unchanged over the past years. However, they showed a spatial difference up to 8 meters (leachate levels between 13 - 21 m+NAP, Fig. F.1 in Appendix F). Three A wells had current data on the leachate levels; they showed an increase in leachate level between 0.2 and 2.0 meters in January 2022 compared to December 2020 and showed spatial differences up to 6 meters (leachate levels between 12 - 18 m+NAP, Fig. F.2 in Appendix F).

5.1.2.1. RESPONSE OF LEACHATE LEVELS TO PRECIPITATION AND ATMOSPHERIC PRESSURE

Precipitation data and atmospheric data collected from KNMI-station Woensdrecht (not on-site) are plotted together with the leachate levels in Figures 5.5 and 5.6. In February, the multiple precipitation events did not lead to an increase in leachate levels (Fig. 5.5). In addition, leachate levels did not appear to decline in the dry period from the end of February until the end of March. In the dry period towards the end of April, leachate levels declined. In the observed period, precipitation events did not impact the leachate levels measured in the waste body. Instead, the leachate levels in the piezometer show an inverse relationship with the atmospheric pressure (Fig. 5.6).

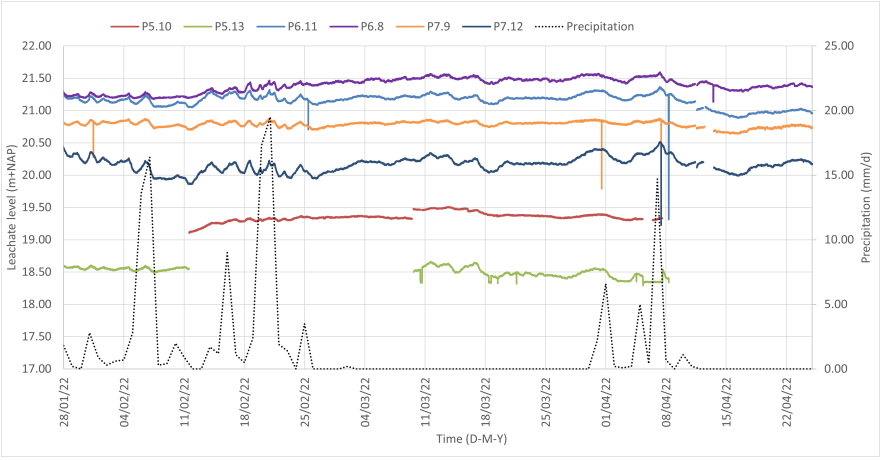

Figure 5.5: Complete time series of measured leachate levels in the new piezometers and the precipitation.

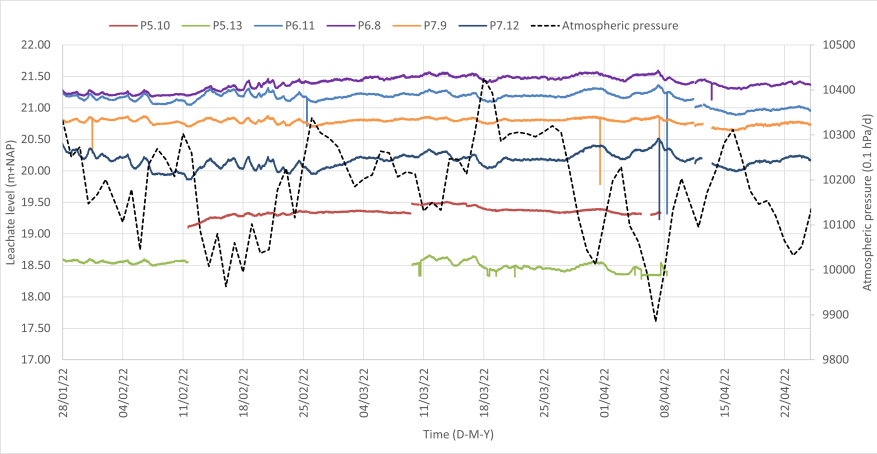

Figure 5.6: Complete time series of measured leachate levels in the new piezometers and the atmospheric pressure.

5

5.1.2.2. RESPONSE OF LEACHATE LEVELS TO LEACHATE INFILTRATION

Figures 5.7a, 5.7b, and 5.7c show that the RIS infiltration was different per drain, both for the volume and the frequency of infiltration. In the plotted period, 03-04-2022 to 05-04-2022, RIS drain 4 infiltrated significantly more than RIS drain 2. However, neither the frequency nor the volume of the infiltration events impacted the leachate levels. There is no apparent difference between the leachate levels in the piezometers of nests 5, 6, and 7.

Figure 5.7: Continuous leachate level measurements in the newly installed piezometers.

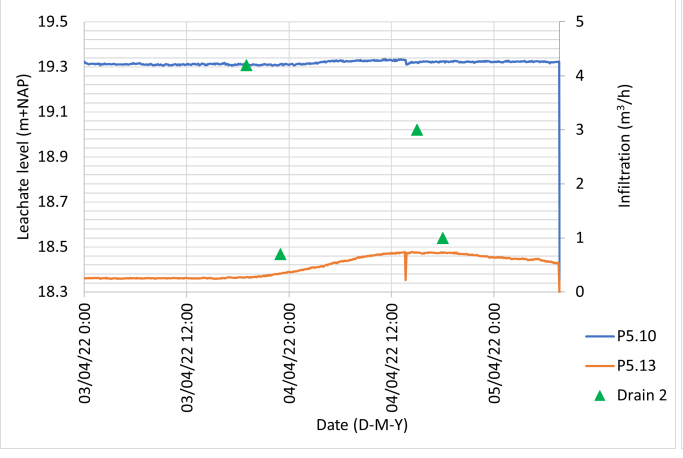

(a) Leachate level piezometer nest 5 with infiltration of drain 2.

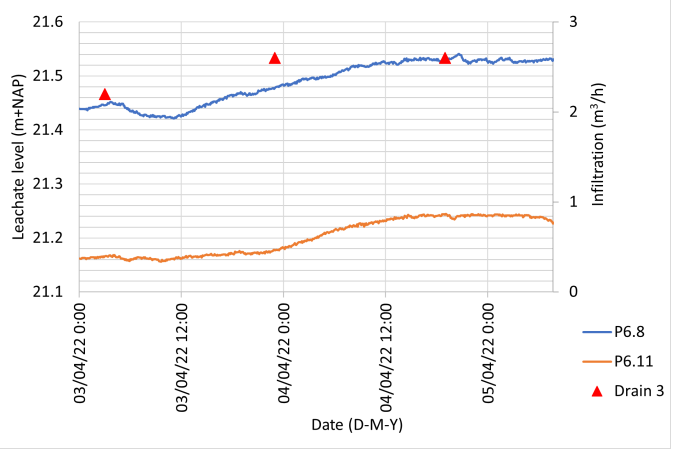

(b) Leachate level piezometer nest 6 with infiltration of drain 3.

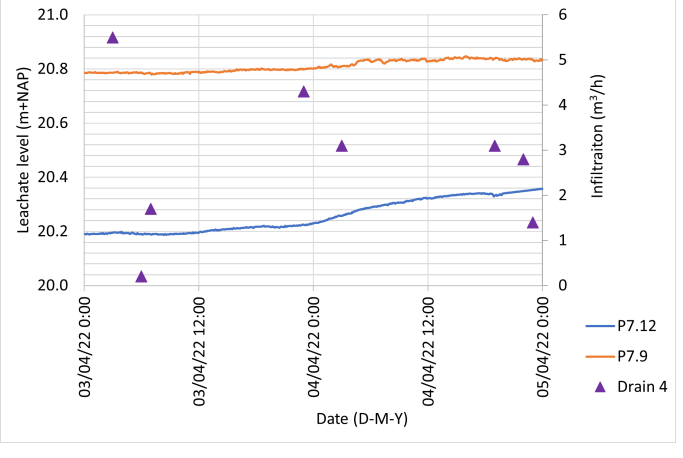

(c) Leachate level piezometer nest 7 with infiltration of drain 4.

5.1.3. LEACHATE LEVELS MEASURED IN THE BASAL DRAINAGE SYSTEM

The basal drains are located between 5.25 and 7.00 m+NAP (Fig. 5.8). 2-meter-high dikes separate the compartments, and a measured leachate level in compartment 3 above 2 meters enables flow to the two neighboring compartments above the dikes. However, there is a 1.75-meter difference in height between the south and north end of the landfill (Fig. 5.8). Therefore, assuming the drainage layer is fully connected, a measured leachate level lower than 1.75 meters indicates that the drainage system on the southern end is dry.

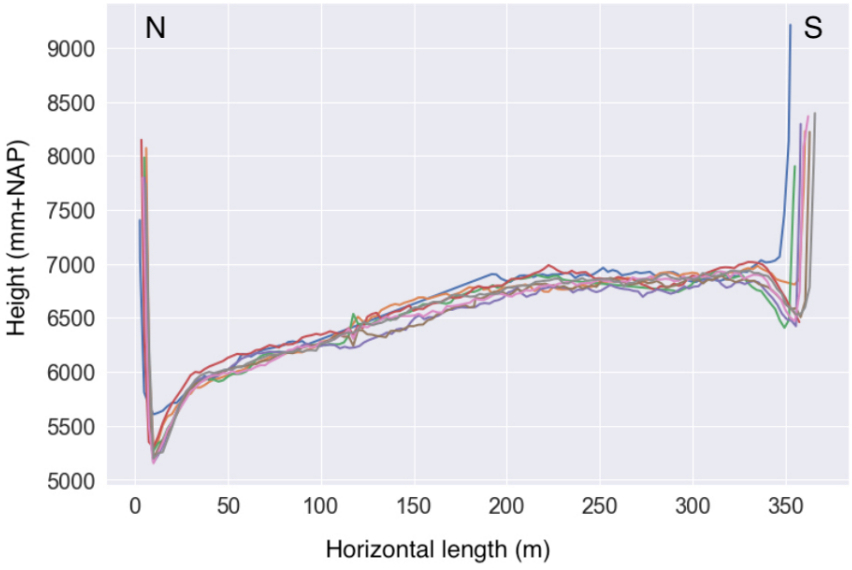

Figure 5.8: Height profile of the basal drainage system. Figure adapted from Hersbach (2021).

The measured leachate levels showed temporal changes in both compartments (Fig. 5.9). Because the basal drains are located on a slope and the level measurements are taken at the lowest point, the variation in leachate level is more dynamic than it would have been if the system was horizontal. In a horizontal system, the leachate would then even out over a larger surface. The variation does not appear to be seasonal, as the leachate level started to rise during a precipitation deficit on several occasions (e.g., January 2019 and August 2019, Fig. 5.10). Additionally, the landfill operators have control over the leachate level in the basal collection pit.

In the months July - October 2018, February - July 2019, October 2019, and November 2021 - July 2022, leachate levels were 1.75 m above the measurement sensor, as indicated by the dashed black line in Figure 5.9. In this period, the basal drains over the length of the landfill (north to south) would have been saturated.

The measured level in compartment 3 was above 2.0 m several times: March-April 2019 and February - June 2022 (pink dashed line in Fig. 5.9). On these occasions, the leachate level measured in the basal drain of compartment 4 tends to be higher. However, from November 2021, the leachate level in compartment 3 was higher than in compartment 4. The leachate level measured in compartment 4 followed the same trends in high and low leachate levels as compartment 3 but declined with a delay.

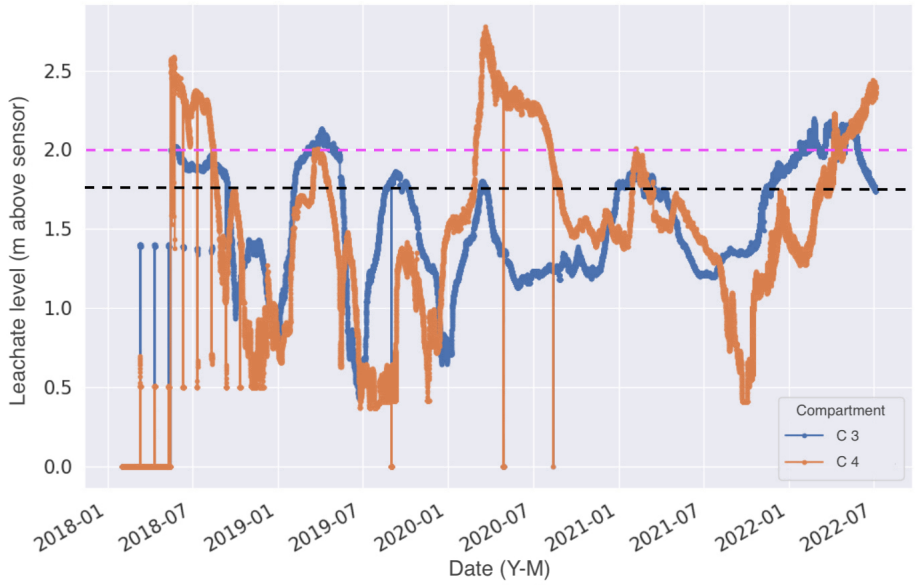

Figure 5.9: Leachate level measured in the basal drains, height in m above the sensor. Figure adapted from Heimovaara (2022, personal communication).

5.1.4. WATER BALANCE ESTIMATION OF DE KRAGGE

Whenever the evaporation was higher than the precipitation, there was a precipitation deficit (Fig. 5.10, marked yellow). Evaporation showed clear seasonal variability, with the lowest evaporation in winter and the highest evaporation in summer. Precipitation

showed less seasonal variability. The cumulative evaporation over four and a half years (02-01-2018 – 04-07-2022) is 2.993 m and the total cumulative precipitation over this period is 3.267 m (KNMI weather station Gilze-Rijnen). Therefore, the rainfall surplus over these 4.5 years is only 0.274 m, much less than the expected 0.300 m/y (Kanen & Kedzia-Kowalski, 2021; Van Turnhout et al., n.d.).

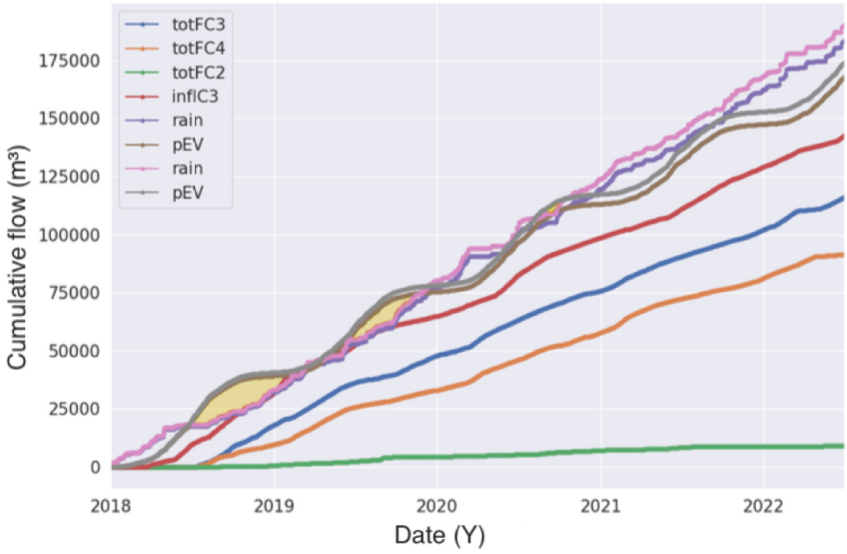

Figure 5.10: Cumulative flows. Blue = total flow extracted from compartment 3. Orange = total flow extracted from compartment 4. Green = total flow extracted from compartment 2. Red = total flow infiltrated in compartment 3. Purple/pink = cumulative rainfall. Grey/brown = total cumulative evaporation. Yellow shaded area indicates a precipitation deficit. Figure from Heimovaara (2022, personal communication).

The infiltration of the RIS drains over the past year changed per day, from 0 m^3/h to over 10 m^3/h. Assuming that all RIS drains (A+B combined) inject 5 m^3/h at the same time for 20 minutes, three times a day, results in a total injection of 35.00 m^3/d. The total area of compartment 3 is around 56000 m^2. If the injected leachate spreads over the entire compartment, this results in a 0.63 mm layer of injected leachate per day. The calculated precipitation surplus over 4.5 years yields a daily surplus of 0.18 mm, according to Figure 5.10. Adding this to the leachate injection leads to a roughly estimated daily recharge of 0.81 mm.

In the operational period of the pilot, the cumulative infiltration of leachate and water

by the RIS into compartment 3 (red line, Fig. 5.10) was higher than the measured outflow (blue line) from the drainage system of compartment 3. Infiltration into compartment 3 appears to slightly follow the same trend as evaporation (a higher increase in the summer months). The volume pumped from the drainage system of compartment 3 was higher than the volume pumped from compartment 4, which in turn was higher than the volume pumped from compartment 2.

The cumulative water balance indicates that more leachate leaves the landfill than is infiltrated (RIS and precipitation surplus) and that the landfill is getting drier (Fig. 5.11). The calculated water balance of compartment 3 (infiltration by the RIS + precipitation surplus - outflow of leachate from compartment 2) indicates an increase in water content up to 32750 m^3. However, this water balance calculation does not account for the possible lateral flow from compartment 3 to compartment 4, which is why it appears that compartment 3 is building up moisture and compartment 4 is losing moisture.

For compartment 4, the only source of inflow in the calculation is precipitation, and the outflow from the compartment is higher, which results in a negative water balance (Fig. 5.10). The cumulative water balance calculation showed that the combined outflow of compartments 2, 3, and 4 were higher than the cumulative infiltration of leachate and water in compartment 3 by the RIS system combined with the precipitation surplus over compartments 3 and 4. It appears unlikely that compartment 3 is building up moisture. The leachate levels measured in the gas wells remained stable over the years. However, the level in two A wells increased by about 1.5-2 between 2020 and 2022 (Figs. F.1 and F.2).

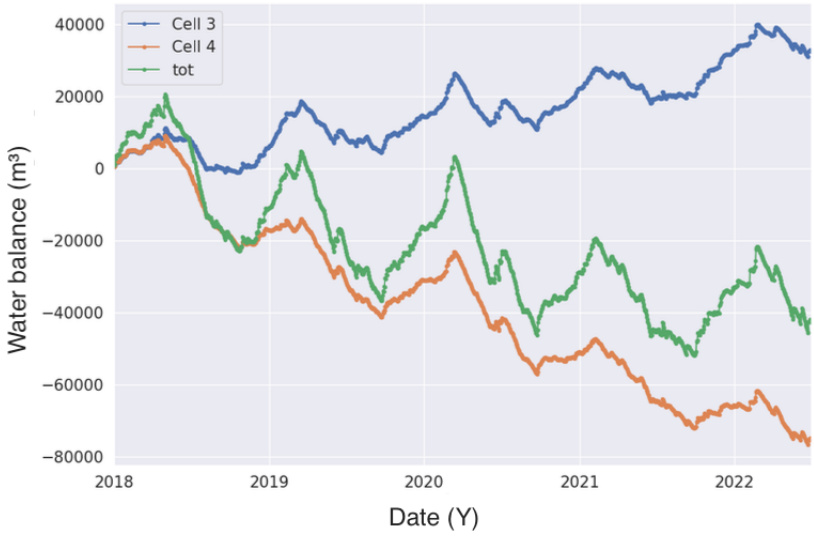

Figure 5.11: Estimated water balance of De Kragge. Blue = water balance for compartment 3. Green = water balance for compartment 4. Orange = cumulative balance for compartments 3 and 4. Figure from Heimovaara (2022, personal communication).

5.1.5. SUMMARY

Within the waste body of compartment 3, the different sections (upper infiltration drains, middle section of waste, basal drains) appear to have little connection. The levels in the basal drainage system were much lower (max. around 7.50 m+NAP) than the levels measured in the piezometers placed in the waste body (16 – 24 m+NAP) and in the infiltration drains (normalized leachate levels between 26.2 – 27.2 m+NAP for drain 2B and between 27.0 – 28.5 m+NAP for drain 3A). This is as expected, as the landfill would not be stable otherwise. The infiltration events of the RIS drains were visible in the leachate levels measured across the infiltration drains; however, the effects were not visible in the measured leachate levels in the piezometers placed in the waste body. If the leachate infiltrated the waste body effectively, it would have been expected that these changes were also visible in the leachate levels measured in the piezometers throughout the waste body. Combining the in and outflow of compartments 2, 3, and 4 resulted in a negative water balance, indicating that the landfill is losing moisture. It is unknown to where this leachate flows, but the different compartments appear to be hydrologically connected.

5.2. LEACHATE FLOW THROUGHOUT THE LANDFILL

In total, 27 wells and piezometers were eligible for a borehole dilution test, as they have a minimum casing diameter of 50 mm and a slotted screen. Because of time restraints, a priority list was made, including the following wells: Z1, Z2, nest 5, 8.18, A1.1, and A5. The priority list was accomplished by drawing a vertical line from north to south throughout the landfill to get spatial representation (Fig. 5.12). In addition, the nested piezometers allow for testing at different depths but at the same approximate location (the piezometers are located 0.5 - 0.6 m from each other). Therefore, if there are alternating saturated and unsaturated waste pockets, the nested piezometers with a 2 m screened section can be used for testing in these different zones. As shown in the last column of Table 2.2, piezometer nests 6 and 7 were tested in addition to the priority list, resulting in a more complete data set.

Besides horizontal velocity, vertical flow is an essential factor in stabilizing the landfill by recirculating leachate. The uniform SBDTs were performed to assess the horizontal velocity, and to conduct a first estimation of the vertical velocity, point injection tests were performed. Point injections were conducted on wells Z1 and Z2 and piezometer 5.13. All dilution tests were performed under the natural hydraulic gradient.

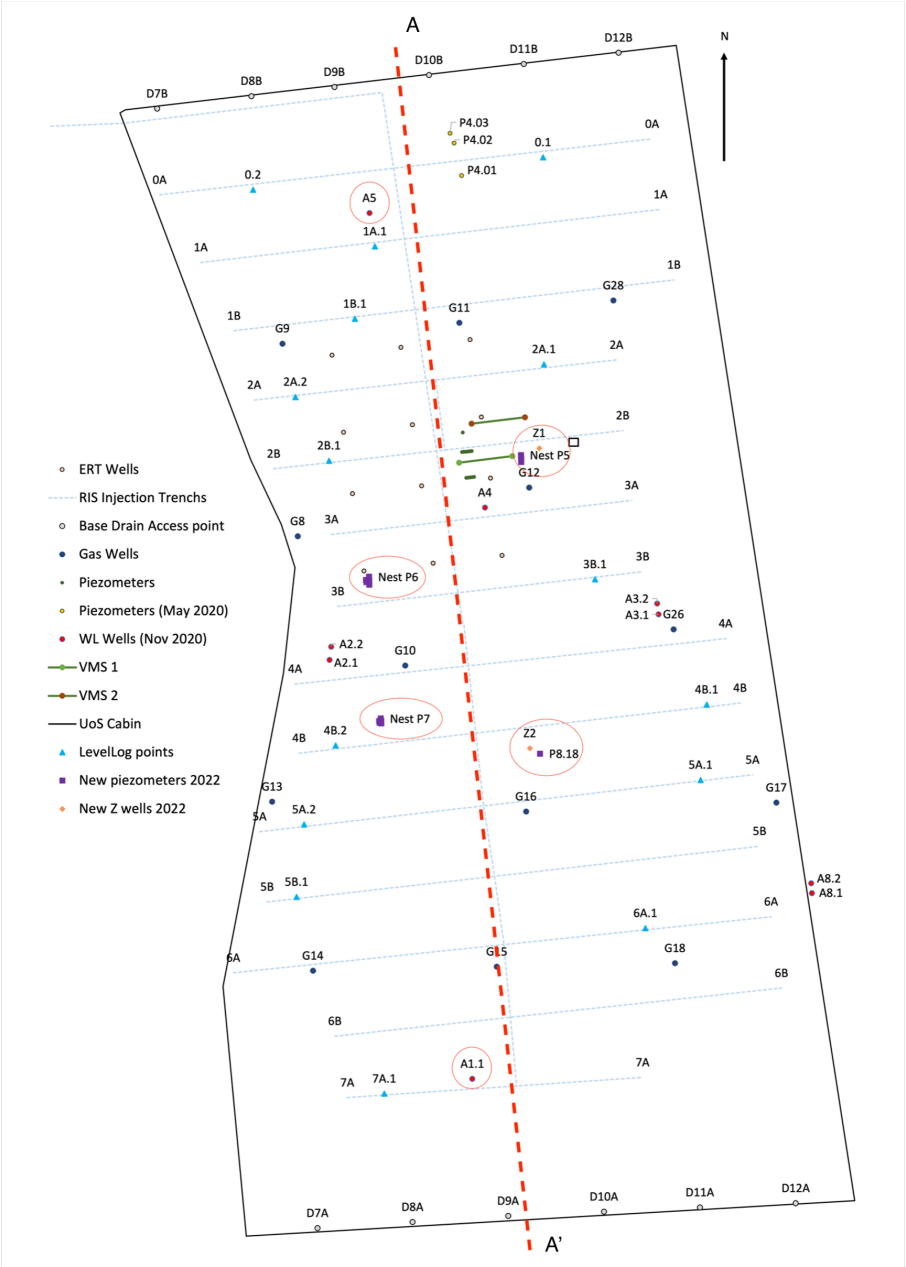

Figure 5.12: Location of wells and piezometers at De Kragge, red circles indicate locations that have been tested, line A-A' the cross-section that was used to determine the priority wells. ERT = Electrical resistivity tomography; RIS = Recirculation infiltration system; WL = Water level; VMS = Vadoze-zone Monitoring System^{TM} (Sensoil); UoS = University of Southampton.

5.2.1. UNIFORM DILUTION TESTS

Dilution tests were performed multiple times on several wells to test their repeatability (Table 5.2). A -1, -2, or -3 was added to the well or piezometer identification to denote repeated tests. Therefore, 5.10-1 is the first test performed on piezometer 5.10, 5.10-2 the second. At De Kragge, there was the possible influence of the infiltration measurements. To investigate whether, and in if so, how much, this affected the horizontal velocity, RIS drains 2 and 3 were temporarily shut off. During this time, dilution tests were conducted on well Z1 and piezometers 5.18, 5.15, and 5.13.

Time constraints prevented from performing tests with infiltration drains turned on during tracer injection. However, per the RIS infiltration scheme, several uniform SBDTs were performed during the infiltration of a drain. For each week, a timeline was established with the performed SBDTs, and the infiltration events of close-by RIS drains (Appendix G). For nest 5 and well Z1 this is drain 2, for nest 6, well Z2 and piezometer 8.18 this is drain 3, and for nest 7 this is drain 4. Wells A5 and A1.1 are located close to drains 0 and 1, and 7, respectively (Fig. 5.12). Infiltration of the drains started within the hour presented in the timeline and lasted for about 20 to 30 minutes.

Table 5.2: Overview of performed single borehole dilution tests. A * denotes the use of an increased diameter to calculate the necessary tracer stock solution. Apart from the tests where it is stated that they were performed without infiltration, all uniform dilution tests were conducted during regular operation of the recirculation infiltration system.

Well	nr.	Type of test	Logged	Manual	Date (D-M-Y)	Target conc. (ppb)
Z1	-1	uniform	x		22-03-2022	1000
	-2	uniform repeat	x		29-04-2022	1000*
	-3	uniform, no infiltration	x		03-05-2022	1000*
	-v-1,2	point	x	x	07-05-2022	
P5.10	-1	uniform	x	x	05-04-2022	750*
	-2	uniform, repeat	x	x	28-04-2022	750*
	-3	uniform, no infiltration	x		04-05-2022	750*
P5.13	-1	uniform	x		18-03-2022	750
	-2	uniform, repeat	x	x	05-04-2022	1000*
	-3	uniform, no infiltration	x (2)		04-05-2022	750*
	-v-1	point		x	08-05-2022	
P5.15	-1	uniform	x		18-03-2022	750
	-2	uniform, no infiltration	x		04-05-2022	750*
P5.18	-1	uniform	x		17-03-2022	1000
	-2	uniform repeat	x		29-04-2022	750
	-3	uniform, no infiltration	x		04-05-2022	1000*
P6.11		uniform	x	x	12-04-2022	750*
P6.14		uniform	x		25-04-2022	750*
P7.9	-1	uniform	(x)	x	12-04-2022	750*
	-2	uniform, repeat	x	x	26-04-2022	1000
P7.12	-1	uniform	x	x	12-04-2022	750*
	-2	uniform, repeat	x		26-04-2022	750*
P7.15	-1	uniform	x		25-04-2022	750*
P7.18	-1	uniform	x		26-04-2022	750*
Z2	-1	uniform	x		06-04-2022	1000*
	-v-1,2,3	point	x	x	07-05-2022	
P8.18		uniform	x		07-04-2022	750*
A5		uniform	x		05-04-2022	750*
A1.1		uniform	x		28-04-2022	750*

5.2.1.1. DECLINE OF TRACER CONCENTRATION OVER TIME

This section elaborates on a few trends in the RWT concentration-time graphs for the uniform SBDTs: uniform and non-uniform distribution of tracer and the possibility of vertical currents inside the well screen. Based on this and the methodology used, an overview was made of the performed tests (section 5.2.1.1). All concentration-time graphs are presented in Appendix H.

Uniform starting concentration

A uniform starting concentration mainly occurred in the most shallow piezometers (e.g., P7.9 and P5.10). SBDT 5.10-3 had a uniform starting concentration over the saturated depth (Fig. 5.13). Over time, the tracer appeared to move faster in the middle section of the leachate column, and there were no signs of vertical currents.

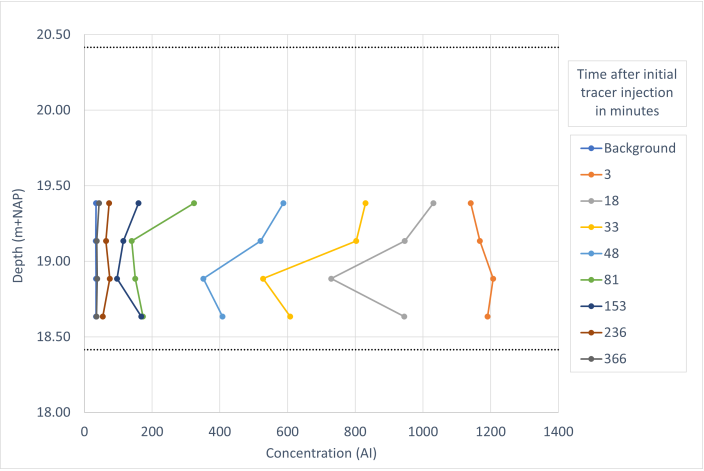

Figure 5.13: Change in RWT (Rhodamine water tracer) concentration over time for dilution test 5.10-3. The dotted lines indicate the screened section: above the upper line, the screen is blind.

Non-uniform starting concentration

A sharp (initial) boundary of the tracer concentration between the blind and screened section of the casing indicates a non-uniform starting concentration. For test 5.15-2, the starting concentration in the screened section was considerably lower than in the blind section (Fig. 5.14). At the base of the piezometer, the concentration was higher, followed by a decline in concentration in the middle of the screen and going up again towards the blind section. A concave shape like this was present in the concentration-depth graphs of tests 5.18-2, 5.18-3, 6.14, 7.15, and 7.18 (varying degrees). While this indicates that the tracer reached the base of the piezometer, the analysis is complicated and might result in inaccurate velocities over depth.

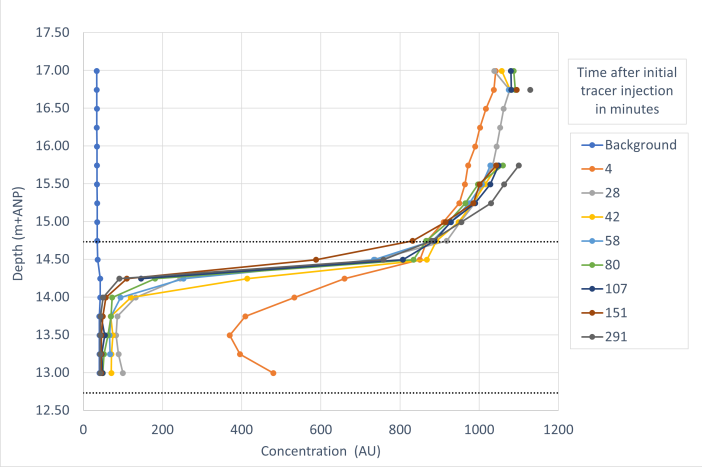

Figure 5.14: Change in RWT (Rhodamine water tracer) concentration over time for dilution test 5.15-2. The dotted lines indicate the screened section: above the upper line, the screen is blind.

Indications of vertical flow

Signs of vertical flow were indicated by a rapid decline in tracer concentration in the blind section of the casing (within 24 hours, piezometers 6.14 and 7.15) or the shape of the concentration-depth logs (well Z1 and Z2). For the test on Z2, the second measurement was taken an hour after the first, and the top meter had almost reached background concentrations again (Fig. 5.15). The section at the top that had returned to background concentration kept increasing in depth over time, while the tracer concentration at the base of the piezometer remained relatively high. This increase in vertical offset indicates vertical flow (Fig. 4.8).

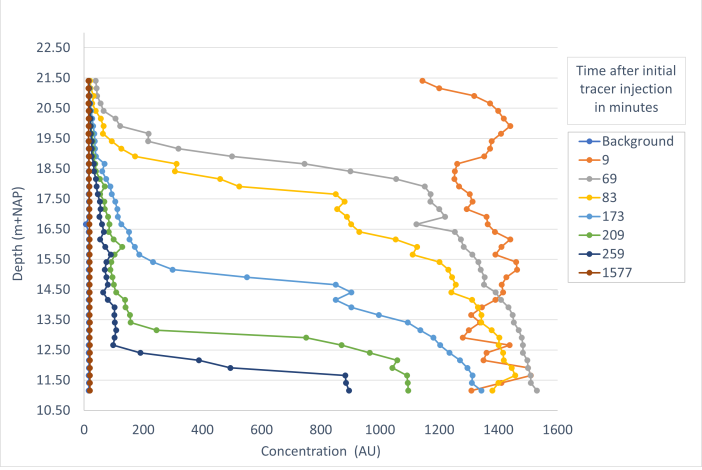

Figure 5.15: Change in RWT (Rhodamine water tracer) concentration over time for dilution test on well Z2. The casing of the well is screened throughout the saturated depth.

No indications of vertical flow

Absence of vertical movement was indicated by a constant RWT concentration in the blind section of the casing or a lack of tracer accumulation at the base of the piezometer or well. Indications of vertical movement were not visible in the concentration-depth graphs for piezometer 8.18: after 24 hours, the tracer concentration in the blind section of the casing had not declined (Fig. 5.16). Instead, the concentration had increased slightly compared to the measurements from the previous day. Piezometer 8.18 is located about 3 m from well Z2, where the concentration-depth graphs did show indications of vertical flow.

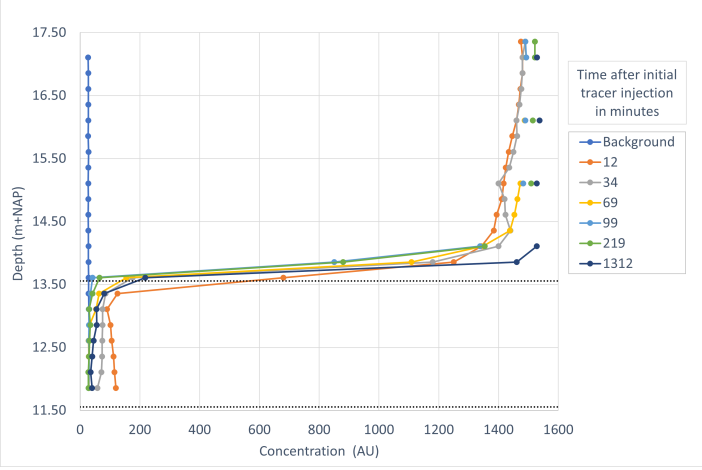

Figure 5.16: Change in RWT (Rhodamine water tracer) concentration over time for dilution test on piezometer 8.18. The dotted lines indicate the screened section: above the upper line, the screen is blind.

Ambiguous

The ambiguous category contains tests where the decrease of RWT concentration in the blind section of the casing had minimal effect on the measured decline of tracer in the screened section, i.e., no accumulation of tracer at the base or an increase in tracer concentration. These piezometers had no or little (< 1.0 m) leachate in the blind section (P5.13) or negligible dilution in the blind section compared to the duration of a dilution test (P7.12, Fig. 5.17).

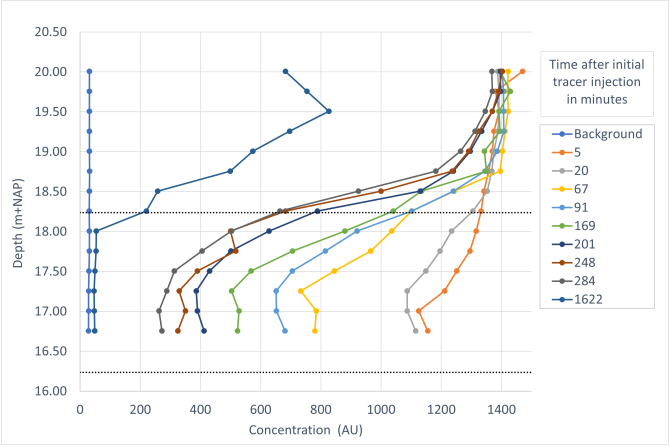

Figure 5.17: Change in RWT (Rhodamine water tracer) concentration over time for dilution test 7.12-1. The dotted lines indicate the screened section: above the upper line, the screen is blind.

Constant depth tests

Logged (overnight) measurements at a constant depth were performed on several piezometers: 5.10, 5.13, 6.11, 7.9, and 7.12. In general, the logged measurements were assumed to be more accurate than manual measurements, as there is no influence from raising and lowering the fluorometer down the leachate column. Additionally, measurements were taken every few minutes, resulting in a complete data set compared to manual measurements taken every 30 minutes. For test 5.13-2, manual measurements were conducted before and after the logged measurements, and for this test, both measurements match up well (Fig. 5.18). The same applies to the logged and manual tests on piezometers 6.11, 7.9, and 7.12, indicating that these manual measurements were performed with minimal errors. However, there is a large difference between the manual and logged measurements for the tests conducted on piezometer 5.10 (test 5.10-2 in particular).

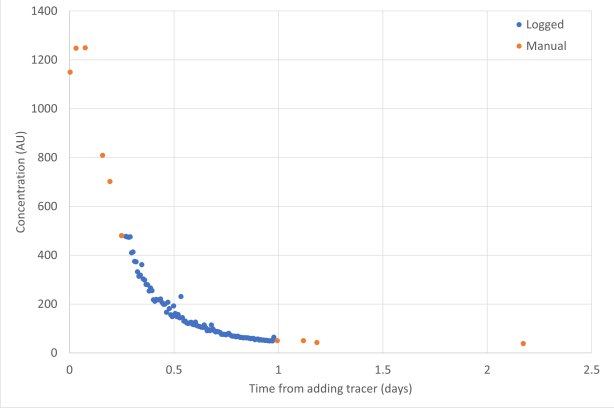

Figure 5.18: Change in RWT (Rhodamine water tracer) concentration over time for logged dilution test 5.13-2. The probe was left at 15.78 m+NAP (12.21 m-GL, about 0.75 m above the base of the piezometer).

Overview of the performed uniform dilution tests

As illustrated above, the decline in tracer concentration showed different behaviors per well and piezometer. A uniform starting concentration is most favorable, as the declining trend in concentration allows for the most straightforward interpretation. Additionally, with a uniform starting concentration, it is visible when a section declines slower than another section (if there is no vertical movement). In theory, an uneven starting concentration should be no problem; the decline in tracer concentration relative to the initial concentration is most important. However, if the starting

concentration is non-uniform, it can be difficult to perform sufficient concentration measurements for calculating the Darcy velocity. The concentration will return to background values faster than the section with a higher starting concentration.

Whenever there are signs of vertical flow in the concentration-depth diagrams, this influences the calculated Darcy velocity, so these calculations are less reliable than tests without any indications of vertical flow. The theory to calculate horizontal flow velocities (Freeze & Cherry 1979) assumes that there is no vertical flow in the borehole. Additionally, there is the possibility that different combinations of vertical and horizontal flow result in similar concentration-depth graphs.

An overview was made of the performed tests in order of reliability: 1A, 2A, 1C, 2C, 1B, 2B (Table 5.3). Furthermore, if there is a difference between logged and manual test data, the logged test is assumed to provide more consistent dilution data than the manual measurements.

Table 5.3: Overview of the performed uniform dilution test categories.

	A) No indications for vertical movement	**B) Indications of vertical movement**	**C) Ambiguous**
1) Uniform initial concentration	5.10-1; A5; 7.9-1; 7.9-2; 5.10-3	Z2; 7.15; 6.14	7.12-1; 7.12-2; 5.13-3; 5.13-2
2) Non-uniform initial concentration	8.18; 5.18-1; 7.18; 5.10-2; 5.18-2; 5.18-3; 5.15-2	Z1-1; A1.1;6.11; Z1-2; Z1-3	5.15-1; 5.13-1

5.2.1.2. CALCULATED HORIZONTAL VELOCITIES

Data analysis

A strong linear correlation (R^2 close to 1.0) between the log of tracer concentration against dilution time (Fig. 4.10) is evidence that the dilution rates are largely due to horizontal flow. To minimize influences other than horizontal flow, the appropriate section of the semi-log graph of RWT concentration dilution against time was selected when logged measurements were performed. In addition, outlying concentration data points due to errors and possible effects of the mixing device were deleted from the manual measurements. Data points were not insubstantially removed (maximum of 1 or 2 data points per horizon), and at least four data points were kept to calculate the Darcy velocity. Several semi-log RWT concentration graphs will be discussed.

Even though the tracer is moving in the blind section, the measured RWT concentration data in the screen formed a good linear curve for the test performed on piezometer 6.11 (R^2 between 0.93 and 0.99). The same applied to piezometer 5.13-2, with an R^2 between 0.90 and 0.99. The overnight logged data had an R^2 of 0.97. Another piezometer where vertical currents moved tracer from the blind section was 6.14, the R^2 values were between 0.83 and 0.98, with one horizon having an R^2 of 0.54. The R^2 for 7.15 were all above 0.92. For tests 5.10-1 and 5.10-2, the R^2 for the logged data is lower than the average of the manual data.

Tests with a relatively low R^2 were: 7.18-1 (R^2 between 0.6 - 0.84), 5.18-2 (R^2 between 0.47 - 0.94), 5.18-3 (R^2 of 0.60 - 0.87). These tests are less reliable than other tests and were all on 'deep' piezometers where it was difficult to reach high RWT starting concentrations. Additionally, the tracer in the screened section diluted quickly.

Table 5.4: Overview of linear correlation (R^2) between the log of tracer concentration against dilution time. Average, minimum, and maximum R^2 belong to manual measurements; the logged R^2 was calculated for a logged test performed at a constant depth. Bold dilution tests are test with an average R^2 of 0.85 or higher.

Well and test ID	Average R^2	Minimum R^2	Maximum R^2	Logged R^2
5.10-1	0.96	0.92	0.99	0.88
5.10-2	0.95	0.89	0.98	0.87
5.10-3	0.96	0.93	0.98	
5.13-1	0.88	0.67	0.95	
5.13-2	0.96	0.90	0.99	0.97
5.13-3	0.93	0.73	0.99	
5.15-1	0.84	0.70	0.96	
5.15-2	0.87	0.76	0.98	
5.18-1	0.82	0.50	0.97	
5.18-2	0.65	0.47	0.94	
5.18-3	0.90	0.60	0.99	
6.11	0.96	0.93	0.99	0.98
6.14	0.83	0.54	0.98	
Z1-1	0.87	0.71	0.97	
Z1-2	0.87	0.38	1.00	
Z1-3	0.89	0.60	0.99	
7.9-1	0.99	0.99	1.00	0.98
7.9-2	0.95	0.89	0.99	0.96
7.12-1	0.94	0.86	0.99	0.96
7.12-2	0.97	0.94	1.00	
7.15	0.96	0.91	0.99	
7.18	0.64	0.60	0.84	
Z2	0.84	0.57	1.00	
8.18	0.84	0.78	0.97	
A5	0.83	0.70	0.91	
A1.1	0.79	0.74	0.85	

Darcy velocities

Darcy velocities were calculated using a borehole correction factor of 2 and the inner diameter of the casing. The velocities are divided into piezometers and wells, and high and low R^2, as discussed above (Fig. 5.19a - 5.20b). For all tests, the first concentration log was discarded in the calculation of the Darcy velocity.

For repeated dilution tests on the same piezometer or well, there was a difference between the calculated horizontal velocities. The calculated velocity for individual depth horizons differed between 79 and 87% for tests 7.9-1 and 7.9-2, while the shape of the graphs was the same. The difference in Darcy velocity between the two logged tests performed on this piezometer was 68%. For piezometer 5.10, the difference between the calculated velocities based on manual data of the first and second tests was 45 - 140%. The difference between the velocity calculated based on the logged tests at the same depth was only 18%. For the tests conducted on piezometer 5.18, the difference was more extensive: up to 200%.

For the manual tests on piezometers 5.10 and 7.9, no measurement errors were noted during the experiments. For the dilution test performed on piezometer 5.18, there was a lack of data points due to the low starting tracer concentration in the screened section. Therefore, the decline in tracer concentration was too fast to capture. Tests 5.18-2 and 5.18-3 had a low linear relation between the log concentration and time (between 0.51 and 0.94, section 5.2.1.2, data analysis).

There was a significant difference between repeated tests, even for tests where the fluorometer was left overnight at only one horizon, and possible error sources are minimal. However, the difference between logged tests is lower than the differences between the manual tests.

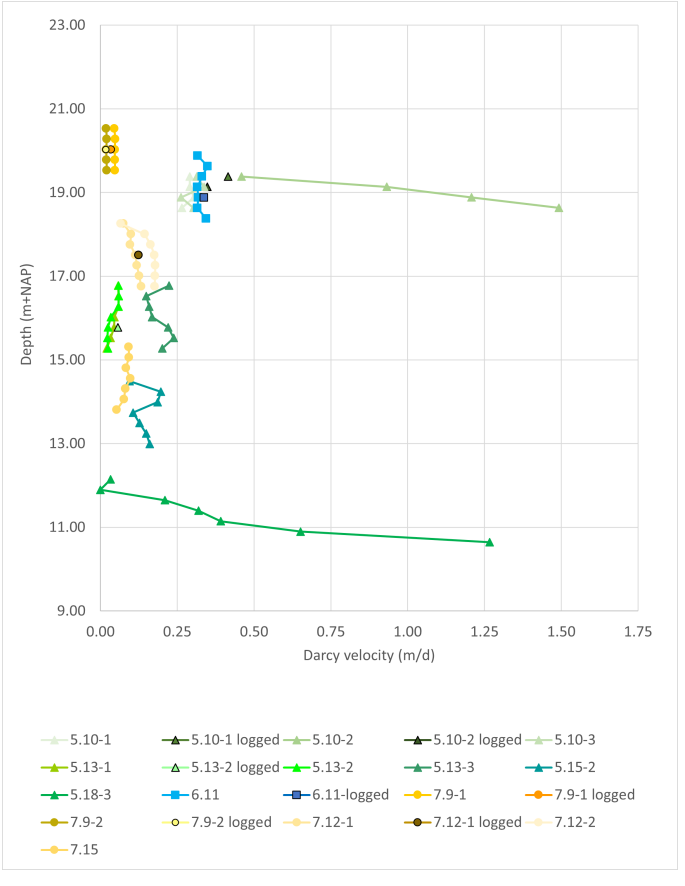

(a) Darcy velocities calculated for the piezometers with linear correlation (R^2) between the log of tracer concentration against dilution time of 0.85 or higher. Borehole correction factor = 2, diameter = inner diameter casing.

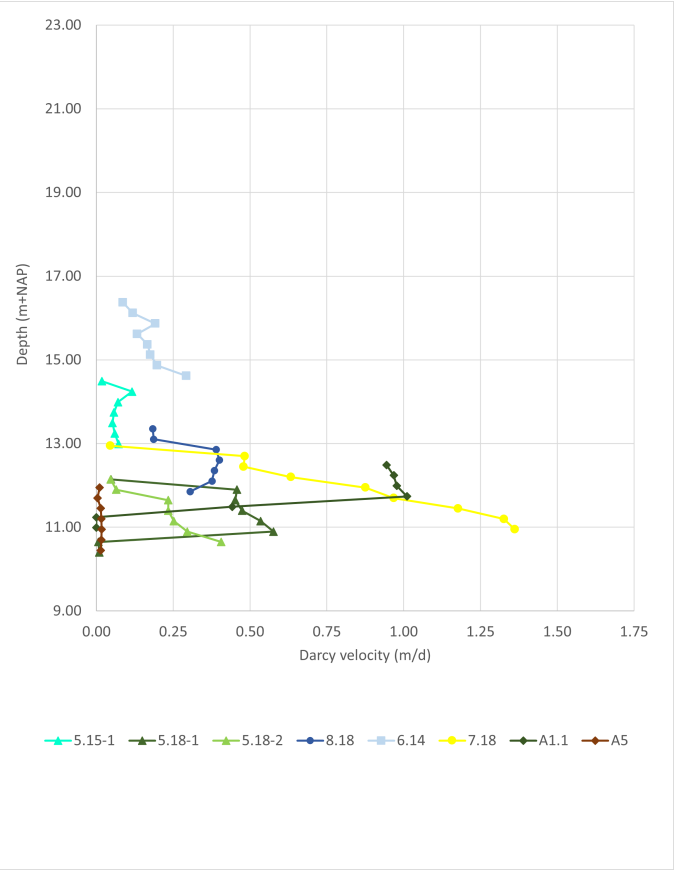

(b) Darcy velocities calculated for the piezometers with linear correlation (R^2) between the log of tracer concentration against dilution time below 0.85. Borehole correction factor = 2, diameter = inner diameter casing.

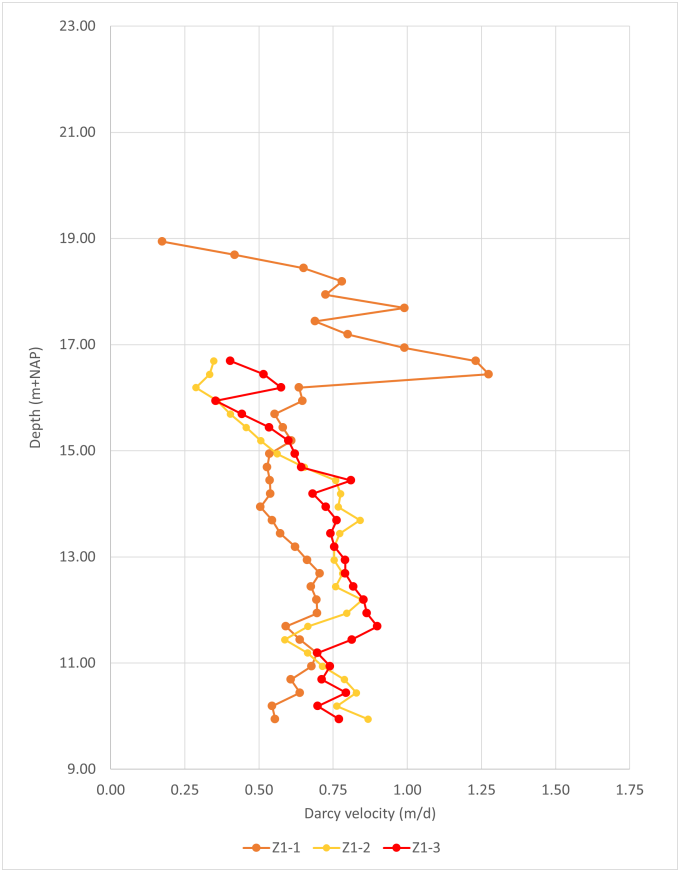

(a) Darcy velocities calculated for the wells with linear correlation (R^2) between the log of tracer concentration against dilution time of 0.85 or higher. Borehole correction factor = 2, diameter = inner diameter casing.

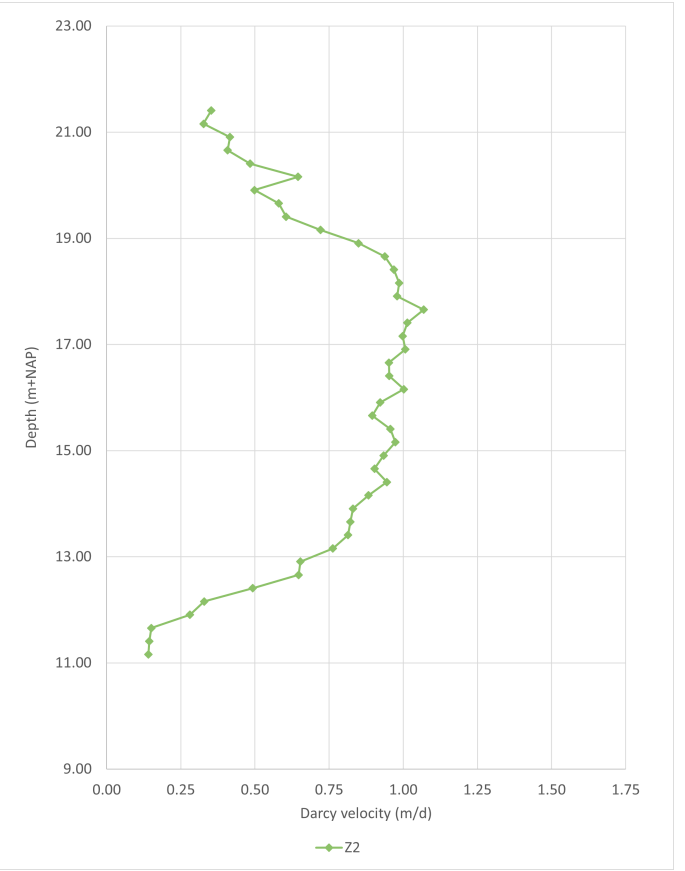

(b) Darcy velocities calculated for the wells with linear correlation (R^2) between the log of tracer concentration against dilution time below 0.85. Borehole correction factor = 2, diameter = inner diameter casing.

5.2.2. POINT DILUTION TESTS

Point dilution tests were performed on wells Z1, Z2, and piezometer 5.13 to estimate the vertical velocity. Figure 5.21 presents the timeline of the point dilution tests, and infiltration of the RIS drains (drains 2 and 3 for 5.13 and Z1, drains 4 and 5 for Z2). Although point dilution tests were performed to assess the vertical velocity, the obtained concentration-time graphs were also used to estimate horizontal flow velocities using the method proposed by Y. Zhang et al. (2020), which applies to wells and piezometers where vertical flow is detected.

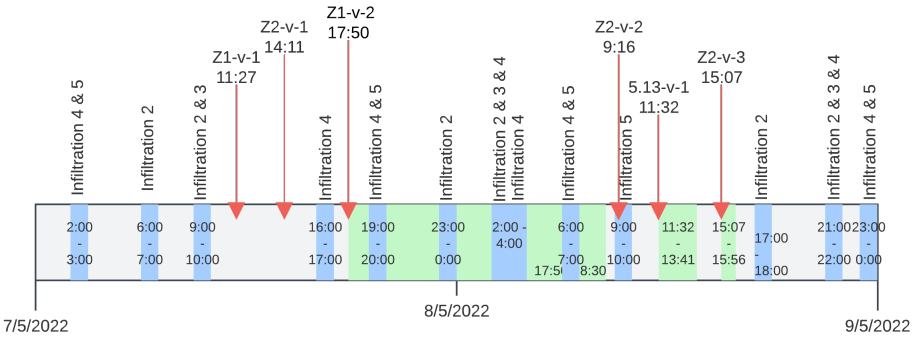

Figure 5.21: Timeline for the point dilution tests.

5.2.2.1. CALCULATED VERTICAL VELOCITIES

Point dilution tests were performed using the chasing- and constant depth technique (Table 5.5). A -1, -2, or -3 was added to the well or piezometer identification to indicate repeated tests. Additionally, the -v indicates that it is a point dilution test. Therefore, Z1-v-1 is the first point dilution test performed on well Z1, and Z1-v-2 the second. Appendix I contains tables that show when the fluorometer detected tracer at a certain depth, after which the fluorometer was moved down. As well as the concentration-time graphs used to calculate the horizontal velocity with the method by Y. Zhang et al. (2020).

Table 5.5: Overview of the performed point dilution tests and resulting vertical flow velocities.

Well and test ID	v_v catching technique (manual) (m/d)	v_v first arrival (constant depth) (m/d)
Z1-v-1	172.3	-
Z1-v-2	-	225.0
Z2-v-1	100.1	-
Z2-v-2	118.0	-
Z2-v-3		150.0
5.13-v-1	-	77.7

Well Z1

For test Z1-v-1, the vertical velocity calculated from the catching technique measurements was 172.3 m/d on average. Two complete concentration-depth profiles were taken after the fluorometer was moved down to the bottom of the well and the tracer had been detected at the base of the well (Fig. 5.22). The graphs indicate that the RWT concentration at the base of the well increased while the concentration at the top decreased.

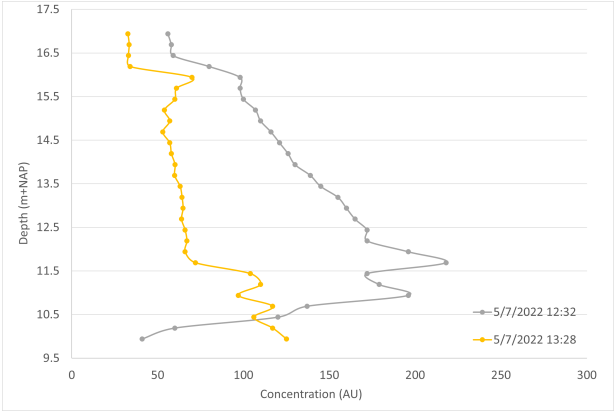

Figure 5.22: Change of (Rhodamine water tracer) concentration over time for point dilution test Z1-v-1.

For the overnight test, Z1-v-2, all of the injected tracer had moved from the well within 15 hours. Figure 5.23 shows the breakthrough curve of RWT at the depth of the fluorometer (5.94 m below the leachate table). After 38 minutes, the tracer slug first reached the fluorometer. The vertical velocity based on the first arrival of the tracer is estimated at 225 m/d. The peak of tracer concentration was reached 74 minutes after

injection, and RWT concentrations were back to background concentration values 358 minutes after injection.

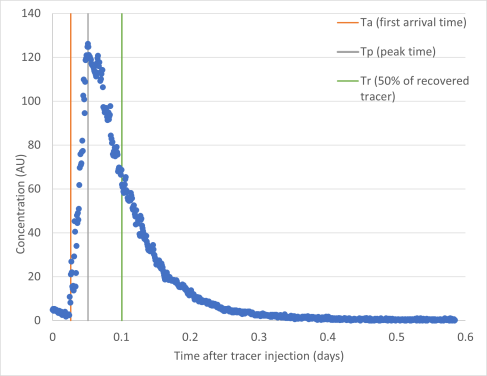

Figure 5.23: Breakthrough curve of RWT (Rhodamine water tracer) concentration for point dilution test Z1-v-2, data normalized by the background RWT concentration.

The calculated vertical velocity from the catching technique was considerably lower than the velocity calculated from the logged breakthrough curve (around 165 m/d versus 225 m/d, respectively). RIS drains 2 and 3 were infiltrated roughly 5 to 2 hours before test Z1-v-1, which was performed using the catching technique (Fig. 5.21). Infiltration does not appear to increase the vertical velocity.

Well Z2

On average, the vertical velocity calculated for point dilution test Z2-v-1 was 100.1 m/d. The RWT concentration-time graphs showed the same behavior as described for the point dilution test performed on well Z1 (Fig. I.1).

For test Z2-v-2, the average vertical velocity using the catching technique was 118.0 m/d. The velocity is about 20 m/d higher than what was calculated for the first point dilution test on Z2. The infiltration timeline indicated that RIS drain 5 was infiltrated between 09:00 and 10:00 at the start of test Z2-v-2 (Fig. 5.21).

For test Z2-v-3, a few moments after the tracer injection, the fluorometer was pulled up to 0.20 m below the leachate table to estimate the starting concentration, which was around 1600 AU. After 49 minutes, the maximum RWT concentration was 800 AU (Fig. 5.24).

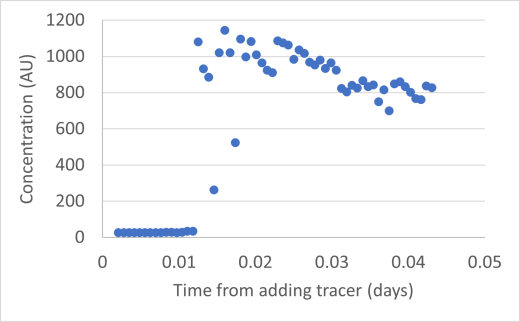

Figure 5.24: Partial breakthrough curve of RWT (Rhodamine water tracer) concentration for point dilution test Z2-v-3. Fluorometer was attached about 2.0 m below the leachate table.

The test had to be terminated 62 minutes after the start of the test because of time constraints, which is why there is not a full breakthrough curve (Fig. 5.24). The first arrival of the tracer was 15 minutes after injection, resulting in an estimated vertical velocity of 150 m/d for the upper 1.50 meters. Compared to the manual measurements using the catching technique at the top of the well during tests Z2-v-1 and Z2-v-2, this is 15-25 m/d higher.

Piezometer 5.13

For test 5.13-v-1, the first arrival of the tracer resulted in an estimated velocity of 77.7 m/d. The (partial) breakthrough curve indicated that the peak concentration of the tracer was not reached after the logging time (168 minutes = 14:20) at 1050 AU (Fig. 5.25). However, a concentration-depth log taken at 14:42 indicated that the RWT concentration had declined to 900 AU at the base. The graph shows that the section of leachate in the blind casing (about 0.75 m) of the piezometer remained at a high concentration of tracer with little dilution (Fig. 5.26). The decline in tracer concentration in the slotted section indicates no tracer accumulated at the base of the well.

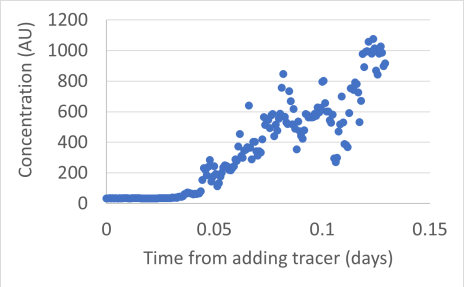

Figure 5.25: Partial breakthrough curve of RWT (Rhodamine water tracer) concentration for point dilution test 5.13-v-1. The fluorometer was attached at 12.75 m-GL, about 0.27 m above the base.

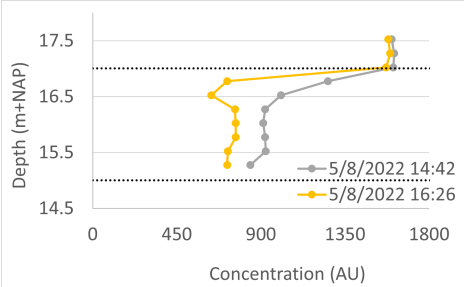

Figure 5.26: Decline in RWT (Rhodamine water tracer) concentration over time for point dilution test 5.13-v-1. Concentration logs were taken after the attempt to log a breakthrough curve.

5

5.2.2.2. CALCULATED HORIZONTAL VELOCITIES

The horizontal flow velocities calculated with the method by Y. Zhang et al. (2020) using the concentration-depth profiles obtained during the point dilution range between 0.047 m/d (piezometer 5.13) and 0.68 m/d (well Z1) (Table 5.6). For piezometer 5.13 and well Z1, these velocities are consistent with the average horizontal velocities calculated in section 5.2.1.2. For well Z2, there is an average difference of about 0.42 m/d.

Table 5.6: Average horizontal Darcy velocities calculated for the point dilution tests, using the method by Y. Zhang et al. (2020).

Well and test ID	Z1-v-1	Z2-v-1	Z2-v-2	5.13-v-1
v_h **(m/d)**	0.68	0.28	0.30	0.047

To check the validity of the method by Y. Zhang et al. (2020), concentration-time logs from the uniform SBDTs performed on piezometer 5.10 and wells Z1 and Z2 were analyzed using this methodology as well. The first RWT concentration log was not taken into account, and when possible, the same data points were used for the calculations performed with Freeze & Cherry (1979) method. For the Freeze & Cherry (1979) method, the calculated Darcy velocities were averaged over the entire saturated depth. All calculations used a borehole correction factor of 2.

Table 5.7 indicates that compared to the Freeze & Cherry (1979) calculated Darcy velocities, applying the method by Y. Zhang et al. (2020) gave either slightly higher or lower velocities with a maximum difference of 0.20 m/d. This difference is not more

significant than the difference between the results of the repeated dilution tests on piezometer 5.10 and well Z1. For well Z2, there is very little difference between the average velocities calculated using both methods (0.06 m/d). It is most likely that the velocity calculations for well Z2 using the concentration graphs of the point dilution tests (Table 5.6) are either lower due to an error in the manual concentration measurements or due to changing hydraulics over time. Overall, the methods compare favorably.

Table 5.7: Comparison of Darcy velocities calculated with two methods for the uniform dilution test performed on wells Z1 and Z2, and piezometer 5.10.

v_h (m/d)	Z1-1	Z1-2	Z1-3	Z2	5.10-1	5.10-2	5.10-3
Zhang et al.	0.47	0.66	0.89	0.78	0.24	0.96	0.46
Freeze & Cherry	0.66	0.66	0.69	0.72	0.29	1.02	0.30

5.2.3. SUMMARY

Horizontal flow was encountered at all tested piezometers and wells. Several piezometers showed considerably lower flow (P7.9, P5.13, and well A5). Overall velocities were estimated to be highest at the base of the measured section of the landfill. However, the tracer concentration data of these deep piezometers show more noise in the measurements (lower R^2). The concentration logs of the Z wells showed clear signs of vertical flow. In several piezometers, the tracer concentration in the blind screen decreased, reducing the reliability of the calculated velocities.

The calculated vertical velocities are much higher (ranging from 77 - 225 m/d) compared to the calculated horizontal Darcy velocities (generally < 1.0 m/d) and the estimated daily recharge ($8.1*10^{-4}$ m/d). The catching technique is susceptible to manual errors. Therefore, tests performed at a constant depth are recommended. The constant depth technique, however, is more time-consuming. Horizontal velocities calculated using the concentration-time diagrams of the point dilution tests using the method by Y. Zhang et al. (2020) comply with the velocities calculated using the method by Freeze & Cherry (1979) for the uniform dilution tests.

6
DISCUSSION

This chapter first discusses the leachate levels and leachate flow throughout the landfill and how they are connected. Furthermore, an overview of possible error sources in the performed measurements is presented. Finally, a conceptual flow model for compartment 3 of De Kragge is presented based on the findings of this research, and the model is compared to other flow models found in literature.

6.1. LEACHATE LEVELS THROUGHOUT THE LANDFILL

The different leachate levels measured throughout the landfill did not appear to be related to each other. It is again important to note that three different leachate levels were analyzed: leachate levels across the infiltration drains, throughout the waste body, and in the basal drainage system.

6.1.1. UNEVEN INFILTRATION OF LEACHATE

The leachate levels measured across the infiltration drains at the top of the landfill were non-uniform, and the leachate levels often increased after the main infiltration event. The extra infiltrating leachate could be excess leachate from the infiltration event, entering the drain with a delay, or the drain could overflow due to the lower infiltration rates, causing spilling. As this phenomenon was most prominent in points 2B.2 and 2B.4 and not in point 2B.3, located in between the two, it is not easy to point out the cause.

The spatial and temporal variation in leachate levels across the infiltration drains makes them difficult to interpret. There was not one point at which the recession consistently went the slowest or fastest. The same applies to the leachate level; there was not one point that consistently had the highest leachate level (Fig. F.6 and F.7). The possible difference in the height of the infiltration drain (the pipe) in relation to the

depth of the CTD-Divers® does not explain this variation in leachate level either (Fig. F.4 and F.5). The infiltration pipe is not entirely horizontal, there is a maximum difference of about 15 cm. Overall, infiltration appears quicker across drain 3A than drain 2B, and leachate levels are more stable across drain 3A.

The uneven infiltration across the drains can result from preferential flow paths along the drain due to differences in permeability due to heterogeneous waste material. Furthermore, a difference in infiltration velocity might be related to the volume of leachate infiltrated and the time between infiltration moments. The direction, speed, and volume of leachate infiltration can be affected by the initial moisture condition of the waste (Bezerra et al., 2022). Therefore, if the leachate level has not receded to its steady-state level, subsequent infiltration is affected, and infiltration across the drain is uneven. Moreover, the infiltration capacity decreases due to clogging. Clogging of the geotextile around the infiltration drain is a known problem at De Kragge (Kanen & Kedzia-Kowalski, 2021). Within the limitations of this research, it was not possible to identify the cause of the spatial variation across the drains.

As interpreted from the leachate level times series of the piezometers located throughout the lower sections of the waste body (so below the infiltration drains), the RIS infiltration does not have a large area of influence outside of the RIS drain itself. The infiltration events were not visible in the observed leachate levels, and there was a 3 to 12.5 m difference in the height of the measured leachate levels in the piezometers placed below the RIS drains and the piezometers in the waste body. Additionally, leachate levels differ up to 3 m throughout the piezometers placed in the waste body. As shown by the research of de Jong (2021) on the pilot landfill in Braambergen, there were significant differences in leachate head (up to 6 m) over short distances, implying that there is poor hydraulic connectivity.

The leachate levels measured in the piezometers throughout the waste body were subject to changes in atmospheric pressure (also called barometric effects), rather than infiltration by precipitation or the RIS system. Barometric effects are well researched in groundwater hydrology (e.g., Price 2009; Spane 1999) and in landfills regarding methane gas emissions (e.g., Kissas et al. 2022; Xu et al. 2014). Gas fills the open pores in the waste and when the atmospheric pressure goes up, the gas bubbles in the pores get compressed, making more space for leachate. Therefore, the leachate level decreases when the air pressure increases, and vice versa. Because the gravel around the RIS

drains is not compressible, and the leachate infiltrates into unsaturated waste, the leachate levels across the RIS drains show little response to atmospheric pressure. Trying to correct the data for the barometric effect lies beyond the scope of this research.

6.1.2. PERCHED LEACHATE ZONES

Trapani et al. (2015) and Di Bella et al. (2012) mention that a low hydraulic conductivity of the middle and lower section of waste body can prevent leachate from percolating downward as fast as it infiltrates from the top layer. This phenomenon causes a (temporary) perched leachate zone, with a saturated horizontal area confined in an otherwise unsaturated area that cannot infiltrate downwards.

The gravel around the infiltration drains at De Kragge has a higher hydraulic conductivity than the waste material. The volume of leachate and water infiltrated into the waste body may cause a perched leachate zone resulting in different measured leachate levels across RIS drains and throughout the waste body. This also explains why the infiltration events were not visible in the measured leachate levels in the waste body, as infiltration is delayed and less effective. In addition, a perched zone enhances lateral leachate migration and outflow from the edges of the landfill (Powrie & Beaven, 1999). At De Kragge, lateral migration from compartment 3 is possible to compartments 2 and 4. Both compartments show a higher outflow of leachate than is infiltrated by precipitation.

The measured leachate outflow from compartment 2 has to be the result of lateral flow coming from compartment 3, as compartment 2 is completely sealed on top, and the compartment does not have infiltration drains. Figure 5.9 showed that the leachate levels in the basal drains reached above the 2-meter-high dikes on several occasions. In addition, there has been a considerable outflow from compartment 4 that does not match up with the possible infiltration from the precipitation surplus. The cumulative outflow from compartment 4 increased even when the measured leachate level in the basal drainage system was below 2.0 meters. Therefore, the compartments appear to be connected hydraulically, and there has to be additional lateral flow from compartment 3 to compartment 4 in the landfill section above the drainage system.

The leachate levels in the basal collection drains were lower than those in the piezometers installed in throughout waste body. This difference indicates that there is

an additional unsaturated zone of waste above the drainage system. A large-scale tracer test conducted by researchers from the University of Southampton showed that the Fluorescein tracer pumped into an infiltration pitch on top of the landfill was never collected in the basal drain access points situated on the north end of the landfill (Fig. 2.5). There appears to be little connectivity between the different saturated zones of the landfill.

Zhan et al. (2015) describe three leachate zones, one of which is a bottom leachate mound within the leachate drainage system. They mention that if the drainage system functions properly, the bottom leachate mound is separated from the primary leachate mound. The primary leachate mound is the section of waste below the general leachate level. The leachate mound in the basal drainage system appears to be separated from the leachate throughout the upper waste body at De Kragge, with the low leachate levels measured in the basal drainage system and the higher levels throughout the waste body.

6.2. LEACHATE FLOW THROUGHOUT THE LANDFILL

The calculation of the Darcy flow velocity depends on the tracer concentration measurements performed with the fluorometer. The fluorometer measures the concentration in AU instead of mg/L or ppb and therefore requires calibration when the concentration is above the linear range. For RWT, the fluorometer used in this research is linear up to 1000 AU, according to the product manual. Calibration was performed using leachate of 6 piezometer and wells. However, the calibration data of the fluorometer were not used, as there were several factors that were not controlled during the calibration process; these include temperature, background fluorescence, and turbidity. Additionally, it was found that the polynomial function gives a good calibration across the full range, but the formula also tries to fit a curve on the linear section, which should be a straight line. Therefore, the polynomial formula is suitable for higher RWT readings (depending on the leachate, above 800 - 1000 AU), but the formula should not be used for lower values that fall within the linear range. For converting AU readings to mg/L or pub, it is thus recommended to use both the linear formula for the lower concentration values and then the polynomial formula only for the higher concentration values.

The background fluorescence was different for each well and piezometer (range between 10 and 75 AU), as well as the temperature (range between 18.5 and 25.0 °C, but

also depends on the season). Calibration should be performed for each well and piezometer separately and at the temperature of the in-situ leachate to overcome the differences in background fluorescence and temperature. Additionally, when injecting the tracer and leachate mixture for a dilution test, these should be at the temperature of the leachate within the well or piezometer. The effect of turbidity is difficult to correct, as this is caused by suspended and dissolved particles within the leachate, but calibrating each piezometer or well separately will help.

If the concentration measurements used for calculating the Darcy velocity are within the linear range, the AU output of the fluorometer equals the concentration in mg/L and ppb, and there is no need for correction. Based on the performed calibrations, it was tried to use only values below 900 AU, but there may still be an error margin in the calculated Darcy velocities, as the AU output might not exactly match the concentration in mg/L or ppb anyway. It is assumed that this error falls within the possible error due to the borehole correction factor (section 6.2.1.2).

6.2.1. HORIZONTAL LEACHATE FLOW

In this section, the influence of the mixing volume, borehole correction factor, and RIS system will be discussed, as well as preferential horizontal flow. Horizontal flow of water and leachate is induced by a pressure gradient or a density gradient. These can include a difference hydraulic head or differences in temperature and concentration, respectively. The possible effect of pressure and density gradients on (vertical) flow will be discussed in detail in subsection 6.2.2, but also apply to the horizontal flow.

6.2.1.1. IMPACT OF THE MIXING VOLUME OF THE SCREENED SECTION

For the piezometers where the leachate table did not reach above the screened section (e.g., P5.10 and well A5), an increase in the diameter used to calculate the required stock concentration resulted in concentrations higher than the target concentration (>1000 ppb). This indicates that the diameter was overestimated as the amount of stock solution needed was calculated using the volume of leachate present in each piezometer or well. For the deeper piezometers where the leachate table reached the blind section (e.g., P8.18), there was a clear distinction in RWT concentration between the screened and blind section. This distinction can result from increased mixing volume due to the (absence of) filter pack around the screen, an overall high horizontal flow velocity, or an error in tracer injection.

For piezometer 8.18, the concentration of RWT in the blind section of the piezometer

casing went up to 1400 AU, whereas the screened section did not reach above 150 AU for the first measurement. It is difficult to distinguish which of the causes mentioned above resulted in the low tracer concentrations in the screen. The RWT concentration in the blind section of piezometer 8.18 did not decline over time, even after a day, indicating limited vertical movement and diffusion of the leachate and tracer. In contrast, the test on piezometer 7.18 had an initial RWT concentration in the screened section of 1200 AU. The second concentration log, after 30 minutes, showed concentrations close to background values, indicating either high horizontal flow velocities or an increased mixing volume.

An improper installation of the wells, piezometers, and filter pack might explain the different starting concentrations and hypothesized increased mixing volume. Under perfect conditions, the exact volume of filter material should be calculated and poured in slowly to allow the filter sand to reach the bottom of the borehole. The casing should be shaken occasionally to get the filter sand down the borehole. Instead, the drilling personnel poured in the filter sand and gravel, and the volume was eyeballed. Due to the improper installation, it is possible that the filter material did not get down to the bottom of the borehole, resulting in a piezometer or well where only a section (or no section at all) of the screen is surrounded by filter material. Installation can differ between the piezometers and wells. Four scenarios are explained and analyzed (Fig. 6.1).

For scenario 1, the well was installed as designed (Fig. 6.1). In this scenario, the volume of tracer stock solution required is either based on the volume of leachate in the casing or on the leachate in the casing combined with the pore volume of the filter pack. Scenario 2 pictures an open borehole around the casing with no installed filter or bentonite seal. The volume of the open borehole is filled with leachate. The volume of tracer stock solution required is either based on the volume of leachate inside the casing or the volume of the borehole. In scenario 3, filter sand was installed unevenly, and the exact volume is unknown. The required volume of tracer stock solution is anywhere between the volume of leachate in the casing and the volume of the borehole. Scenario 4 illustrates a casing without any filter sand and bentonite installed, and the borehole collapsed against the casing. The maximum diameter for the mixing volume is the inner diameter of the casing. Therefore, the required tracer stock solution volume is based on the volume in the casing.

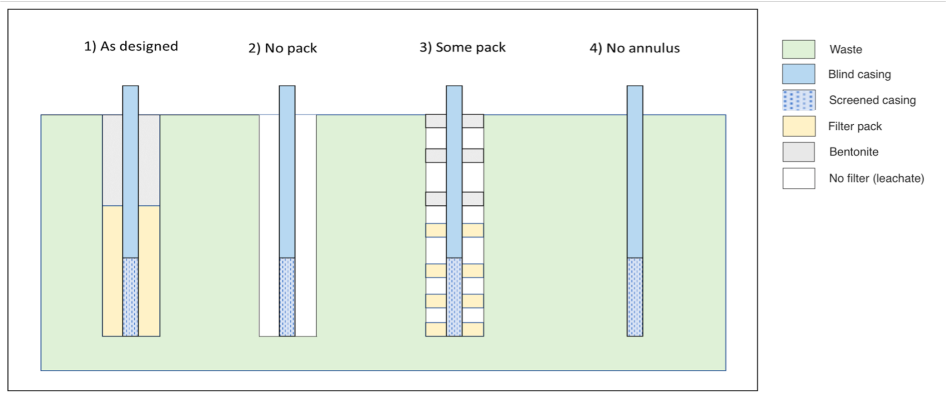

Figure 6.1: Four possible scenarios for the construction of the new wells and piezometers. Figure adapted from Rees-White (2022, personal communication).

Table J.1 shows the calculation process behind the four scenarios, in this case for dilution test 5.10-1. The different maximum and minimum tracer masses needed were compared to the used stock masses by changing the target concentration to the average initial concentration. Scenario 4, a piezometer without any annulus, appears unlikely, as well as the minimum tracer masses for all four scenarios (Table J.1). For dilution test 5.10-3, 7.5 ml of stock solution led to an average initial concentration of 1191 AU (1191 ppb); this concentration is within the minimum and maximum tracer masses for scenarios 1, 2, or 3. Analysis of the other tests on piezometers 5.10, 5.18, and well Z1 support scenario 2 or 3. Tests conducted on piezometer 5.18 showed high initial RWT concentrations at the base of the screen, lower concentrations in the middle, and higher concentrations at the top. These differences in concentration imply scenario 3, where the filter pack is non-uniformly distributed over the screened section.

Considering the installation process, it is doubtful that the piezometers and wells were installed entirely correctly (scenario 1). It is impossible to validate whether any filter material reached the screened section. Because of the depth, getting the filter material down the borehole was more challenging for deep piezometers (e.g., 15 - 18 meters: P5.15, P5.18). Differences in the installation of the filter pack can explain the differences between the sharp concentration discrepancy for the 18-meter deep piezometers in contrast to the uniform tracer concentrations for the 9-10 meter deep piezometers.

To back-calculate the appropriate diameter of the screened casing, the equation for the

volume of stock solution required to reach the target concentration was used:

$$W = \pi * \left(\frac{r}{2}\right)^2 * h * x \tag{6.1}$$

Here, W is the volume of stock added [L^3], r is the diameter and h is the leachate head, both [L], and x is the average initial concentration over the saturated depth [AU].

Back-calculation of the diameter depends on the time between tracer injection and the first concentration log. The more time between injection and the first concentration log, the lower the concentration. First logs were not performed at the same time after injection, as indicated in Table 6.1. The average initial output was used for these analyses, assuming that the concentration was uniformly distributed over the screened section. For well Z1 and piezometer 5.18, this was not the case.

Table 6.1: The number of minutes between injection of the tracer and the first concentration log.

Well and test ID	5.10-1	5.10-2	5.10-3	5.18-1	5.18-2	5.18-3	Z1-1	Z1-2	Z1-3
Minutes	3	10	3	9	5	4	7	7	6

For piezometer 5.18, the volume of stock solution was calculated for the screened section (2 m), and the initial concentration was averaged only over the screened part. The average back-calculated diameter for well Z1 is 0.175 m (Table 6.2). The average back-calculated diameter for piezometer 5.10 is 0.0821 m, and 0.0886 m for piezometer 5.18.

There is a significant difference between the back-calculated diameter of individual wells. The tests were not repeated enough to accurately calculate the average diameter and corresponding standard deviation. However, these data suggest that the actual mixing volume is bigger than the piezometers and well casing diameters and that there is a difference between individual piezometers and wells.

A bigger diameter results in an increased volume; thus, a higher flow velocity is needed to remove the tracer from the well. Relating this to the borehole correction factor: decreasing the correction factor increases the calculated Darcy velocity (section 6.2.1.2). The inner diameter of the casing is the minimum diameter and, therefore, the most conservative option regarding Darcy flow velocities. Horizontal flow velocities were calculated using an increased diameter of 0.0821 m (5.10), 0.0886 m (5.18), 0.175

m (Z1), and 0.129 m (Z2).

Table 6.2: Back-calculated casing diameter of the screened section.

Well ID	Stock solution (ml)	Average initial concentration (AU)	Back-calculated diameter (m)
Z1-1	76	283	0.191
Z1-2	115	819	0.222
Z1-3	155	906	0.178
Z2	185	1360	0.129
5.10-1	8	1309	0.0783
5.10-2	7.5	1173	0.0838
5.10-3	7.5	1191	0.0842
5.18-1	2.74	254	0.0829
5.18-2	5.56	464	0.0873
5.18-3	10	696	0.0956

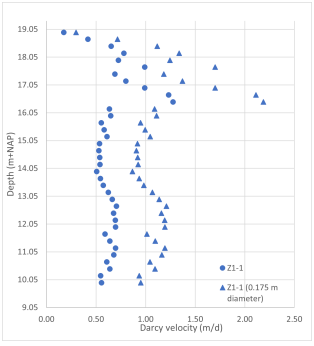

Figure 6.2: Darcy velocity calculated for test Z1-1, with a diameter of 0.108 m and increased diameter of 0.175 m.

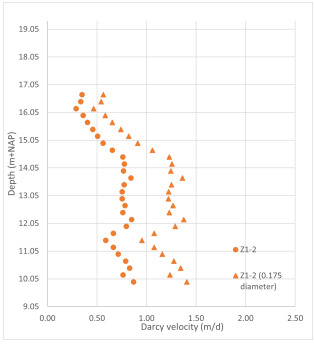

Figure 6.3: Darcy velocity calculated for test Z1-2, with a diameter of 0.108 m and increased diameter of 0.175 m.

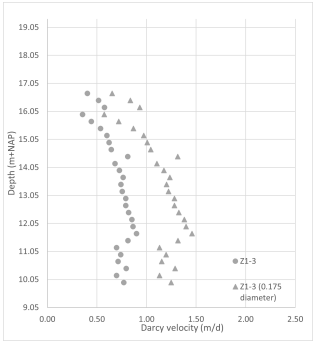

Figure 6.4: Darcy velocity calculated for test Z1-3, with a diameter of 0.108 m and increased diameter of 0.175 m.

As shown in Figures 6.2, 6.3, and 6.4 a proportional increase in diameter over the saturated depth does not increase the Darcy velocity proportionally: an increase in diameter has a more significant effect on already higher Darcy velocities. There is a linear relationship between diameter and the Darcy velocity, Eq. (4.10). Additionally, Darcy velocities were calculated for piezometers 5.10 and 5.18 using the bigger diameters (Appendix J).

6.2.1.2. IMPACT OF THE BOREHOLE CORRECTION FACTOR

In previous Darcy velocity calculations, a general borehole correction factor (α) of 2 was used. The correction factor can be calculated with Eq. (4.11) if several hydraulic parameters are known. As indicated in section 6.2.1.1, there is a lack of knowledge about the state of the well design and aquifer parameters. The mixing volume of the screened section exceeded the internal diameter of the casings. This hypothesized increased mixing volume is related to the borehole correction factor. The correction factor accounts for the convergence of streamlines towards a well or piezometer. The hydraulic conductivity of De Kragge landfill is unknown and can vary spatially. The equation to calculate the correction factor (Eq. (4.11)), assumes that the filter is installed evenly around the screened filter. As section 6.2.1.1 discussed, this is likely not the case at De Kragge.

The hydraulic conductivities were estimated based on literature findings, and the radii were based on the casing and drilling rig diameter.

- As an estimation of the hydraulic conductivity of the waste (K_3), values found by de Jong (2021) were used. de Jong (2021) performed pumping tests on the pilot landfill in Wieringermeer. Hydraulic conductivities between 10^{-3} and 10^{-9} m/s are reported in literature for landfills (e.g., Powrie & Beaven 1999; Beaven 2000; Staub et al. 2009; Reddy et al. 2009). Values calculated by de Jong (2021) fall within this range.
- The hydraulic conductivity of the filter material (K_2, sand for the piezometers and gravel for the Z wells) was estimated using the grain size (1.0-1.6 mm for the sand, unknown for the gravel).
- The hydraulic conductivity of the well screen (K_1), was estimated using the size of the slots. The slot size of the piezometers was 0.3 mm, and the slot size of the Z wells was 2.0 mm. Englert (2003) estimated the values for a screened casing with a slot size of 0.5 mm to be between 1.00×10^{-4} and 3.10×10^{-3} m/s. Verreydt et al. (2015) mention that the hydraulic conductivity for wells with a slot size of 0.3 mm is 0.09 m/s and 0.30 m/s for a slot size of 1.0 m/s. Therefore, a different K_1 was calculated for both.
- The radius of the borehole (r_3) is the radius of the drilling rig and r_1 and r_2 are the inner and outer radius of the casing.

Table 6.3: Input parameters for borehole correction factor equation. The value of the hydraulic conductivity of the well screen (K_1) without parenthesis is estimated using Englert (2003), value in parenthesis and with an * is estimated using Verreydt et al. (2015). K_2 is the hydraulic conductivity of the filter material, K_3 the hydraulic conductivity of the waste, r_1 the inner radius of the casing, r_2 the outer radius of the casing, and r_3 the radius of the borehole.

Parameter	Value (piezometer)	Value (Z well)
K_1 (-)	1.00×10^{-4} (0.09*)	3.10×10^{-3} (0.685*)
K_2 (-)	1.00×10^{-4}	1.00×10^{-3}
K_3 (-)	1.00×10^{-7} - 6.00×10^{-4}	1.00×10^{-7} - 6.00×10^{-4}
r_1 (m)	0.024	0.054
r_2 (m)	0.025	0.055
r_3 (m)	0.075	0.125

Calculating the borehole correction factor with the values presented in Table 6.3 resulted in a range between 0.60 - 3.68 for the piezometers and 3.12 - 3.39 for the Z wells (Table 6.4).

Table 6.4: Calculated values for the borehole correction factor (α) for the piezometers and wells using Eq. (4.11). Value without parentheses is α calculated using K_1 =1.00×10^{-4} and 3.10×10^{-3}, value in parentheses is α calculated using K_1 = 0.09 or 0.685 for the hydraulic conductivity of the well screen; following table 6.3.

Hydraulic conductivity (K_3)	α Piezometers	α Wells
1.00×10^{-7}	3.56 (3.68*)	3.26 (3.39*)
6.00×10^{-4}	0.60 (0.63*)	3.12 (3.25*)

Drost et al. (1968) theoretically derived the correction factor, calculating values between 0.5 and 4.0. Englert (2003) calculated a mean value for the correction factor of 1.95 in an aquifer dominated by gravelly and sandy floodplain deposits, using Eq. (4.11) and estimations of the hydraulic parameters. Lloyd et al. (1979) used a value of 1.0, commenting that this is valid for boreholes with an outer diameter ≤ 100 mm. Rollinson (2020) performed forced gradient SBDTs on two wells in a UK landfill to estimate the borehole correction factor. Three tests with different flow rates were performed, resulting in an average of 0.9 and 2.7 per well (averaging 1.8). The estimated correction values of this research (0.60 - 3.68) are within the domain set by Drost et al. (1968) and the values mentioned above.

Based on the range of borehole correction values, a sensitivity analysis was performed using values from 0.5 to 4.0, with increments of 0.5. Here, a correction factor of 1 is

equal to the filtration velocity. As illustrated in Table 6.5, the filtration velocity (α = 1) equals twice the Darcy velocity calculated with a correction factor of 2. Figures 6.5 and 6.6 visualize that the equation is more sensitive to a lower correction factor. The lower the value of the borehole correction factor, the lower the hydraulic connectivity is assumed to be.

Table 6.5: Borehole correction parameter (α) sensitivity analysis. The effect of increasing or decreasing the borehole correction parameter compared to a value of 2 is presented.

α (-)	0.5	1.0	1.5	2.0	2.5	3.0	3.5	4.0
% of change in Darcy velocity compared to α = 2	300	100	33	0	-20	-33	-43	-50

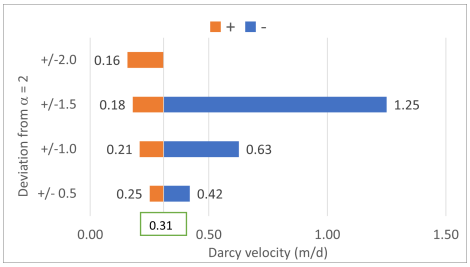

Figure 6.5: Influence of the borehole correction factor on the Darcy velocity, test 5.10-1 at 19.34 m+NAP.

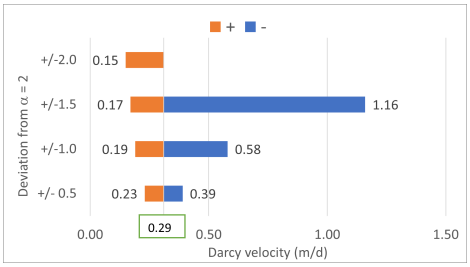

Figure 6.6: Influence of the borehole correction factor on the Darcy velocity, test 5.10-3 at 19.34 m+NAP.

The Darcy velocity was calculated using the range of calculated values for the borehole correction factor (Fig. 6.7 - 6.14). Based on the composed overview of SBDTs and assessment of the linear correlation (R^2) between the log of tracer concentration against dilution time (Table. 5.4), several tests with an R^2 of 0.85 or higher are pictured. Figures for piezometers 6.11, 7.15, and well Z1, as well as the remaining piezometers and wells with an R^2 below 0.85, can be found in Appendix K. All ranges of possible velocities are presented in Table 6.6. In the figures, the blue dot is the horizontal Darcy velocity calculated using a borehole correction factor of 2, and the error bars indicate the range of velocities. An orange dot is the velocity calculated using measurements of a logged test at a specific horizon.

Minimum average velocities for the deepest piezometers (5.18, 7.18, and 8.18), corrected for a lower borehole correction factor, are all over 0.10 m/d (Table. 6.6). Even

with a possible increase in borehole correction factor (compared to $\alpha = 2$), velocities at the base are likely the highest. Maximum average velocities reach above 5 m/d (test 5.18-3). Velocities in piezometers 5.13 and 7.9, and well A5 remain the lowest and can be as low as 0.010 m/d.

As mentioned in this section, the Darcy velocity is more sensitive to a decrease in the borehole correction factor, and changing the correction factor has a more significant effect on a higher initial velocity. Therefore, velocities calculated for piezometers 7.9 and 5.13, and well A5 show little change (around 0.05 m/d), while the average velocity for piezometer 5.18 (test -3) changed with 4.22 m/d on average (Table. 6.6).

Table 6.6: Average horizontal Darcy velocities per test, including average Darcy velocity using a borehole correction factor (α) of 2, and the high and low α according to Table 6.4. A * indicates a logged test, and bold tests are tests where the linear correlation (R^2) between the log of tracer concentration against dilution time was 0.85 or higher.

Piezometer / well ID	**Measurements between (m+NAP)**		**Average velocity α_2 (m/d)**	**Average velocity α_{low} (m/d)**	**Average velocity α_{high} (m/d)**
5.10-1	18.44	20.44	0.29	0.96	0.16
5.10-2	18.44	20.44	1.02	3.41	0.56
5.10-2*		19.14	0.35	1.12	0.19
5.10-3	18.44	20.44	0.30	1.01	0.17
5.13-1	15.01	17.01	0.05	0.15	0.02
5.13-2	15.01	17.01	0.04	0.14	0.02
5.13-2*		15.78	0.06	0.19	0.03
5.13-3	15.01	17.01	0.19	0.65	0.11
5.15-1	12.74	14.74	0.06	0.21	0.03
5.15-2	12.74	14.74	0.15	0.49	0.08
5.18-1	10.28	12.28	0.32	1.07	0.17
5.18-2	10.28	12.28	0.22	0.73	0.12
5.18-3	10.28	12.28	0.57	1.32	0.26
Z1-1	9.71	19.05	0.66		0.39
Z1-2	9.71	16.69	0.66		0.39
Z1-3	9.71	16.69	0.69		0.41
6.11	18.30	20.30	0.33	1.09	0.18
6.11*		18.88	0.34	1.13	0.18
6.14	14.40	16.40	0.17	0.57	0.09
7.9-1	19.32	21.32	0.05	0.07	0.03
7.9-1*		20.03	0.04	0.12	0.02
7.9-2	19.32	21.32	0.02	0.07	0.01
7.9-2*		20.03	0.02	0.06	0.01
7.12-1	16.50	18.50	0.12	0.38	0.06
7.12-1*		17.51	0.12	0.41	0.07
7.12-2	16.50	18.50	0.16	0.52	0.08
7.15	13.55	15.55	0.08	0.28	0.04
7.18	10.71	12.71	0.48	0.16	0.26
8.18	11.56	13.56	0.32	0.62	0.10
Z2	10.91	21.41	0.91		0.54
A1.1	10.69	12.69	0.62	2.07	0.34
A5	10.13	12.13	0.01	0.04	0.01

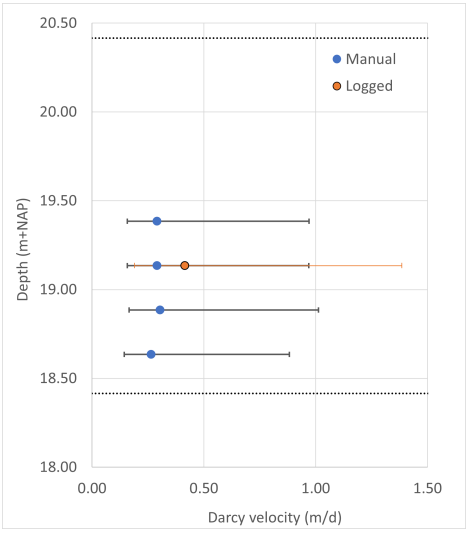

Figure 6.7: Darcy velocities calculated for test 5.10-1, error bars indicate the range of velocities based on the estimated borehole correction factors.

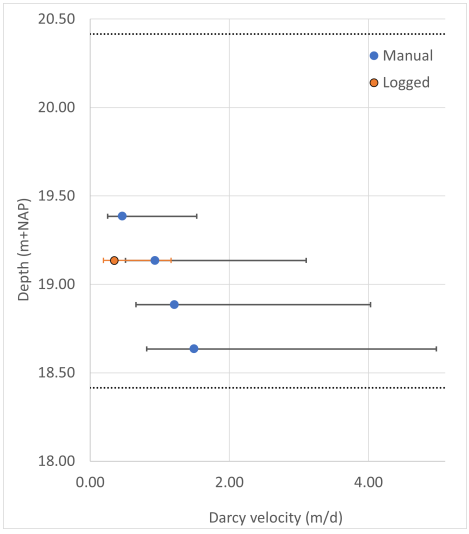

Figure 6.8: Darcy velocities calculated for test 5.10-2, error bars indicate the range of velocities based on the estimated borehole correction factors.

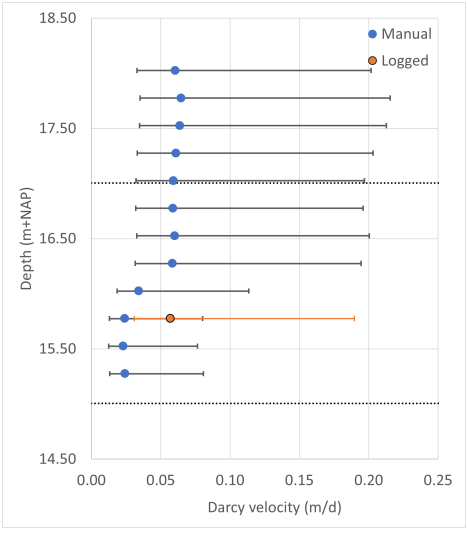

Figure 6.9: Darcy velocities calculated for test 5.13-2, error bars indicate the range of velocities based on the estimated borehole correction factors.

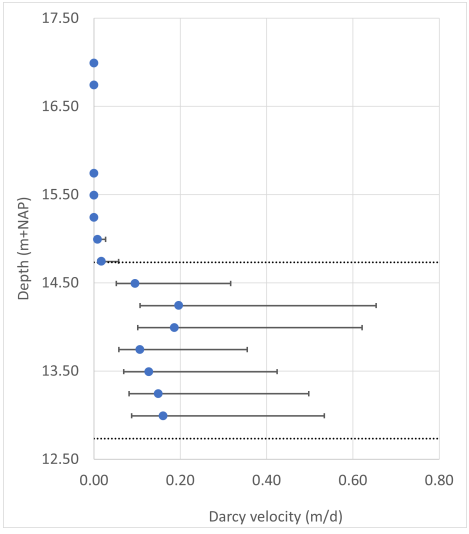

Figure 6.10: Darcy velocities calculated for test 5.15-2, error bars indicate the range of velocities based on the estimated borehole correction factors.

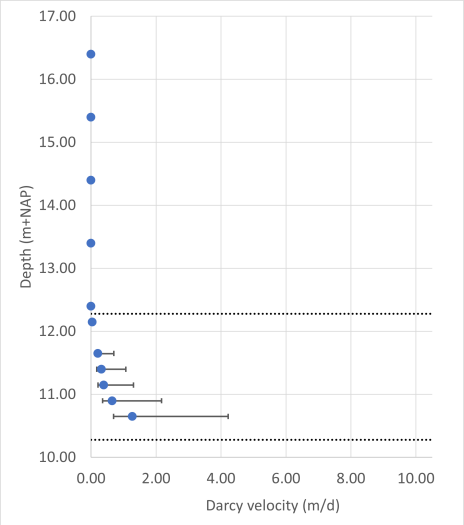

Figure 6.11: Darcy velocities calculated for test 5.18-3, error bars indicate the range of velocities based on the estimated borehole correction factors.

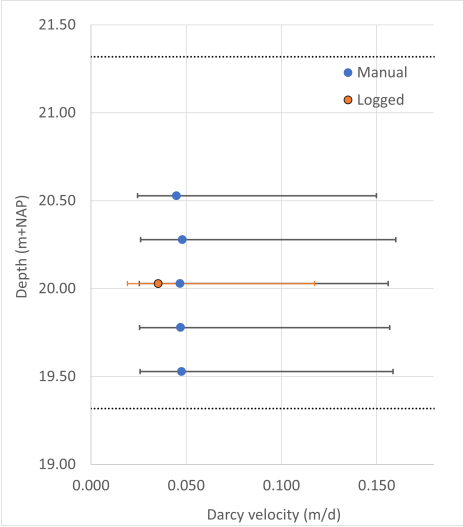

Figure 6.12: Darcy velocities calculated for test 7.9-1, error bars indicate the range of velocities based on the estimated borehole correction factors.

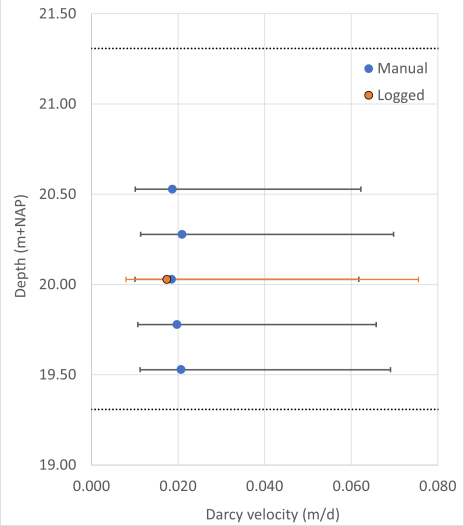

Figure 6.13: Darcy velocities calculated for test 7.9-2, error bars indicate the range of velocities based on the estimated borehole correction factors.

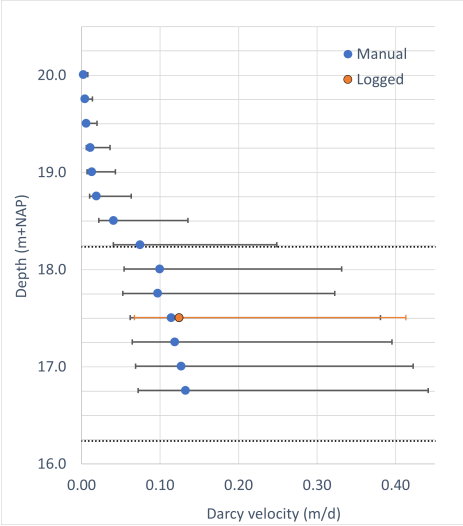

Figure 6.14: Darcy velocities calculated for test 7.12-1, error bars indicate the range of velocities based on the estimated borehole correction factors.

6.2.1.3. IMPACT OF THE LEACHATE RECIRCULATION INFILTRATION SYSTEM

The piezometers and wells are all located between 2.5 and 9 meters from an infiltration drain. Well Z1 is located closest to its respective drain, followed by the piezometers of nest 5 and well A1.1 (Table 6.7).

Table 6.7: Distances between piezometers or wells and the nearest infiltration drain. All distances are approximate. RIS = Recirculation Infiltration System.

ID	Nest P5	Well Z1	Nest P6	Nest P7	P8.18	Well Z2	Well A5	Well A1.1
RIS drain	2B	2B	3B	4B	4B	4B	1A	7A
Distance (m)	5 - 6	2.5	7 - 8	6 - 9	8	7	9.5	3

Tests 5.10-3, 5.13-3, 5.15-2, 5.18-3, and Z1-3 were performed when RIS drains 2 and 3 had been turned off 2 days prior to testing (Fig. G.7). The tests on piezometer 5.10 and well Z1 did not result in significant differences compared to previous tests. Test 5.13-3 resulted in velocities about four times as high as the previous two tests, where the RIS drains were operating according to schedule (horizontal Darcy velocity around 0.20 m/d instead of 0.050 m/d). The same applies to test 5.15-2, where the calculated velocities were about 2 to 3 times as high as the test performed during normal infiltration (0.15 m/d and 0.064 m/d, respectively). The dilution test on piezometer 5.18 without the RIS drains operating resulted in velocities higher than the second test but lower than the first test.

Several previous tests were performed right before or right after infiltration by a nearby drain (Appendix G). These are discussed briefly to check whether any significant differences are found.

RIS drains 0 and 1 were infiltrated right at the start of the test performed on well A5 (Fig. G.3). In addition, the system was infiltrated multiple times during the span of the dilution test, which lasted 3 days. There does not appear to be an influence of the infiltration system in this well, as the calculated velocities are low (average 0.013 m/d) and there were no signs of vertical flow. The test on well A1.1 was performed during the infiltration of drains 6 and 7 (Fig. G.6), and this test did indicate vertical flow (Fig. H.11a). The resulting average horizontal Darcy velocity (0.87 m/d) of well A1.1 was relatively high, especially compared to the horizontal Darcy velocity measured in well A5. Both wells are located halfway down the slope of the landfill, with A5 on the northern slope and A1.1 on the southern slope (Fig. 5.12). It was therefore not expected

that well A5 would have low flow velocities, as the overall movement of leachate within the waste body is towards the north, and the vegetation and ground surface point to seepage and flow out the sides of the landfill.

The SBDT performed on piezometer 6.11 started right after infiltration by drains 3 and 4 (Fig. G.4). As only one test was performed on P6.11, it is difficult to comment on the influence of the infiltration system. Horizontal velocities were the same as piezometer 5.10 (around 0.35 m/d), located at the same depth. The horizontal velocities calculated using the data from test 7.9-2 resulted in velocities twice as low as for test 7.9-1 (0.020 m/d and 0.047 m/d, respectively). Drain 4 was infiltrated prior to test 7.9-1 (Fig. G.4), and during the logged test 7.9-2, drain 4 was infiltrated twice (Fig. G.5). However, possible effects of the infiltration were not visible in the RWT concentration-time graphs (Fig. H.7d). There is, therefore, no indication that the infiltration prior to test 7.9-1 led to higher velocities.

Test 5.13-1 started right after and during infiltration of drains 2 and 3 (Fig. G.1), resulting in the same average horizontal Darcy velocity (0.040 m/d) as test 5.13-3, which was performed when drains 2 and 3 were shut off (Fig. G.7). SBDTs on well Z2 and piezometer 8.18 started after infiltration by RIS drains 2, 3, and 4 (Fig. G.3). Tests on these wells were not repeated. The concentration depth graph of well Z2 did show signs of vertical movement, but the graph of piezometer 8.18 did not.

All in all, only the uniform SBDT performed on well A1.1 shows the possible influence of a RIS drain close by infiltrating at the exact moment of a performed dilution test (Fig. 5.12). A1.1 is the well that is located the closest to an infiltration drain. As discussed in section 6.1, the RIS drains do not appear to have a large area of influence; it can be that only well A1.1 is located within this area. With the limitations of this research, it is not possible to comment on whether the injection of leachate resulted in more flow paths overall, e.g., if a bigger part of the landfill is flushed. No previous leachate flow research had been conducted.

6.2.1.4. PREFERENTIAL FLOW PATHS

Horizontal preferential flow paths in the waste around the piezometer or well are indicated by a significantly higher velocity at certain horizons than at other horizons. Tracer concentration measurements were taken every 0.25 m, and with a 2-meter screen, only 4 - 8 measurements were taken for the piezometers. Therefore, making a

statement on preferential flow paths around a single piezometer is difficult. Piezometers 5.10, 5.15, 6.11, 7.9, 7.12, and well A5 showed relatively uniform Darcy velocities over depth, indicative of heterogeneous material. Piezometers 5.15, 5.18, 6.14, and 7.18 indicated increasing Darcy velocities with depth. For well A1.1, there appeared to be no horizontal movement at the base of the well, and it is difficult to relate whether this resulted from preferential flow paths in the waste, a clogged well, or incorrectly installed wells.

As a result of the vertical movement of the RWT tracer in wells Z1 and Z2, the calculated Darcy velocities are more accurate when the total average of the velocity is calculated over the measured column (section 5.2.2 elaborates on this). Specific horizons for the velocity graphs of the Z wells can not be compared.

Reviewing the horizontal velocities spatially over the landfill but at the same depth, piezometers 7.9 and 5.13 showed lower velocities compared to other piezometers around 9 - 11 m below ground level (piezometers 5.10 and 6.11, and piezometer 6.14, respectively). The low velocities could result from surrounding waste with low hydraulic conductivity, blocking the horizontal flow. The same applies to well A5, which had the lowest calculated velocities of tested piezometers and wells. The lack of connection between velocity and depth supports the hypothesis of preferential flow in landfills.

Overall, the estimated horizontal velocity was higher at the deepest piezometers, indicating a zone with higher flow velocities. Öman & Rosqvist (1999) report that the velocity of solute transport increased with landfill depth because the water volume that participates in leachate flow decreases significantly with the landfill depth. Fellner & Brunner (2010) mention that leachate is funneled into preferential pathways, increasing with depth.

6.2.1.5. COMPARISON WITH VELOCITIES FOUND IN LITERATURE

Literature values of Darcian velocities in landfill waste samples and from a landfill field study vary (Table 6.8). It should be noted that, apart from the velocities reported by Rollinson (2020), these are 'overall' Darcy velocities based on the travel time of the used tracer rather than horizontal Darcy velocities.

Bendz et al. (1998) performed a laboratory study on well-degraded waste from an experimental landfill and found velocities of 0.85 m/d. The studies by Rosqvist & Bendz (1999) and Rosqvist & Destouni (2000) were conducted on waste samples from the same

landfill. Rosqvist & Destouni (2000) performed a field study on the pilot-scale landfill itself. Rosqvist & Bendz (1999) performed tracer tests under sprinkling conditions and reported Darcy velocities between 0.85 and 1.38 m/d. The Darcian velocities reported by Rosqvist & Destouni (2000) were dependent on the age of the waste and decomposition level and the application method of water irrigation (steady-state or transient). Velocities ranged between 0.010 and 3.72 m/d, with higher velocities for the tests performed under ponding conditions.

Rollinson (2020) performed SBDTs on four landfills in the UK, without infiltration and recirculation measures, and reported Darcy velocities between 2.60×10^{-3} and 1.50 m/d. Rollinson (2020) found no relation between depth and horizontal flow rate. Finally, velocities reported by Statom et al. (2006) are based on a fitted parameter for a variably saturated dual-domain model based on long-term temporal chloride data. Choi et al. (2020) performed a tracer field experiment on a South-Korean bioreactor landfill where leachate is injected by vertical drains installed throughout the waste body over the entire depth. Bulk estimates of the hydraulic conductivity reported by Woodman et al. (2017) range from 3.89 - 14.69 m/d and de Jong (2021) reported hydraulic conductivities between 0.01 - 51.84 m/d. de Jong (2021) performed pumping tests on landfill Braambergen, which currently under aeration measures.

Table 6.8: Literature review of Darcy velocities in waste reactors and landfills. Velocities marked with * are hydraulic conductivities.

Source	**Darcy velocity (m/d)**	**Method**
Bendz et al. (1998)	0.85	Laboratory study
Rosqvist & Bendz (1999)	0.85 - 1.38	Laboratory study
Rosqvist & Destouni (2000)	0.010 - 3.72	Laboratory + field study
Statom et al. (2006)	0.27	Numerical model
Woodman et al. (2017)	3.89* - 14.69*	Field study
Rollinson (2019)	2.60×10^{-3} - 1.50	Field study
Choi et al. (2020)	0.34 - 0.45	Field study
de Jong (2020)	0.01* - 51.84*	Field study

Horizontal Darcy velocities calculated within this research fall in the range of Darcian velocities reported by the studies mentioned above. The upper boundary of hydraulic conductivities by de Jong (2021) and Woodman et al. (2017) are relatively high compared to the Darcy velocities, but it expected that in a landfill cell the Darcy velocity is less than the hydraulic conductivity (Statom et al., 2006). The vertical velocities

reported in this research do not, but those are likely not representative of the actual velocities in the waste. Only Rollinson (2020) calculated horizontal velocities, and those values correspond with what was encountered at De Kragge. As the landfill researched by Rollinson (2020) was not subjected to leachate infiltration, this could further point to the RIS not having a large area of influence in compartment 3 and, thus, an insignificant effect on the velocities.

Choi et al. (2020) performed tracer tests on a section without leachate infiltration in addition to the measurements in the cell with infiltration. They found that the velocity was lower in the cell without leachate infiltration (0.25 m/d compared to 0.34 - 0.49 m/d). At De Kragge, there is no information on flow velocities within compartment 4 (where there is no infiltration system). However, there was a significant measured outflow coming from compartment 4 (subsection 5.1.4) and, therefore, potentially a measurable velocity.

6.2.2. VERTICAL LEACHATE FLOW

Just as horizontal flow, vertical flow results from a pressure or density gradient (concentration or density), these possible effects will be discussed in this section. A vertical gradient was present in the leachate level data, where deeper piezometers had a lower leachate level (Fig. 5.6).

The calculated vertical velocities (ranging from 77 - 225 m/d) are high compared to the estimated horizontal Darcy velocities (generally < 1.0 m/d) and compared to the maximum possible recharge of 8.10×10^{-4} m/d as estimated in section 5.1.4. It is very likely that these vertical wells, and possibly the piezometers, act as a preferential channel. Generally, the vertical hydraulic conductivity in a landfill is lower than the horizontal hydraulic conductivity (Powrie & Beaven, 1999). Lateral flow through the bulk of the waste body is directed to these preferential channels, as mentioned by Fellner & Brunner (2010). The calculated vertical velocities from the wells and the piezometer might not represent the actual localized vertical velocities throughout the waste.

There was a difference between individual measurements for all of the performed point dilution tests on wells Z1 and Z2 using the chasing technique. This difference can be caused by a manual error that comes with this technique since the probe was moved manually, and the results are subjective to the person performing the test. Another

possibility is that the vertical velocity differentiates over depth. In addition, the fluorometer was not moved down at the same output. It was tried to move the fluorometer down at the first arrival of the RWT tracer, but with fluctuating background values, this was hard to determine.

Well Z2 and piezometer 8.18 are located in a section that used to have puddles of water and leachate on the surface of the landfill due to an overflowing RIS drain. In April, there was a significant difference between this section of the landfill and the rest, which was dry. Following the installation of the Z2 well in January 2022, the landfill operators noted that the wetness had gone down. The drier surface could be a combined result of less precipitation and RIS infiltration, and the installation of well Z2 is highly likely to have played a part in this by acting as a preferential channel where leachate flows along the side of the borehole or casing of the well (Fig. 6.15). The concentration-time graphs of the uniform dilution tests from well Z2 clearly show vertical movement (measured to be around 100-150 m/d using the point dilution tests). In contrast, the graphs of piezometer 8.18 did not. The lack of vertical movement measured in piezometer 8.18 can result from the smaller diameter, the surrounding waste, or correct installation which eliminates vertical flow along the side of the casing. The measured vertical flow implies a difference in pressure head (Fig. 6.16).

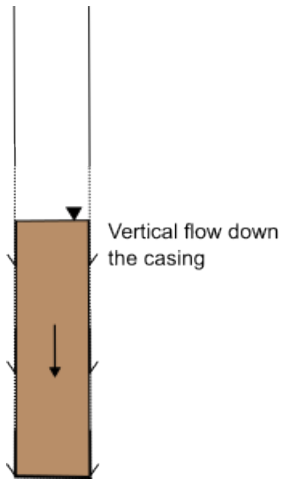

Figure 6.15: A well with vertical flow down the sides of the casing, inducing vertical flow inside the well.

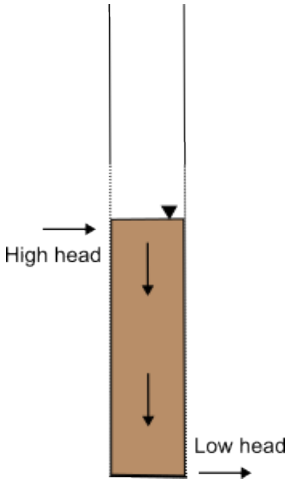

Figure 6.16: A well crossing a section with a high and low head, and the resulting vertical flow inside the borehole, adapted from Maurice (2009).

The decline in tracer concentration in the blind section of a piezometer (e.g., P7.15) has to result from vertical flow, as leachate cannot flow out of the blind laterally. However, for the piezometers where leachate comes up to the blind casing, there is no influx of fresh leachate from the top to replenish the leachate. The top of the casing is blind, and the piezometer is capped. If the piezometer has leachate flowing down the sides of the casing, this cannot dilute the RWT concentration inside the blind casing. Subsection 5.1.2 mentions the head differences measured in the piezometers by the CTD-Divers®, which were about 0.10-0.15 m maximum over 12 hours. It is unlikely that a head difference of 0.10-0.15 m can result in the dilution of three meters of leachate in the blind section; the same applies to the calculated possible daily recharge of 8.10×10^{-4} m.

Dilution of RWT inside the blind casing during the manual uniform dilution tests could result from moving the fluorometer up and down. The fluorometer has a diameter of 2.23 cm, almost half the inner diameter of the piezometer. Although the fluorometer was pulled up and down with care, this movement could have induced vertical flow. However, this does not explain the overnight decrease of RTW concentration in the blind sections of piezometers 5.13, 6.14, 7.15, and 7.12. Improper installation of the piezometers was discussed in subsection 6.2.1.1; it could be that instead of two meters of the screened casing, four were installed or that the casing sections were not sealed together correctly. Additionally, a high horizontal flow through the screened section of the piezometer can cause turbulence inside the casing resulting in more mixing and, therefore, a decline in concentration in the blind section of the casing.

In general, the density of the used RWT tracer should not be a concern as only small amounts have been used (maximum of 0.2 mg RWT), and the density is close to the density of leachate. During the fieldwork period, it was relatively cold, and cold tracer has an increased density and can thus be denser than the leachate. If there is a density difference, the tracer will sink toward the bottom of the well or piezometer, which can be mistaken for vertical flow. The average temperature in the testing period was 7.3 °C in March, 9.3 °C in April, and 14.0 °C in May (KNMI). The temperature of the leachate in the waste fluctuated around 22 °C. The tracer stock solution was always at air temperature. If the leachate used to mix with the tracer stock solution before injection also reached the air temperature, this could slightly increase the density of the injected tracer and leachate solution compared to the leachate present in the well or piezometer and could result in a downward movement of the tracer.

The breakthrough curve of test Z1-v-2 shows a slightly longer tail. An elongated tail results from a delay in the movement of part of the RWT solute, pointing to a local non-equilibrium effect where the leachate is mobile in part of the system and immobile in the rest of the system (Ward et al., 1998). Molecular diffusion allows for solute (RWT) exchange between the mobile and immobile zones. The formula used to calculate the Darcy velocity does not correct for possible effects due to molecular diffusion. The effects of molecular diffusion can be measured by performing multiple dilution tests using different dye tracers (for example, RWT, fluorescein, and eosin) or by combining the different tracers into one dilution test, and then comparing the results in terms of dilution time. The tracers have different differential coefficients (caused by, e.g., molecule size and temperature). If molecular diffusion is the dominant cause of the decline in tracer concentration within the wells or piezometers, this will show in the dilution rates per used tracer.

The effects of diffusion by a concentration gradient has been mentioned by Pitrak et al. (2007), who recommends removing the first few concentration measurements which is what has been done in this research. Within the well, diffusion could play a role when the tracer concentration within the blind casing remains higher than the tracer concentration in the section of the slotted screen (which dilutes through horizontal flow). However, the uniform dilution test performed on piezometer 8.18 showed that the RWT tracer concentration in the blind section of the casing did not decline after 24 hours, even though the RWT concentration in the screened section of the casing had reached background values. This points to limited diffusion and density effects, at least for the vertical velocity within the well.

6.3. ASSESSMENT OF POSSIBLE UNCERTAINTIES DURING FIELD EXPERIMENTS AND DATA ANALYSIS

In the previous sections, several factors have been identified that can influence the accuracy and reliability of the measured data in the field, the analysis of the data, and estimated Darcy velocities. These possible error sources are summarized in Table 6.9, divided into water level measurements and dilution tests. The table lists the parameter to be obtained with the corresponding action, likelihood, effect, and uncertainty of the error source. Suggestions to mitigate the error are offered, and it is indicated to which tests the possible error applies.

Table 6.9: Assessment of the uncertainties associated with leachate level and flow measurements and analyses.

Test		Action	Parameter	Uncertainty	Likelihood	Effect	Explanation	Mitigation	Applicable to performed tests
Leachate level measurement		Leachate level measurement with dip meter	Leachate head	Error in measurement	Low	High	Measurements of the leachate level are used in analysis of the leachate levels throughout the landfill, an error in the measuremend can lead to a wrong interpetation. In addition, dip measurements of the leachate level inside a piezometer/well were taken before dilution tests to calculate the volume of tracer needed.	Perform two meausrements	-
		Leachate level measurement with pressure gauge (CTD-Diver®)	Leachate head	Error in measurements (wrong calibration, etc.)	Low - Medium	High	Measurements of the leachate level are used in analysis of the leachate levels throughout the landfill, an error in the measuremend can lead to a wrong interpetation.	Calibrate correctly and use manual measurements	-
Uniform and point dilution tests	Preparation	Purging of new wells and piezometers		Incorrect purging	High	Medium	If purging is not performed correctly or long enough, it will not remove suspended sediment which can block the signal of the RWT tracer picked up by de fluorometer.	Pump out 3-5 times the volume of leachate inside the well or piezometer	Purging of piezometer 7.12 indicated that there was still suspended sediment inside the piezometer after purging
		Callibration of fluorometer to convert AU output to ppb		Incorrect calibration	High	High	Parameters of influence that are difficult to control/investigate are turbidity and sorption, temperature, natural background fluorescence, salinity, and electrical conductivity	Extensive reserach on possible parameters of influence	All, AU was not converted to ppb
	Performing the experiment	Injection of tracer in the well or piezometer. Uniform and point dilution tests.	Starting RWT concentration (C_0)	Bad vertical mixing	High	Low - Medium	An uneven flow of RWT tracer out of the hosepipe during injection. Mostly applicable to uniform dilution tests.	Using a cone promotes mixing by going up and down the well. Bad vertical mixing can lead to a wrong interpretation when data points for further analysis are not carefully selected. It is only a problem if flow is so fast that it is not measurable anymore because of the low initial concentration.	Table 5.2, section 2: 8.18, 5.18-1, 7.18, 5.10-2, 5.18-2, 5.18-3, 5.15-2, 5.13-2, Z1-1, A1.1, 6.11, Z1-2, Z1-3, 5.15-1
			Starting RWT concentration (C_0)	Bad horizontal mixing	Medium - High	Medium	This can result in an increase in RWT concentration over time as the concentration evens out over the horizontal plane. Mostly applicable to unfirom dilution tests.	Using a cone promotes mixing by going up and down the well. Omit the first concentration log right after injection (Maurice, 2009).	5.13-2, 5.15-1, 5.15-2, 5.18-1, 5.18-2, 7.9-2, 7.12, 7.18, 8.18, A5

Test		Action	Parameter	Uncertainty	Likelihood	Effect	Explanation	Mitigation	Applicable to performed tests
Uniform and point dilution tests	Performing the experiment	Manual concentration measurements. Manual uniform dilution tests and chasing technique point dilution tests.	RWT concentration (C)	Additional mixing during measurements.	Medium	High	For uniform tests: going up and down with the fluorometer causes extra mixing and redistribution of the tracer. Dropping the sensor has the same effect. For point dilution test: chasing technique requires carefull handeling of the fluorometer to not promote additional mixing. Results in lower linearity (R^2) between the log of concentration and time.	Carefull selection of data points to be used in further analysis or performing a dilution test with the fluoromoter probe at a constant depth, logging the data at a certain interval.	5.13-1, 5.15-1
			RWT concentration (C)	Misreading output from data logger	Low	Medium - High	Misreading the value on the datalogger or noting down the wrong value. Results in lower linearity (R^2) between the log of concentration and time.	Carefull selection of data points to be used in further analysis	-
	Data analysis	Analysis of concentration-time data. Uniform and point dilution tests.	Horizontal Darcy velocity (v_f)	Mixing volume (r)	High	Medium	The diameter (/mixing volume) depends on whether or not the filter pack was installed correctly	Couple with borehole correction factor. The correction factor corrects for the convergence of the streamlines towards the borehole and the faster flow inside the well.	All
			Horizontal Darcy velocity (v_f)	Incorrect borehole correction factor (α)	High	High	The parameter is difficult to determine. There is an overall lack of knowledge about the state of the well and the waste body.	Estimate the borehole correction factor either analytically or theoretically and make error bars in Darcy velocity graph	All
			Horizontal Darcy velocity (v_f)	Effects from diffusion and sorption	Medium	High	Including the initial fast decline and possible diffusion effects over-estimates the Darcy velocity	Omit the first concentration log right after tracer injection (Pitrak et al., 2007)	All

6.4. CONCEPTUAL FLOW MODEL

Based on the finding of this research, a conceptual model of compartment 3 of De Kragge was composed (Fig. 6.17). The model is a cross section from north to south, including several wells and piezometers. Flow process included in the model are: preferential horizontal flow, channelling of leachate towards the wells, lateral flow towards neighbouring compartments, and several unsaturated and saturated zones.

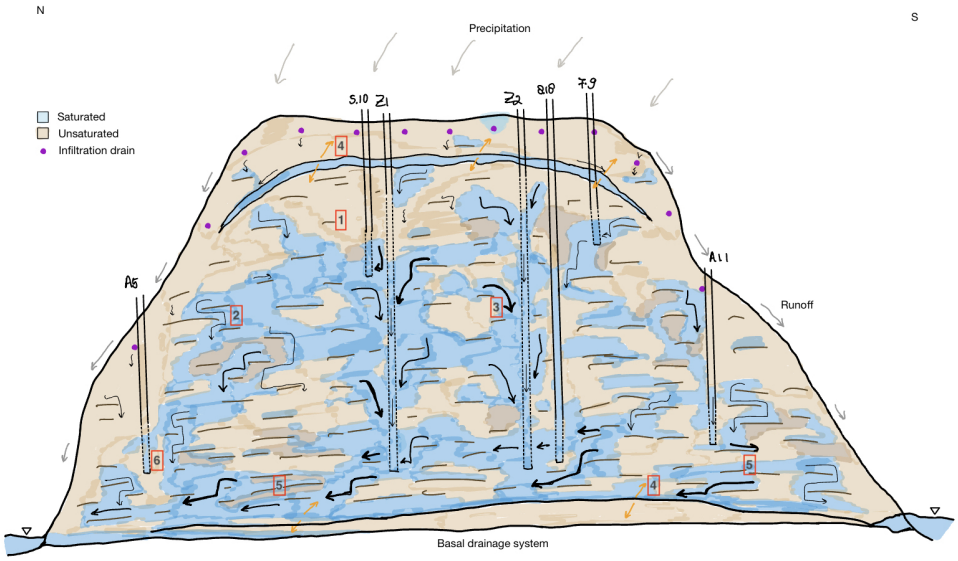

Figure 6.17: Conceptual flow model of landfill De Kragge. A thicker arrow indicates higher flow velocities. 1) Horizontally-oriented waste; 2) Leachate flow; 3) Channeling towards wells; 4) Lateral flow to neighboring compartments; 5) Deeper zones of higher compaction; 6) Waste potentially blocking leachate flow.

Literature that illustrates leachate flow in a conceptual model is not extensive; generally, the analysis either describes or illustrates landfill characteristics such as preferential flow and perched leachate zones but does not combine them. In their conceptual model, Statom et al. (2006), state that a landfill is a reservoir containing potentially contaminated solutes, and by flushing clean water through the waste body, these solutes are depleted over time. They describe a dual-domain system with the following mobile zones for their test cell in the US: the cover of the landfill which is composed of sand, the first section of waste close to the cover, and preferential flow paths throughout the waste. The interior section of the waste is the immobile region. The waste was unsaturated at De Kragge to approximately 6 m below ground level. Therefore dilution

test could not be performed within this zone. The leachate level and RIS analysis did point out that leachate is not infiltrating efficiently and does not affect leachate levels below this upper unsaturated zone. The infiltrated leachate might be transported by preferential pathways within this unsaturated zone and, therefore, not show in the leachate levels throughout the waste body. The variety in Darcy velocities fits the dual-domain system but also shows that the interior waste section is not immobile.

Several authors who conducted research at De Kragge or the pilot landfill in Braambergen note a 'bucket' model for the leachate distribution (Ren 2021; de Jong 2021). Within these buckets, leachate is reported to be stagnant. Apart from the lack of flow at the base of well A1.1 and low velocities in well A5, this research did not find compelling evidence for isolated waste buckets with stagnant leachate. Regardless, isolated saturated waste is likely to be present at the site since the previous drilling for the installation of wells did indicate unsaturated waste zones below saturated waste zones. There might always be flow in these bucket zones. Alternatively, the piezometers were not installed within these zones, or the drilling drastically changed the hydraulics around the piezometers and wells, therefore not representing the initial condition.

In the field of landfill hydrology (Trapani et al., 2015; Zhan et al., 2015; Di Bella et al., 2012) and groundwater (slope) hydrology (Debieche et al., 2012; Nastev et al., 2008), several authors note that perched leachate and water bodies decrease the infiltration and downward movement of leachate and water. At De Kragge, there is a perched, saturated zone below the RIS drains resulting from infiltrated leachate and water (section 6.1). The effectiveness of the infiltration towards the deeper waste body is decreased, as the infiltration events were not visible in the levels measured in the piezometers (nests P5 - P8 and Z wells). The results of the UoS tracer test support the decrease in infiltration. Perched leachate zones enhance lateral flow (Trapani et al. 2015). This increased lateral flow is indicated at De Kragge by the measurable outflow of compartments 2 and 4. In addition, the enhancement of lateral flow correlates with the higher measured velocities in the deep piezometers (P5.18, P7.18, and P8.18), which are located approximately 3.5 - 6 m above the basal drains.

The difference in horizontal velocities over depth and location indicate preferential flow paths as discussed in section 6.2.1.4). Preferential flow within landfills has been described by numerous authors based on different tracer tests conducted on waste in an experimental set-up (e.g., Rosqvist et al. 2005; W. J. Zhang & Yuan 2019) and at fieldscale landfills (e.g., Oonk et al. 2013; Rees-White et al. 2021; Woodman et al. 2017; Rollinson 2020).

7

CONCLUSIONS AND RECOMMENDATIONS

This chapter first answers the sub-questions, followed by a conclusion to the main research question 'How does leachate flow vary spatially through the waste body of De Kragge landfill?' and general conclusions on the methodology of this research and in-situ stabilization measures at De Kragge. Finally, recommendations are provided for further research.

7.1. CONCLUSIONS TO THE RESEARCH QUESTIONS

How fast does the leachate infiltrate through the recirculation infiltration system?

Leachate level rise in the piezometers below the drains due to infiltration was relatively uniform (in terms of the time it takes to infiltrate). The decline of the leachate levels after infiltration took up to 12 hours, and the leachate levels did not always return to the starting level. Leachate levels measured across the drain were not uniform after infiltration. There does not appear to be a relation between leachate level height and location across the drain. In addition, there was temporal variation. There appears to be either leachate spilling or overflow towards the drains, as there were often additional, non-uniform infiltration peaks after an infiltration event.

Can the leachate levels be linked to the infiltration and each other?

Leachate levels measured in the piezometers throughout the waste body (piezometer nests 5, 6, and 7, and piezometer 8.18) did not pick up any leachate level rise or fall due to the infiltration. Thus indicating that the infiltration drains only have a small area of influence around the drain and the possibility that leachate flows laterally to neighboring compartments. Leachate levels measured in the piezometers in the waste body all follow the same rises and declines, responding to atmospheric pressure rather than infiltration. The leachate levels measured in the basal drains are much lower than

in the waste body. There appear to be several saturated and unsaturated zones within the waste body.

What are the Darcy flow velocities?

Assuming a borehole correction factor of 2 resulted in horizontal Darcy velocities (averaged over the screened section) between 0.02 and 1.0 m/d for the piezometers and around 0.70 m/d for the two Z wells. Several uncertainties and possible sources of error have been identified; the main uncertainty and influence is the borehole correction factor, which makes it challenging to conclude absolute Darcy velocities. In addition, parameters might differ from well to well due to anisotropy of the waste and well installation. Point dilution tests suggest higher vertical velocities (77 m/d for piezometer 5.13 and 225 m/d for well Z1). The uniform and point borehole dilution tests showed that leachate inside the landfill is not stagnant.

Is there any variation with depth?

Calculated horizontal velocities differed within the saturated zone of a piezometer or well, and with depth of the landfill. Overall, the highest velocities were measured in the deepest piezometers, located about 5 meters above the base of the landfill.

Can zones of preferential flow be distinguished from zones with negligible flow?

Spatially distributed over the landfill, velocities measured in several piezometers differed considerably from other measurements at the same depth, indicating preferential flow. The borehole dilution tests performed in both Z wells with a 10 - 12 m screen showed a difference in flow velocity over depth, but the vertical movement made comparison of the different horizons difficult. The high measured vertical flow results from these wells acting as a preferential channel and are not representative of the possible vertical velocities in the waste body.

Does the recirculation infiltration system influence the flow velocity?

No evidence from this research supports the hypothesis that the recirculation and infiltration of leachate and water resulted in higher horizontal flow velocities. Dilution tests performed with infiltration drains turned off did not result in lower calculated velocities than when the infiltration drains were performing according to schedule. Additionally, calculated velocities match with velocities in landfills without infiltration measures found literature.

7.2. GENERAL CONCLUSIONS

How does leachate flow vary spatially through the waste body of De Kragge landfill?
There was spatial variability in the measured flow velocities, without a clear pattern, apart from higher velocities measured in the deep piezometers closest to the base of the landfill; this might be linked to the perched leachate zone above the basal drains promoting lateral flow. The variation in flow velocities supports the hypothesis of preferential flow paths. Additionally, the large wells provided a channel for vertical flow. The results of the dilution tests showed a variation with repeated tests, also the logged tests at a set horizon. Calculated velocities between two logged tests differed up to 68%, and calculated velocities for manual dilution tests differed up to 200%. Temporal variation due to changes in hydraulics is difficult to differentiate from variation due to noise and possible errors. As there are no long-term measurements, e.g., dilution tests performed in previous years or tests performed before the recirculation measures, it is challenging to comment on whether there have been changes in the landfill hydraulics resulting from the infiltration measures.

Regarding the leachate levels, there is at least an unsaturated zone below the infiltration drains, an unsaturated zone above the basal drains, and likely smaller zones throughout the landfill (indicated by previous research). Leachate levels below the infiltration drain differed up to 1.5 m following infiltration events, while leachate levels in the waste body showed little temporal differences. Leachate levels in the basal drains showed a yearly variation of up to 2 m.

Methodology of performed tests
The installation of the additional wells and piezometers in January 2022 allowed for quite a complete overview of leachate flow at De Kragge. Due to the vertical flow within the well, the monitoring wells (110 mm diameter and fully screened) are less suitable for uniform dilution tests where the aim is to produce a full-depth Darcy velocity profile. The issue of vertical flow is less prominent in the piezometers, but these only have a 2 m screened section. Therefore, the piezometers are more suitable for performing uniform dilution tests and monitoring leachate levels than the bigger, fully screened wells. The bigger wells can be used for other tests, such as pumping tests (and point dilution tests).

The benefits of the performed dilution tests are that one person can perform them, only requires cheap materials, and the test itself is straightforward. Additionally, a manually performed test allows for a Darcy velocity profile over the entire saturated depth of a

well (when there is no vertical flow). The disadvantage of the dilution tests is that it takes a lot of effort and time to inject the tracer and monitor the decline of tracer concentration. Injection of the tracer always has to be performed manually (which can easily result in errors), but monitoring tracer decline can also be performed logged. There are few alternatives to performing borehole dilution tests. An alternative would be installing flow meters inside the wells; however, this is considerably more costly and might not be worth it.

The manual concentration measurements had to be refined whenever there was a manual error (dropping the fluorometer down the piezometer) or noise in the data (additional flow processes). Therefore, logged measurements at a fixed horizon are more reliable, and the concentration data needs less refinement than data collected by manual measurements. Performing a point dilution test with the fluorometer sensor at a specific depth resulted in a tracer breakthrough curve. The breakthrough curve is more reliable than the measurements of the chasing technique, which are easily susceptible to manual errors. The point dilution tests provided a good insight into the vertical flow velocities within the wells.

Regarding the method to calculate the Darcy velocity, the method by Y. Zhang et al. (2020) is more robust than the method by Freeze & Cherry (1979), as the velocity is based on the total decline of the tracer over the slotted section. Therefore, the method is suitable even when there is vertical flow within the well, and the method of Freeze & Cherry (1979) is not. The only drawback is that the method by Y. Zhang et al. (2020) results in one overall velocity rather than a velocity per horizon; if there is no vertical flow within the well, the method by Freeze & Cherry (1979) is preferred.

In-situ stabilization measures

Injecting leachate at the top with the infiltration trenches (drains) appears less effective than desired at De Kragge. There are unknown problems with the connectivity of different leachate zones within the waste, and a significant volume of leachate appears to flow laterally to compartment 4. Improvements regarding the recirculation and infiltration system include installing additional horizontal drains at a deeper level (e.g., 4-5 m below ground level) between the already installed infiltration drains. Vertical infiltration drains are another option. However, the point dilution tests performed in the Z wells indicated that leachate is channeled toward these vertical wells, which might also happen to infiltration wells, decreasing the infiltration efficiency. Using an

infiltration blanket increases the area of infiltration at the top and might help distribute the leachate more uniformly. However, all these measures are very rigorous and expensive; it would be advised to leave the landfill as it is for now and continue monitoring and testing.

Installation of additional wells and piezometers on top of the landfill with the purpose of conducting additional dilution tests would not be recommended for future research. This research showed a variation in flow velocity and leachate distribution throughout the landfill; additional wells and piezometers likely result in the same conclusion. Additionally, installing wells and piezometers into the landfill disturbs the hydraulics within the landfill and can create additional preferential flow paths. The channeling of leachate towards the wells takes away from the flushing capacity of the landfill, as leachate is short-circuiting towards the base of the landfill along these wells and piezometers instead of horizontally moving throughout the landfill. This decreases the effect of the stabilization through leachate recirculation. However, installing additional piezometers (or wells) on the northern or southern slope of the landfill can be helpful. The relative absence of flow in well A5 (northern slope) was not expected. Additional piezometers installed on the slopes can help investigate whether this flow absence is only present around well A5 or if there is little flow along the entire slope section.

If there is the desire to expand the existing data set, dilution tests can be repeated on the already installed wells and piezometers in compartment 3 (elaborated further in section 7.3, recommendations), especially on the deeper piezometers (P5.18, P7.18, and P8.18) where initial concentrations remained low and performing sufficient concentration measurements was difficult due to the quick dilution of tracer. To further investigate what effect the leachate infiltration has on the leachate levels and the flow velocity, the infiltration system could be stopped for a prolonged period (e.g., a month). Leachate levels and leachate outflow from all three compartments should be monitored to test whether there are any changes, and dilution tests should be repeated.

7.3. RECOMMENDATIONS

The following recommendations are suggested based on the findings of this study:

1. **Perform borehole dilution tests on a landfill section without recirculation measures.** This could validate whether the measured horizontal and vertical flow results from the recirculation measures. The neighboring compartment 4 at De

Kragge is not under leachate recirculation. Possible measured horizontal flow in compartment 4 could either result from infiltration by precipitation or flow from compartment 3.

2. **Additional research into the error sources.** This would complement and validate the results of this research. Possible sources of error mentioned are related to the calibration of the Rhodamine water tracer fluorometer, the mixing volume of the borehole, and the borehole correction factor (α). The fluorometer can be calibrated better by performing calibration measurements at the temperature of the in-situ leachate (around 22 °C) and doing the calibration process for each well and piezometer separately due to the difference in background concentration. More information is needed to assess the borehole correction factor, i.e., the hydraulic conductivity of the landfill. The hydraulic conductivity can be investigated by pumping tests and measuring the drawdown.
3. **Additional point dilution tests.**To give more insight into the possible vertical flow within the saturated length of the piezometer or well. For the deeper piezometers (e.g., 5.18 and 8.18), the Rhodamine water tracer can be added to the top of the leachate column. There is no recharge of leachate from the top; therefore, no flow is expected in the blind section of the casing. Moreover, performing uniform borehole dilution tests with packers eliminates influences of vertical flow.
4. **Perform dilution tests one at a time.** Uniform dilution tests should not be performed simultaneously, the Rhodamine water tracer concentration sometimes declines too fast to capture accurately. Going up and down the well or piezometer every 10 minutes is not recommended as this disturbs the leachate column and causes additional mixing, leading to less reliable data. The fluorometer can be at a specific horizon in the screen to take minute-by-minute measurements between (half-)hourly manual measurements. This way, reliable logged data is collected, and complete concentration-depth profiles can be used to check whether the tracer is also moving from the blind section.
5. **Extended research on the leachate level measurements from the infiltration drains (and piezometers and wells).** There is much variation in leachate levels, both spatially and temporally. This variation has not been investigated in depth in this research. It is suggested to investigate this more and possibly try to calculate hydraulic conductivities.

REFERENCES

Beaven, R. (2000). *The hydrogeological and geotechnical properties of household waste in relation to sustainable landfilling.* (PhD dissertation, University of London, London).

Bendz, D., Singh, V., & Berndtsson, R. (1997). The flow regime in landfills – implications for modelling. In *Proc. sardinia '97* (pp. 97–108). Sixt International Landfill Symposium, Cagliari, Italy II.

Bendz, D., Singh, V. P., Rosqvist, H., & Bengtsson, L. (1998). Kinematic wave model for water movement in municipal solid waste. *Water Resources Research, 34*(11), 2963–2970. doi: 10.1029/98WR01109

Bezerra, P. H. L., Coutinho, A. P., Lassabatere, L., Neto, S. M. D. S., de Melo, T. D. A. T., Antonino, A. C. D., … Montenegro, S. M. G. L. (2022, 2). Water Dynamics in an Infiltration Trench in an Urban Centre in Brazil: Monitoring and Modelling. *Water (Switzerland), 14*(4). doi: 10.3390/w14040513

Blight, G., Ball, J., & Blight, J. (1992). Moisture and suction in sanitary landfills in semiarid areas. *Journal of Environmental Engineering, ASCE 118*, 865–877.

BNNVARA. (2018, 3). *Lekkende vuilnisbelt vervuilt grondwater natuurgebied.* Retrieved from `https://www.bnnvara.nl/vroegevogels/artikelen/lekkende-vuilnisbelt-vervuilt-grondwater-natuurgebied`

Brabants Dagblad. (2022, 2). *Lekt oude vuilstort in Rosmalen ook?* Retrieved from `https://www.bd.nl/den-bosch-vught/lekt-oude-vuilstort-in-rosmalen-ook~a7060302/?referrer=https%3A%2F%2Fwww.google.com%2F`

Choi, H. J., Choi, Y., & Rhee, S. W. (2020, 1). Estimation on migration characteristics of leachate using analysis of hydraulic conductivity at bioreactor landfill. *Waste Management and Research, 38*(1), 59–68. doi: 10.1177/0734242X19873705

Darcy, H. (1856). *Les fontaines publiques de la ville de Dijon.* Paris: Dalmont.

Debieche, T. H., Bogaard, T. A., Marc, V., Emblanch, C., Krzeminska, D. M., & Malet, J. P. (2012, 7). Hydrological and hydrochemical processes observed during a large-scale infiltration experiment at the Super-Sauze mudslide (France). *Hydrological Processes*, *26*(14), 2157–2170. doi: 10.1002/hyp.7843

de Jong, T. (2021). *Spatial and temporal variability of hydrological behaviour and leachate composition in a landfill stabilized by in-situ aeration.* (MSc thesis, Delft University of Technology, Delft). Retrieved from `http://repository.tudelft.nl/`

Di Bella, G., Di Trapani, D., Mannina, G., & Viviani, G. (2012, 3). Modeling of perched leachate zone formation in municipal solid waste landfills. *Waste Management*, *32*(3), 456–462. doi: 10.1016/j.wasman.2011.10.025

Drost, W., Klotz, D., Koch, A., Moser, H., Neumaier, F., & Rauert, W. (1968). Point Dilution Methods Investigating Ground Water Flow by Means of Radioisotopes. *Water Resources Research*, *4*(1).

Englert, A. (2003). *Measurement, Estimation and Modelling of Groundwater Flow Velocity at Krauthausen Test Site.* (PhD thesis, RWTH Aachen University, Aachen). Retrieved from `https://publications.rwth-aachen.de`

Fahrmeier, N., Goeppert, N., & Goldscheider, N. (2021). Comparative application and optimization of different single-borehole dilution test techniques. *Hydrogeology Journal*, *29*, 199–211.

Fan, H. j., Shu, H. Y., Yang, H. S., & Chen, W. C. (2006, 5). Characteristics of landfill leachates in central Taiwan. *Science of the Total Environment*, *361*(1-3), 25–37. doi: 10.1016/j.scitotenv.2005.09.033

Fellner, J., & Brunner, P. H. (2010, 11). Modeling of leachate generation from MSW landfills by a 2-dimensional 2-domain approach. *Waste Management*, *30*(11), 2084–2095. doi: 10.1016/j.wasman.2010.03.020

Fetter, C. W. (2001). *Applied Hydrogeology* (4th ed.). Upper Saddle River, New Jersey: Prentice Hall.

Freeze, R., & Cherry, J. (1979). *Groundwater.* Englewood Cliffs; NY: Prentice-Hall.

Gebert, J., Comans, R., Heimovaara, T., Dieudonné, A., Powrie, W., Beaven, R., ... Kalbitz, K. (2020). *Coupled multi-process research for reducing landfill emissions (CURE) - NWO Proposal* (Tech. Rep.).

Gomo, M. (2020, 6). Effects of Artefacts on Natural Gradient Single-Borehole Tracer Dilution Tests. *Natural Resources Research*, *29*(3), 2227–2235. doi: 10.1007/s11053-019-09557-7

Hersbach, R. (2021). *Modelleren van de waterbalans van stortplaats de Kragge - Hoe goed is de waterbalans?* (Unpublished BSc thesis, Delft University of Technology, Delft).

Ishak, A. R., Mohamad, S., Soo, T. K., & Hamid, F. S. (2016, 6). Leachate and Surface Water Characterization and Heavy Metal Health Risk on Cockles in Kuala Selangor. *Procedia - Social and Behavioral Sciences*, *222*, 263–271. doi: 10.1016/j.sbspro.2016.05.156

Kanen, T., & Kedzia-Kowalski, S. (2021). *Voortgangsrapportage iDS Kragge* (Tech. Rep.).

Käss, W. (1998). *Tracing Technique in Geohydrology*. Rotterdam: A.A. Balkema.

Kedzia-Kowalski, S. (2021). *iDS installatie Bergen op Zoom - 'as built' rapport* (Tech. Rep.). Attero B.V.

Kissas, K., Ibrom, A., Kjeldsen, P., & Scheutz, C. (2022, 2). Methane emission dynamics from a Danish landfill: The effect of changes in barometric pressure. *Waste Management*, *138*, 234–242. doi: 10.1016/j.wasman.2021.11.043

Lei, Y., Shen, Z., Huang, R., & Wang, W. (2007). Treatment of landfill leachate by combined aged-refuse bioreactor and electro-oxidation. *Water Research*, *41*(11), 2417–2426. doi: 10.1016/j.watres.2007.02.044

Libby, J. L., & Robbins, G. A. (2014, 1). An unsteady state tracer method for characterizing fractures in bedrock wells. *Groundwater*, *52*(1), 136–144. doi: 10.1111/gwat.12045

Lloyd, J. W., Ramanathan, C., & Pacey, N. (1979). The use of point dilution methods in determining the permeabilities of land-fill materials. *Water Services*, *83*, 843–846.

Ma, J., Li, J., & Li, Y. (2021). Effects of leachate recirculation quantity and aeration on leachate quality and municipal solid waste stabilization in semi-aerobic landfills. *Environmental Technology & Innovation*, *21*.

Marius, M., Stringfellow, A., Smallman, D., & Atkinson, T. (2010). *FLUORESCENT TRACERS-A TOOL FOR LANDFILL INVESTIGATION AND MANAGEMENT* (Tech. Rep.).

Maurice, L. (2009). *Investigations of rapid groundwater flow and karst in the Chalk* (Unpublished doctoral dissertation). University College London.

Meza, N. (2021). *Project Sustainable Landfill Management. Internal report project CURE (Coupled Multiprocess Research to Reduce Landfill Emissions)* (Tech. Rep.).

Nastev, M., Morin, R., Godin, R., & Rouleau, A. (2008, 3). Developing conceptual hydrogeological model for Potsdam sandstones in southwestern Quebec, Canada. *Hydrogeology Journal*, *16*(2), 373–388. doi: 10.1007/s10040-007-0267-9

Nordqvist, R., Gustafsson, E., Andersson, P., Thur, P., & Ab, G. (2008). *Svensk Kärnbränslehantering AB Groundwater flow and hydraulic gradients in fractures and fracture zones at Forsmark and Oskarshamn* (Tech. Rep.). Retrieved from `www.skb.se` .

Ogata, Y., Ishigaki, T., Nakagawa, M., & Yamada, M. (2016, 6). Effect of increasing salinity on biogas production in waste landfills with leachate recirculation: A lab-scale model study. *Biotechnology Reports*, *10*, 111–116. doi: 10.1016/j.btre.2016.04.004

Öman, C., & Rosqvist, H. (1999). Transport fate of organic compounds with water through landfills. *Water Research*, *33*(10), 2247–2254.

Omroep Gelderland. (2018, 1). *Zorgen over 'lekkende' vuilnisbelt.* Retrieved from `https://www.gld.nl/nieuws/2302788/zorgen-over-lekkende-vuilnisbelt`

Oonk, H., Zomeren, A. v., Rees-White, T. C., Beaven, R. P., Hoekstra, N., Luning, L., ... Woelders, H. (2013, 10). Enhanced biodegradation at the Landgraaf bioreactor test-cell. *Waste Management*, *33*(10), 2048–2060. doi: 10.1016/j.wasman.2013.03.003

Piccinini, L., Fabbri, P., & Pola, M. (2016, 6). Point dilution tests to calculate groundwater velocity: an example in a porous aquifer in northeast Italy. *Hydrological Sciences Journal*, *61*(8), 1512–1523. doi: 10.1080/02626667.2015.1036756

Pitrak, M., Mares, S., & Kobr, M. (2007, 1). A simple borehole dilution technique in measuring horizontal ground water flow. *Ground Water*, *45*(1), 89–92. doi: 10.1111/j.1745-6584.2006.00258.x

Powrie, W., & Beaven, R. (1999). Hydraulic properties of household waste and implications for landfills. *Proceedings of the Institution of Civil Engineers - Geotechnical Engineering*, *137*(4), 235–237.

Price, M. (2009). Barometric water-level fluctuations and their measurement using vented and non-vented pressure transducers. *Quarterly Journal of Engineering Geology and Hydrogeology*, *42*(2), 245–250. doi: 10.1144/1470-9236/08-084

Raghab, S. M., Abd El Meguid, A. M., & Hegazi, H. A. (2013, 8). Treatment of leachate from municipal solid waste landfill. *HBRC Journal*, *9*(2), 187–192. doi: 10.1016/j.hbrcj.2013.05.007

Reddy, K. R., Hettiarachchi, H., Parakalla, N. S., Gangathulasi, J., & Bogner, J. E. (2009, 2). Geotechnical properties of fresh municipal solid waste at Orchard Hills Landfill, USA. *Waste Management*, *29*(2), 952–959. doi: 10.1016/j.wasman.2008.05.011

Rees-White, T. C., Woodman, N. D., Beaven, R. P., Barker, J. A., & Rollinson, J. (2021, 6). Single-well injection-withdrawal tests as a contaminant transport characterisation tool for landfilled waste. *Waste Management*, *128*, 142–153. doi: 10.1016/j.wasman.2021.04.047

Ren, Z. (2021). *Explanation of Water Distribution Variations in the Landfill Using Electrical Resistivity Tomography*. (MSc thesis, Delft University of Technology, Delft). Retrieved from `http://repository.tudelft.nl/`

Rollinson, J. (2020). *Hydrogeological techniques for the in-situ characterisation of saturated landfilled waste in relation to contaminant flushing*. (MSc thesis, University of Southampton, Southampton). Retrieved from `https://eprints.soton.ac.uk`

Rollinson, J., Rees-White, T., Barker, J., & Beaven, R. (2010). A single borehole dilution technique to measure the hydrogeological properties of saturated landfilled waste. *Waste 2010 conference*.

Rosqvist, H., & Bendz, D. (1999). An experimental evaluation of the solute transport volume in biodegraded municipal solid waste. *Hydrology and Earth System Sciences*, *3*(3), 429–438.

Rosqvist, H., Bendz, D., Beaven, R., & Hudson, A. (2014). Controlled tracer tests through solid waste in two large-scale experimental set-ups. In *Nordic geotechnical meeting*.

Rosqvist, H., Bendz, D., Öman, C., & Meijer, J. (1997). Water flow in a pilot-scale landfill. In *Proc. sardinia '97* (pp. 85–96). Sixt International Landfill Symposium, Cagliari, Italy II.

Rosqvist, H., & Destouni, G. (2000). *Solute transport through preferential pathways in municipal solid waste* (Vol. 46; Tech. Rep.). Retrieved from `www.elsevier.comrlocaterjconhyd`

Rosqvist, H., Dollar, H. L., & Fourie, B. A. (2005). Preferential flow in municipal solid waste and implications for long-term leachate quality: Valuation of laboratory-scale experiments. *Waste Management and Research*, *23*(4), 367–380. doi: 10.1177/0734242X05056995

Spane, F. A. (1999). *Effects of Barometric Fluctuations on Well Water-Level Measurements and Aquifer Test Data* (Tech. Rep.). United States. doi: 10.2172/15125

Statom, R. A., Mccray, J. E., & Thyne, G. D. (2006). Conceptual Model for Landfill Hydrologic Transport Developed Using Chloride Tracer Data and Dual-Domain Modeling. *Environmental & Engineering Geoscience*, *7*(1), 67–78.

Staub, M., Galietti, B., Oxarango, L., Khire, M. V., & Gourc, J.-P. (2009). Porosity and hydraulic conductivity of MSW using laboratory-scale tests. In *Third international workshop "hydro-physico-mechanics of landfills"* (pp. 10–13). Braunschweig, Germany.

Tate, T., Robertson, A. S., & Gray, D. A. (1970). The hydrogeological investigation of fissure-flow by borehole logging techniques. *Quarterly Journal of Engineering Geology*, *2*.

Trapani, D. D., Di Bella, G., Mannina, G., Nicosia, S., & Viviani, G. (2015). Influence of the Height of Municipal Solid Waste Landfill on the Formation of Perched Leachate Zones. *Journal of Environmental Engineering*, *141*(8). doi: 10.1061/(ASCE)EE.1943

Van Essen Instruments B.V. (2022). *Product Manual CTD-Diver® DI28x Series* (Tech. Rep.). Retrieved from `www.vanessen.com`

Van Turnhout, A. G., Oonk, H., & Heimovaara, T. J. (n.d.). *Verbreding Toepasbaarheid Duurzaam Stortbeheer* (Tech. Rep.). Retrieved from `http://repository.tudelft.nl/`.

van Vossen, W., Heyer, K.-U., & van Meeteren, M. (2009). *Feasibility study sustainable emission reduction at the existing landfills Kragge and Wieringermeer in the Netherlands. Generic report: Processes in the waste body and overview enhancing technical measures Dutch Sustainable Landfill Foundation IFAS Consultants for Waste Management* (Tech. Rep.). Den Bosch: Royal Haskoning.

Vereniging Afvalbedrijven. (2015). *Deelplan van Aanpak Verduurzamingspilot Op Stortplaats De Kragge 2* (Tech. Rep.).

Vermeijden, L. (2018). *A water balance model for landfill De Kragge II - Supporting the development of a sustainable aftercare approach.* (MSc thesis, Delft University of Technology, Delft). Retrieved from `http://repository.tudelft.nl/`.

Verreydt, G., Bronders, J., Van Keer, I., Diels, L., & Vanderauwera, P. (2015, 11). Groundwater Flow Field Distortion by Monitoring Wells and Passive Flux Meters. *Groundwater*, *53*(6), 933–942. doi: 10.1111/gwat.12290

VROM. (1991). Richtlijn voor dichte eindafwerking op afval- en reststofbergingen. , *634/EA91/D006/19895*.

VROM. (1993). Richtlijn onderafdischingsconstructies voor stort- en opslagplaatsen. *Publicatiereeks Bodembescherming*, *1993*(2).

Ward, R., Williams, A., Barker, J., Brewerton, L., & Gale, I. (1998). *Groundwater Tracer Tests: A Review and Guidelines for Their Use in British Aquifers* (Tech. Rep.). British Geological Survey Technical Report WD/98/19.

Werkgroep Afvalregistratie. (2021). *Afvalverwerking in Nederland, gegevens 2019* (Tech. Rep.). Utrecht: Rijkswaterstaat. Retrieved from `www.afvalcirculair.nl`

West, L. J., & Odling, N. E. (2007, 1). Characterization of a multilayer aquifer using open well dilution tests. *Ground Water*, *45*(1), 74–84. doi: 10.1111/j.1745-6584.2006.00262.x

Woodman, N. D., Rees-White, T. C., Beaven, R. P., Stringfellow, A. M., & Barker, J. A. (2017). Doublet tracer tests to determine the contaminant flushing properties of a municipal solid waste landfill. *Journal of Contaminant Hydrology*, *203*, 38–50. doi: 10.1016/j.jconhyd.2017.05.008

Woodman, N. D., Rees-White, T. C., Stringfellow, A. M., Beaven, R. P., & Hudson, A. P. (2014, 11). Investigating the effect of compression on solute transport through degrading municipal solid waste. *Waste Management*, *34*(11), 2196–2208. doi: 10.1016/j.wasman.2014.06.022

Xu, L., Lin, X., Amen, J., Welding, K., & McDermitt, D. (2014). Impact of changes in barometric pressure on landfill methane emission. *Global Biogeochemical Cycles*, *28*(7), 679–695. doi: 10.1002/2013GB004571

Zhan, T. L. T., Xu, X. B., Chen, Y. M., Ma, X. F., & Lan, J. W. (2015). Dependence of Gas Collection Efficiency on Leachate Level at Wet Municipal Solid Waste Landfills and Its Improvement Methods in China. *Journal of Geotechnical and Geoenvironmental Engineering*, *141*(4). doi: 10.1061/(ASCE)GT.1943-5606

Zhang, W. J., & Yuan, S. S. (2019, 2). Characterizing preferential flow in landfilled municipal solid waste. *Waste Management*, *84*, 20–28. doi: 10.1016/j.wasman.2018.11.023

Zhang, Y., Wang, H., Zhang, X., Dong, H., & Mao, C. (2020, 7). Groundwater velocity determination by single-borehole dilution test. In *Iop conference series: Earth and environmental science* (Vol. 525). IOP Publishing Ltd. doi: 10.1088/1755-1315/525/1/012175

A

LANDFILL SPECIFICS

At De Kragge, compartments 1 and 2 have a permanent top cover, whereas compartments 3 and 4 are not sealed (Fig. A.1). In compartment 3, the leachate level of the basal drain is measured in the collection pit, indicated by the star in Figure A.2.

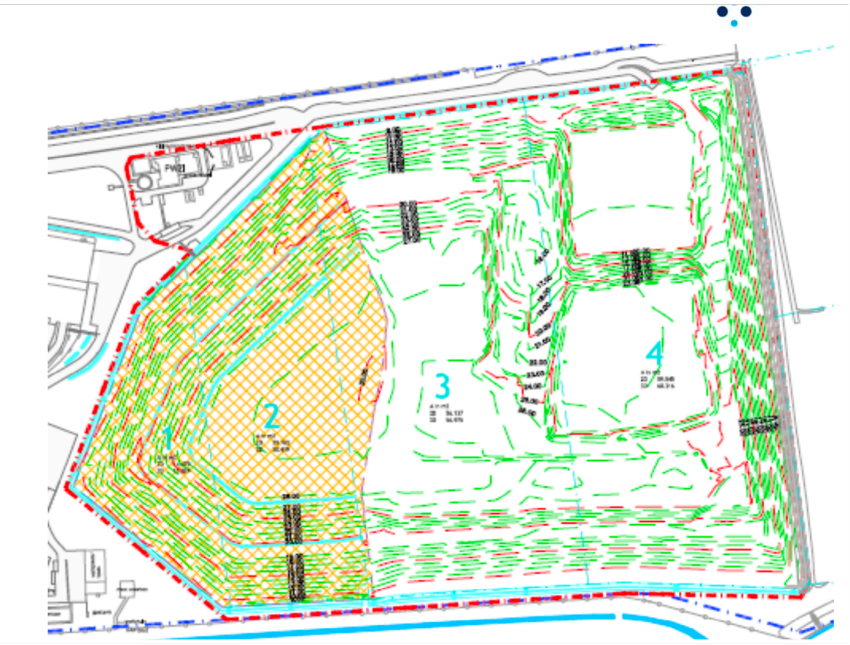

Figure A.1: Top view of landfill De Kragge. The marked area is sealed with a permanent impermeable combination cover (compartments 1 and 2, and a small area of compartment 3), the unmarked area is not sealed with an impermeable cover. Figure by Vereniging Afvalbedrijven (2015).

A

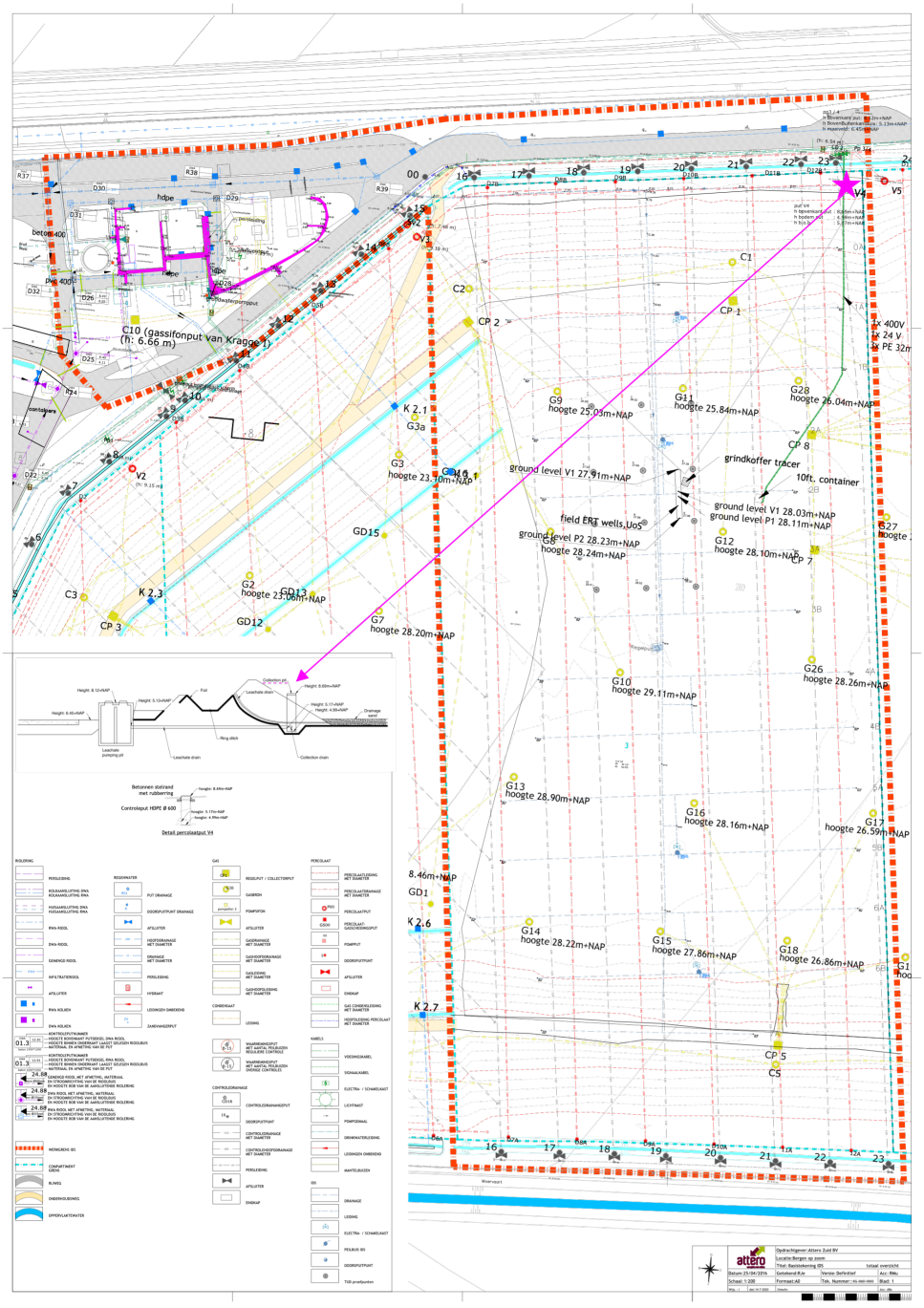

Figure A.2: Top view of landfill De Kragge, indicating the location of the collection pit with the pink star. The collection pit is where the leachate level of the drainage system is measured. Figure adapted from Vereniging Afvalbedrijven (2015).

B

WELL AND PIEZOMETER DESIGN

Several new wells and piezometers were installed in January 2022. The wells (Z1 and Z2) were designed to be installed with approximately 12 m of gravel pack around the screened section of the casing, followed by sand and a bentonite seal up to ground level (Fig. B.1). The piezometers were designed to have approximately 3 m of gravel pack, as the screened section of the casing is 2 m (Fig. B.2). The gravel pack is followed by a bentonite seal up to ground level.

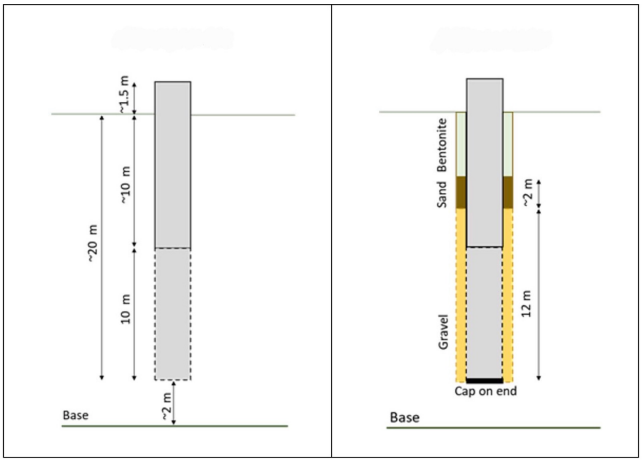

Figure B.1: Schematic example of the Z1 and Z2 well (110 mm outer diameter). Figure by Rees-White (2021, personal communication).

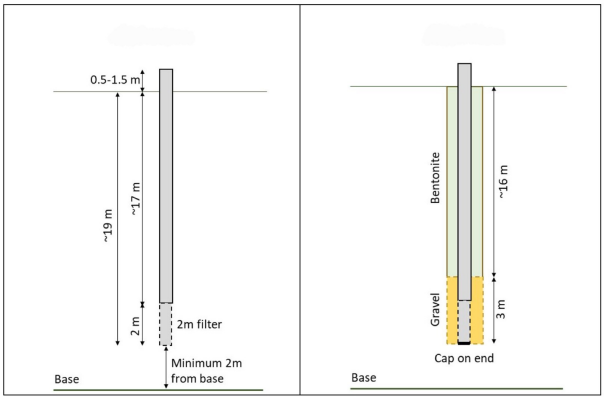

Figure B.2: Schematic example of the installed piezometers (50 mm outer diameter). Figure by Rees-White (2021, personal communication).

C

LEACHATE LEVEL MEASUREMENT POINTS ACROSS THE INFILTRATION DRAINS

Across infiltration drains 2B and 3A, several piezometers were installed to measure the leachate levels following infiltration. The depth of the piezometers and CTD-Divers® differs (Table. C.1).

Table C.1: Extensive table with depth information on piezometers and CTD-Divers® (conductivity, temperature, and depth pressure gauges) installed across drains 2B and 3A. A * signifies a depth that may vary from reality.

Depths all in m+NAP	**2B.2**	**2B.3**	**2B.4**	**2B.5**	**3A.1**	**3A.2**	**3A.4**	**3A.5**	**3A.6**	**3A.8**
Top piezometer	29.1	29.3	29.2	29.5	28.7	29.7	28.9	29.7	29.7	29.5
Ground level	27.9	28.1	28.0	28.0	27.9	28.7	28.5	28.6	28.5	28.4
Gravel box top*	27.4	27.4	27.4	27.4	27.9	27.9	27.9	27.9	27.9	27.9
Drain*	27.3	27.3	27.3	27.3	27.8	27.8	27.8	27.8	27.8	27.8
Gravel box base*	26.6	26.6	26.6	26.6	27.1	27.1	27.1	27.1	27.1	27.1
Diver	24.6	25.2	24.8	25.0	27.3	26.1	27.0	25.5	24.9	26.5
Base piezometer	24.3	24.4	24.9	24.8	27.0	25.9	26.2	25.4	24.7	26.0

D

DEVELOPMENT OF METHODOLOGY

D.1. TRIAL UNIFORM DILUTION TEST ON WELL Z1

The first borehole dilution test at De Kragge was performed on well Z1, using an electric pump after injection of the tracer to promote mixing. The use of the pump resulted in decreased concentration values of the tracer, close to background values (Fig. D.1).

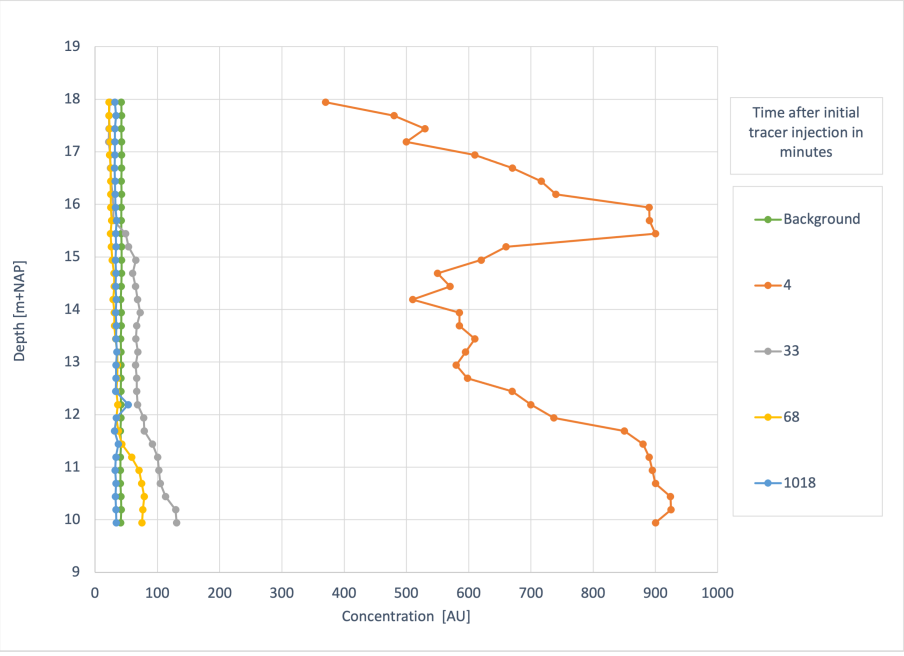

Figure D.1: First borehole dilution test performed on well Z1.

D.2. PURGING OF THE NEW PIEZOMETERS

The newly installed piezometers were purged to remove suspended and settled sediment.

D.2.1. METHODOLOGY

The following steps were performed to purge the piezometers:

- Before purging, the depth to leachate was measured using a dip-meter, as well as the base of the piezometer. The volume of leachate inside the well was calculated using this information and the inner diameter of the piezometer.
- A water sampling pump (PowerPack Tubing Actuator, Waterra) was attached to a bench above the piezometer (Fig. D.2). The pump could not be attached to the piezometer itself because it is not strong enough to withstand the the vibrations.
- The tube of a inertial pump, with the valve first, was inserted into the piezometer until about a meter above the base.
- The tube of the inertial pump was connected to the actuating arm of the water sampling pump and the fixed discharge point on the actuator. The tubing actuator was then turned on to oscillate the tubing-valve assembly up and down.
- Pumping was continued until 3-5 times the volume of the piezometer was discharged into a bucket.
- After, the tube was disconnected from the actuating arm and removed from the piezometer.

Figure D.2: Purging set-up, the water sampling pump was strapped to a bench and the leachate was collected in a bucket (not visible on picture).

D.2.2. RESULTS

The two 110 mm wells could not be purged as this would take a very long time using the water sampling pump and there was a possibility for the inertial pump to get clogged if there was too much suspended sediment. Piezometers 5.7, 5.10, 5.13, 5.15, 5.18, and 8.18 were purged on 09-03-2022 (Table. D.1). As seen in Table D.1, it was only possible to pump out 1.5 L of leachate from piezometer 5.7, so pumping was terminated after about 5 minutes as there was not enough leachate in the piezometer to allow the inertial pump to oscillate up and down without touching the base of the piezometer.

Table D.1: Purging details of piezometer nest 5 and piezometer 8.18.

Piezometer	Volume inside piezometer (L)	Volume pumped, approx. (L)
5.7	1.34	1.5
5.10	2.68	25
5.13	5.19	35
5.15	10.15	45
5.18	13.43	70
8.18	10.91	70

Piezometers 6.11, 6.14 7.9, 7.12, and 7.18 from nest 6 and 7 were purged on 11-04-2022 and 12-04-2022 (Table D.2). Piezometers 6.5 and 6.8 did not contain enough leachate to purge and piezometer 6.18 was damaged and had foam coming out of the top, so it was not suitable to conduct any sort of test on. Pumping took anywhere from 5 minutes (P5.7) to 36 minutes (P5.13). The difference was due to the volume that was pumped out and the recovery speed of the piezometer. For all piezometers, except P5.7 and P7.9, it was possible to continuously pump leachate out of the piezometer.

Table D.2: Purging details of piezometer nests 6 and 7.

Piezometer	Volume inside piezometer (L)	Pumped out (L)
5.7	1.34	1.5
5.10	2.68	25
5.13	5.19	35
5.15	10.15	45
5.18	13.43	70
8.18	10.91	70

D.3. CALIBRATION OF THE RHODAMINE FLUOROMETER

The fluorometer (Cyclops-7F) output was calibrated by measuring the output for a 400 mL sample of leachate with increasing RWT concentration.

D.3.1. METHODOLOGY

The following steps were performed to calibrate the RWT fluorometer:

- The background fluorescence of the sample was measured using the fluorometer. The temperature of the sample was also measured.
- The RWT stock solution (1% active ingredient RWT, see section E.1) was diluted by 10 and added in 0.5 ml increments to the 400 ml of leachate sample.
- The measurements were taken in the dark (as dark as it could get) to minimize the possible effect of sunlight. Measurements from the datalogger were read using a flashlight.
- A maximum of 4.0 - 5.0 ml of the RWT solution was added. The concentration of the leachate sample was measured before every extra addition of RWT solution.
- The obtained data was plotted as RWT concentration in ppb (parts per billion) to fluorometer output (AU).

D.3.2. RESULTS

The calibration curve for P5.10 is linear up to 625 ppb, P5.13 is linear up to about 875 ppb (Fig. D.4), P5.15 is linear up to 750 ppb (Fig. D.5), P5.18 up to 1000 ppb (Fig. D.6), well Z1 up to 875 (Fig. D.7, and P8.18 up to 875 ppb (Fig. D.8).

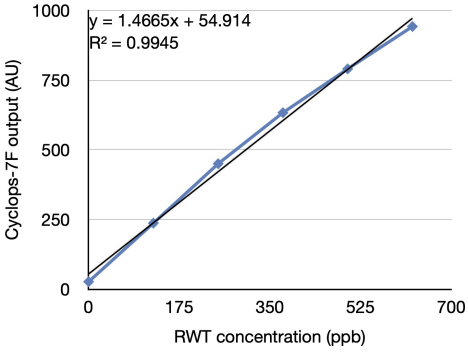

Figure D.3: Linear calibration curve for the RWT (Rhodamine water tracer) fluorometer performed on piezometer 5.10.

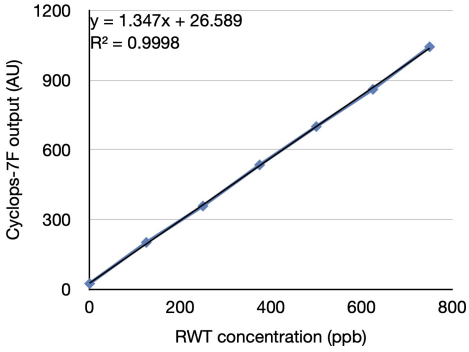

Figure D.4: Linear calibration curve for the RWT (Rhodamine water tracer) fluorometer performed on piezometer 5.13.

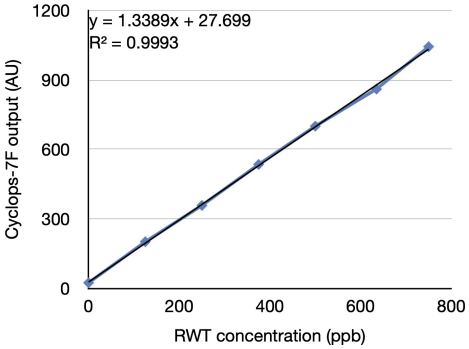

Figure D.5: Linear calibration curve for the RWT (Rhodamine water tracer) fluorometer performed on piezometer 5.15.

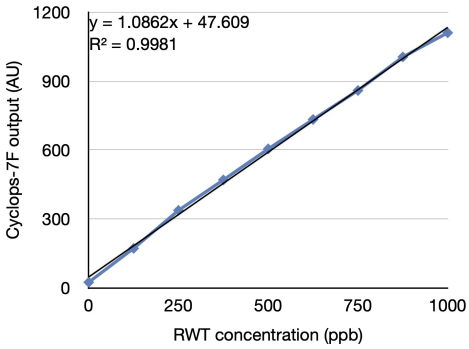

Figure D.6: Linear calibration curve for the RWT (Rhodamine water tracer) fluorometer performed on piezometer 5.18.

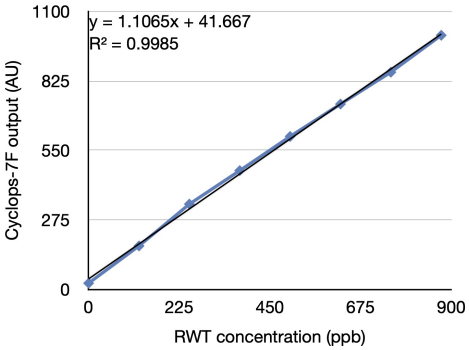

Figure D.7: Linear calibration curve for the RWT (Rhodamine water tracer) fluorometer performed on well Z1.

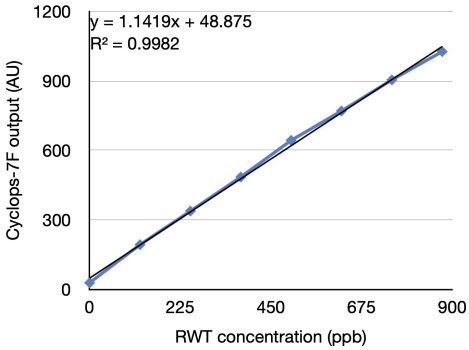

Figure D.8: Linear calibration curve for the RWT (Rhodamine water tracer) fluorometer performed on piezometer 8.18.

E

UNIFORM BOREHOLE DILUTION TESTS

E.1. MAKING A STANDARD STOCK SOLUTION

A stock tracer solution was prepared because RWT is sold as a 20% active ingredient solution, a concentration too high to be measured using a fluorometer.

- 5 grams of the RWT (20% active ingredient) was weighed into a measuring cup with a pipette.
- The measured RWT was diluted into a volumetric flask of 1 L, making sure all the RWT from the measuring cup got into the volumetric flask. The RWT was diluted until the 1 L mark with a combination of distilled and tap water. The dilution leads to a stock solution with a concentration of 1 ppt (parts per thousand).
- The diluted mixture was thoroughly mixed by putting a cap on the flask, inverting, and waiting for air bubbles to rise. Then the flask was swirled for a few seconds and righted again, waiting for the bubbles to rise. These steps were repeated a few times.

E.2. OVERNIGHT SET UP

To perform overnight logged measurement of the concentration, the datalogger and an external battery were secured in a box to protect from possible rain and moisture (Fig. E.1).

Figure E.1: Overnight set-up of a dilution test, datalogger and external battery were secured in a plastic box. The rod with the fluorometer was attached to the piezometer with tape. A hole in the box allowed for the rod to attach to the datalogger.

F

LEACHATE LEVELS

F.1. LEACHATE LEVELS MEASURED IN THE WASTE BODY

Leachate levels in the gas wells and the A wells were measured by the landfill operators using a dip-meter (Fig. F.1 and F.2). Measurements were conducted weekly. Leachate levels of the newly installed piezometer nests (5, 6, 7, and 8) and wells (Z1 and Z2) were performed manually and in light of this research (Fig. F.3).

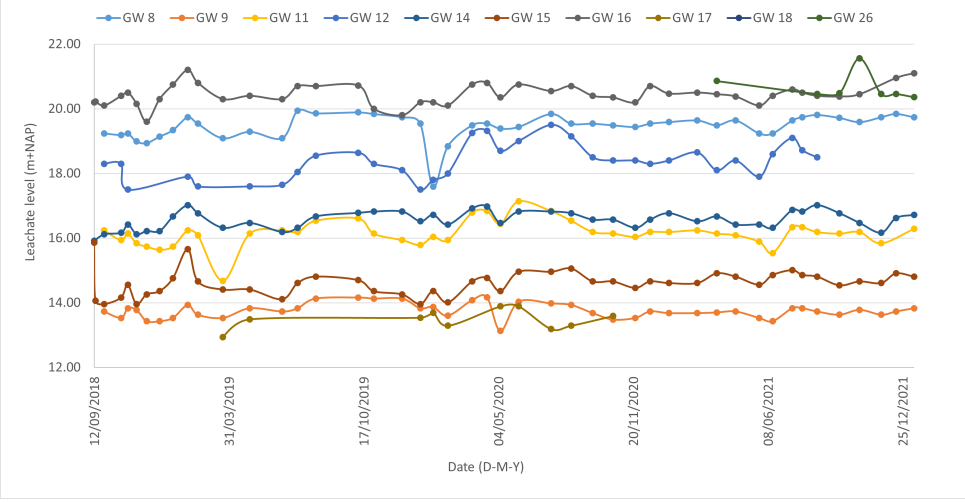

Figure F.1: Leachate levels measured in the gas wells throughout compartment 3 using a dip-meter.

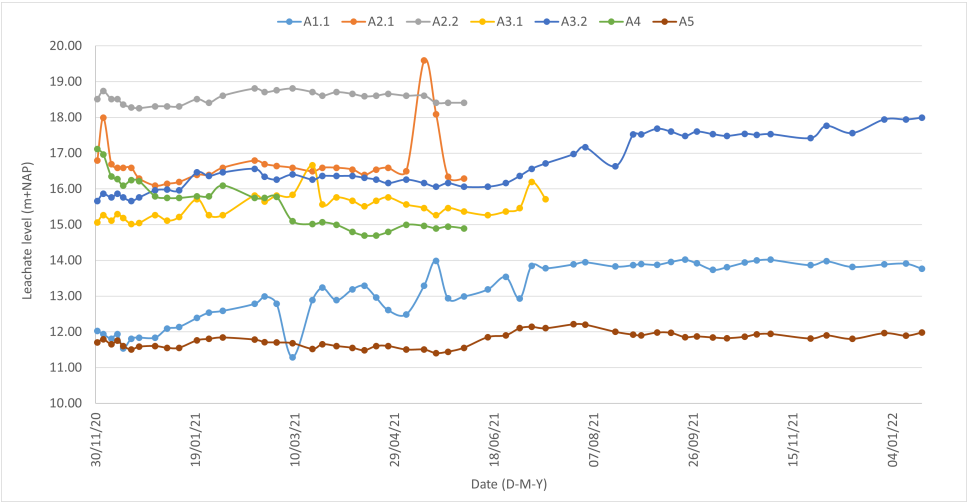

Figure F.2: Leachate levels measured in the A wells throughout compartment 3 using a dip-meter.

Figure F.3: Leachate levels measured in the newly installed piezometers using a dip-meter.

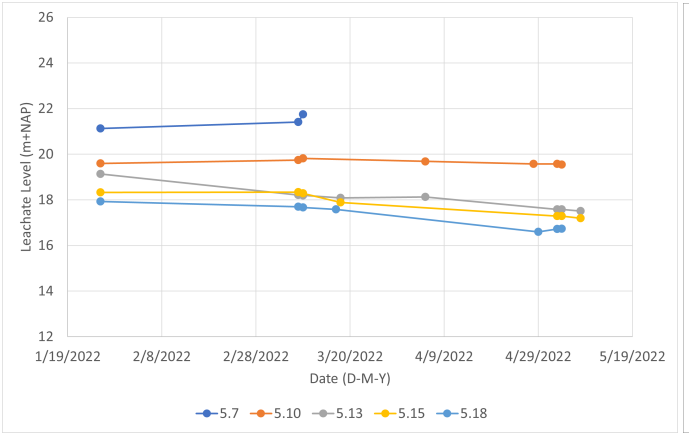

(a) Leachate level measurements of piezometer nest 5.

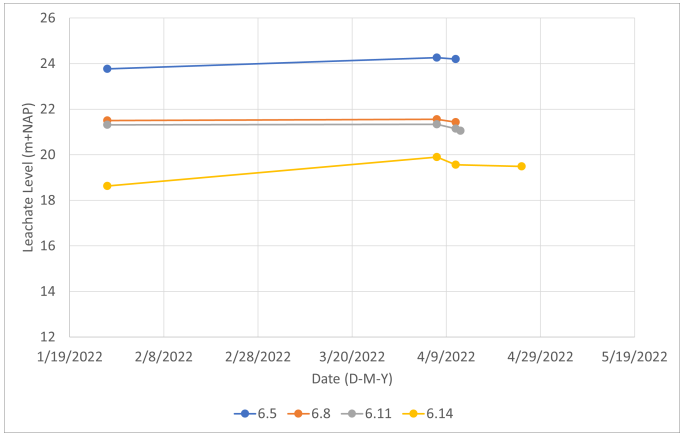

(b) Leachate level measurements of piezometer nest 6.

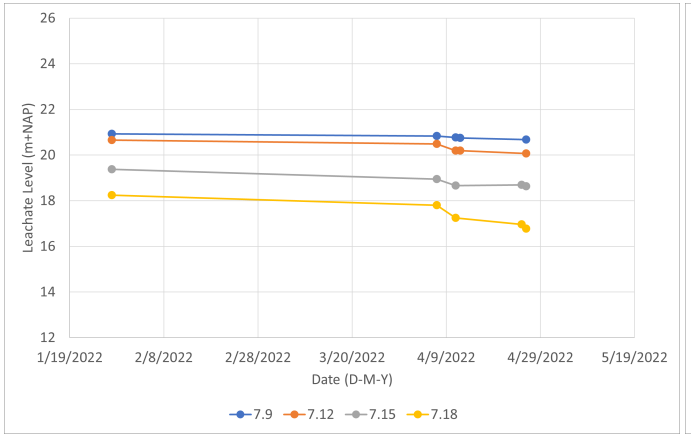

(c) Leachate level measurements of piezometer nest 7.

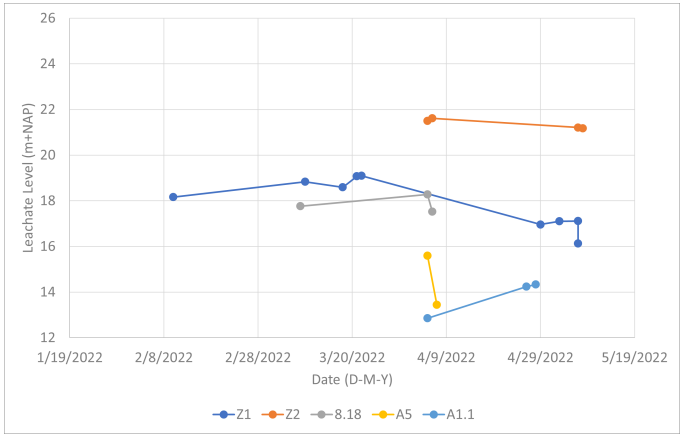

(d) Leachate level measurements of the Z wells, wells A1.1 and A5, and piezometer 8.18.

F.2. LEACHATE LEVELS MEASURED ACROSS THE INFILTRATION DRAINS

Leachate levels across the infiltration drains were measured by CTD-Divers. More information about the piezometers installed across the drains and their measurement depth can be found in Appendix C. The infiltration drains are located approximately 0.5-0.9 m below ground level and the drains are not entirely horizontal (Fig. F.4 and F.5). Normalized leachate levels across RIS drain 2B and 3A are pictured in Figures F.6 and F.7.

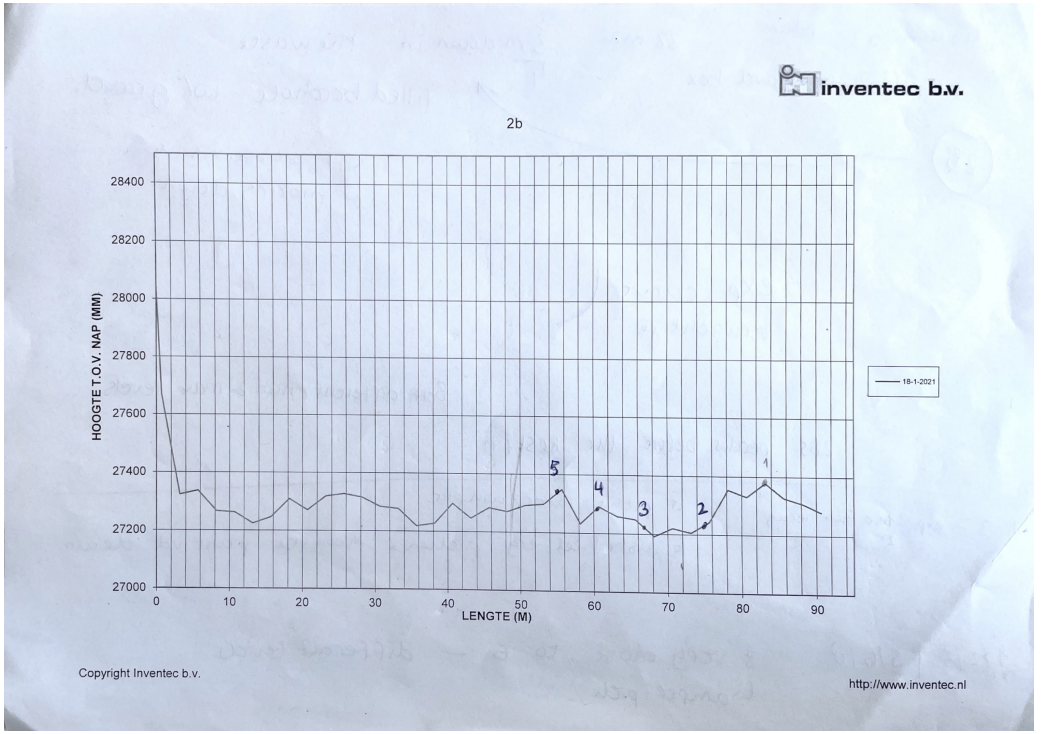

Figure F.4: Location of pressure gauge points in drain 2B compared to the height of the infiltration pipe.

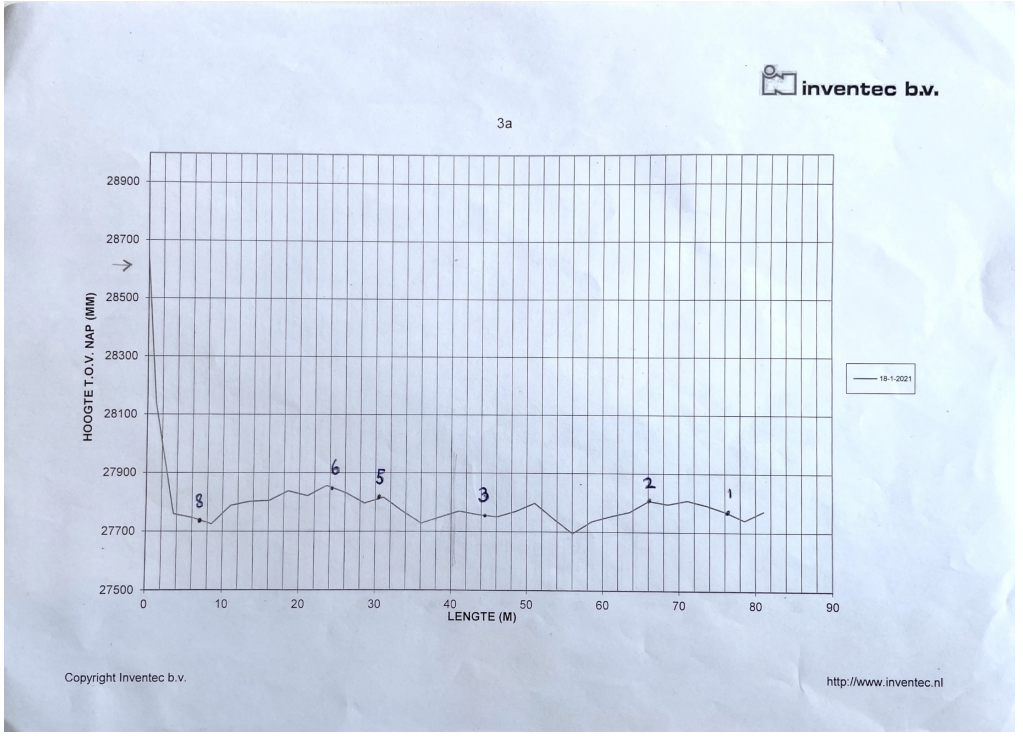

Figure F.5: Location of pressure gauge points in drain 3A compared to the height of the infiltration pipe.

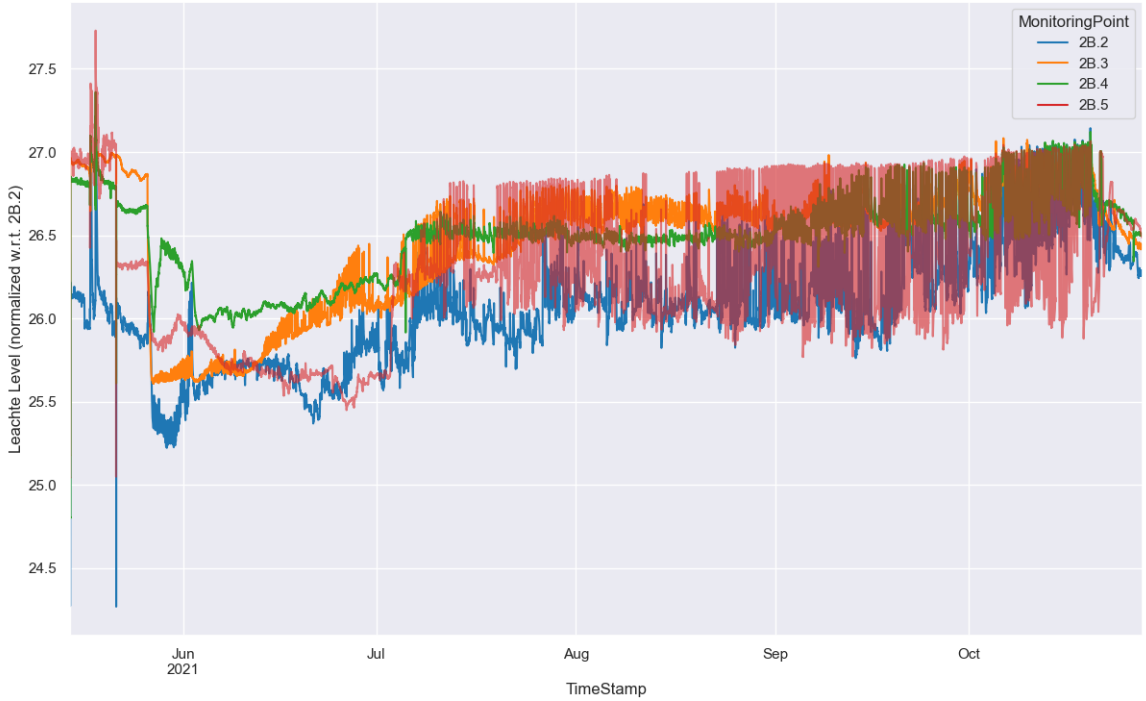

Figure F.6: Leachate levels measured by pressure gauges across RIS drain 2B, normalized with respect to point 2B.2.

Figure F.7: Leachate levels measured by pressure gauges across RIS drain 3A, normalized with respect to point 3A.1.

G

TIMELINE OF PERFORMED TESTS

For every week, the performed dilution tests are indicated in a timeline, together with the infiltration of the drains (Fig. G.1 - G.7).

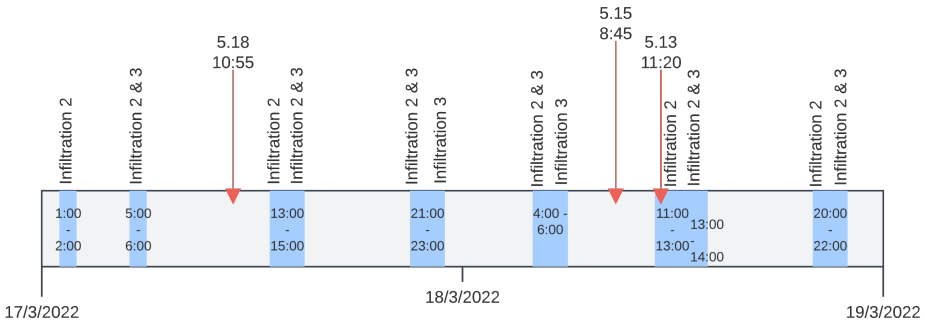

Figure G.1: Timeline of the infiltration and performed borehole dilution tests in week 11.

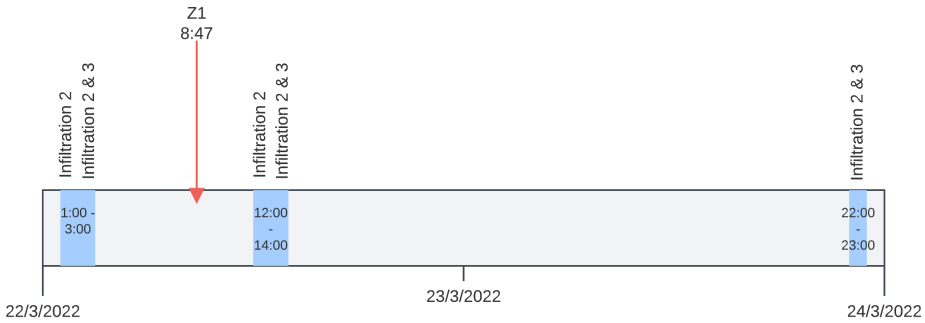

Figure G.2: Timeline of the infiltration and performed borehole dilution tests in week 12.

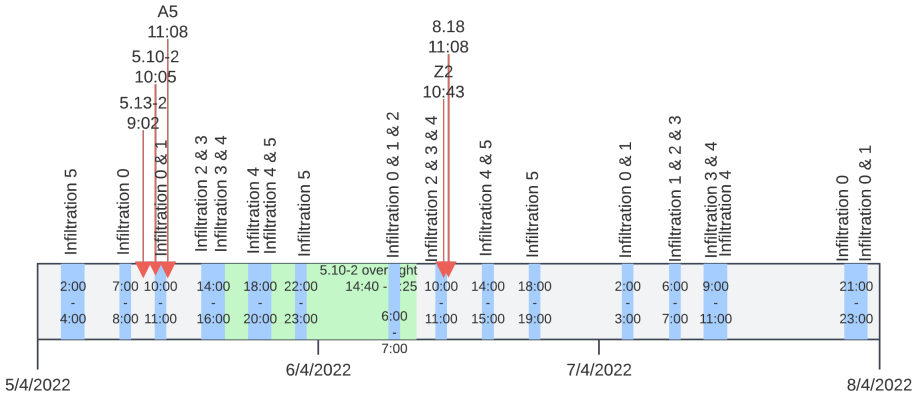

Figure G.3: Timeline of the infiltration and performed borehole dilution tests in week 14.

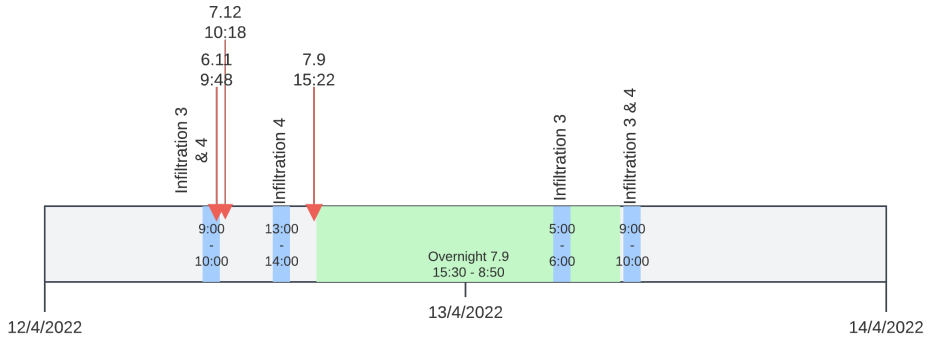

Figure G.4: Timeline of the infiltration and performed borehole dilution tests in week 15.

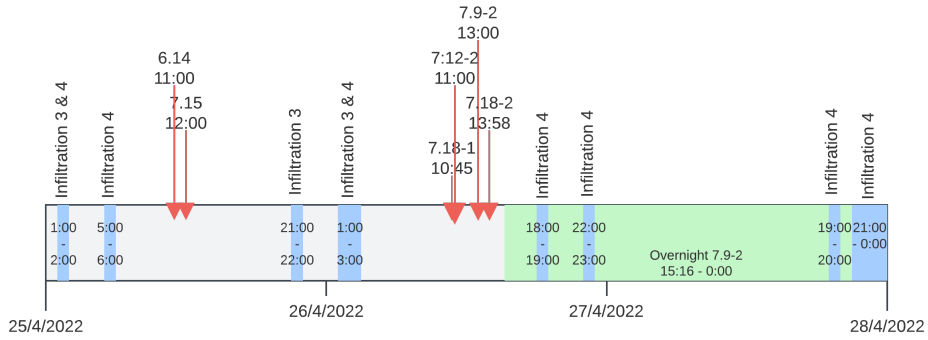

Figure G.5: Timeline of the infiltration and performed borehole dilution tests in week 17, part 1.

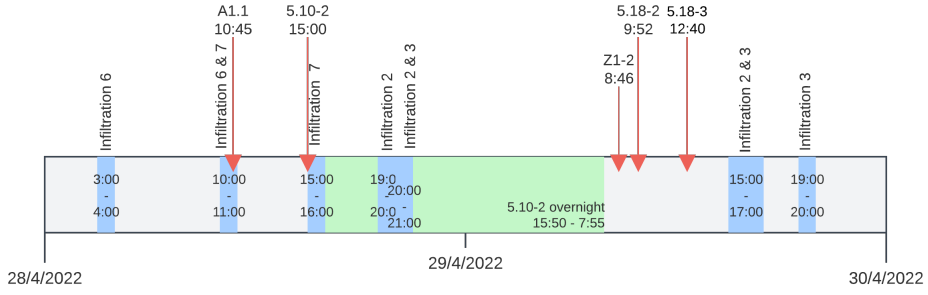

Figure G.6: Timeline of the infiltration and performed borehole dilution tests in week 17, part 2.

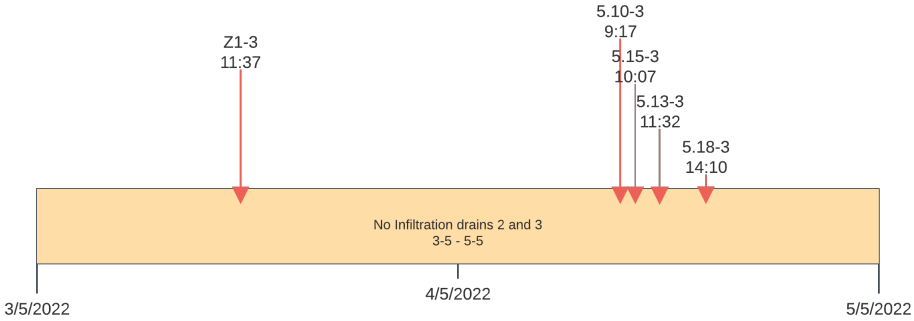

Figure G.7: Timeline of the infiltration and performed borehole dilution tests in week 18.

H

RWT CONCENTRATION-DEPTH GRAPHS

This Appendix contains all of the RWT concentration-depth diagrams. The tests are ordered by location: nest 5 and well Z1 (Fig. H.1a - H.5a), nest 6 (Fig. H.6a - H.6c), nest 7 (Fig. H.7a - H.9a), piezometer 8.18 and well Z2 (Fig. H.10a and H.10b), and wells A1.1 and A5 (Fig. H.11a and H.11b).

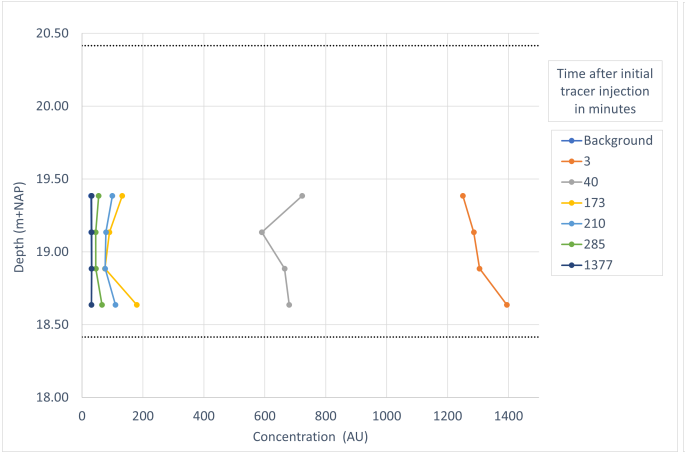

(a) Decline of Rhodamine water tracer concentration for test 5.10-1.

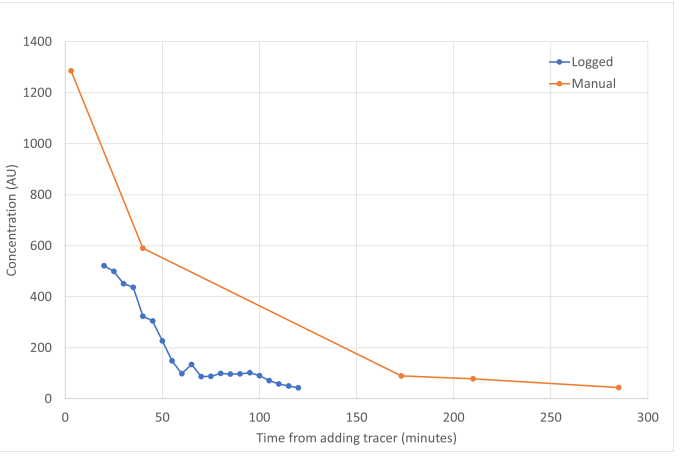

(b) Decline of Rhodamine water tracer concentration for overnight logged test 5.10-1.

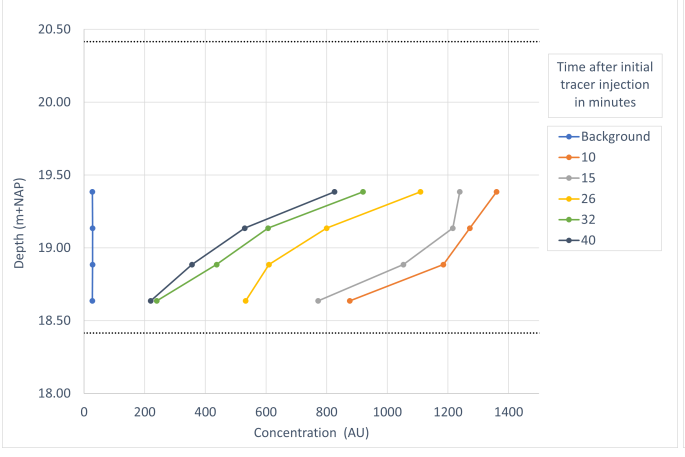

(c) Decline of Rhodamine water tracer concentration for test 5.10-2.

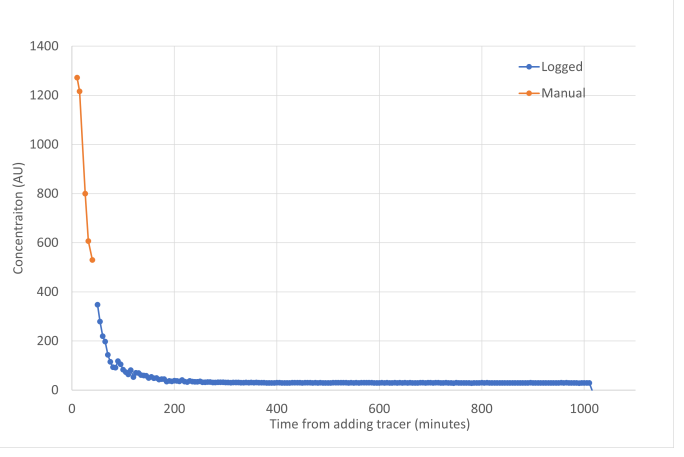

(d) Decline of Rhodamine water tracer concentration for overnight logged test 5.10-2.

Figure H.1: Decline of Rhodamine water tracer concentration over depth for test 5.10-1 and 5.10-2.

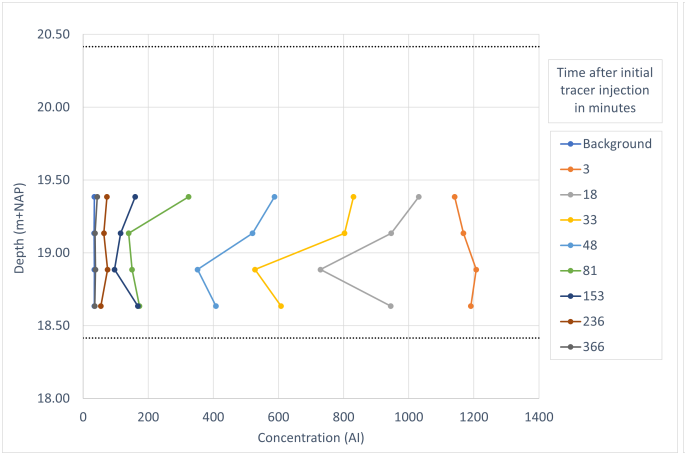

(a) Decline of Rhodamine water tracer concentration for test 5.10-3.

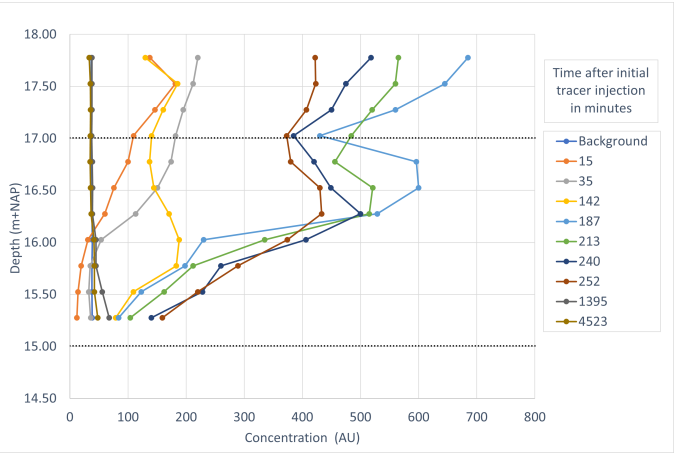

(b) Decline of Rhodamine water tracer concentration for test 5.13-1.

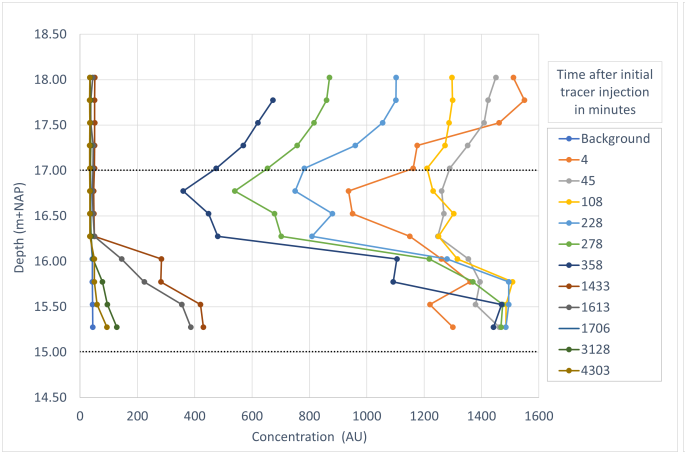

(c) Decline of Rhodamine water tracer concentration for test 5.13-2.

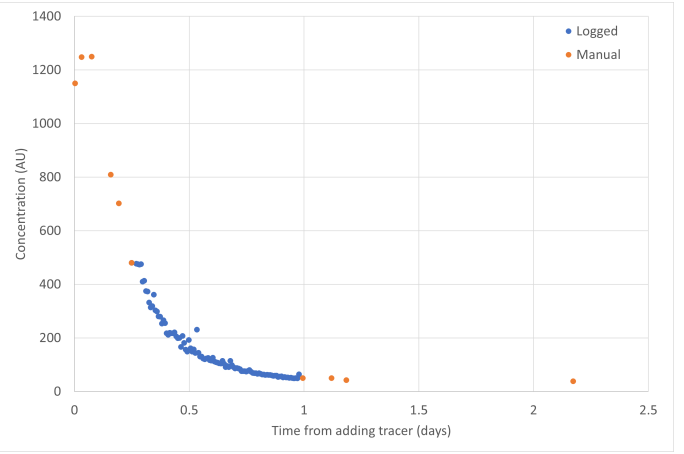

(d) Decline of Rhodamine water tracer concentration for overnight logged test 5.13-2.

Figure H.2: Decline of Rhodamine water tracer concentration over depth for test 5.10-3, 5.13-1, and 5.13-2.

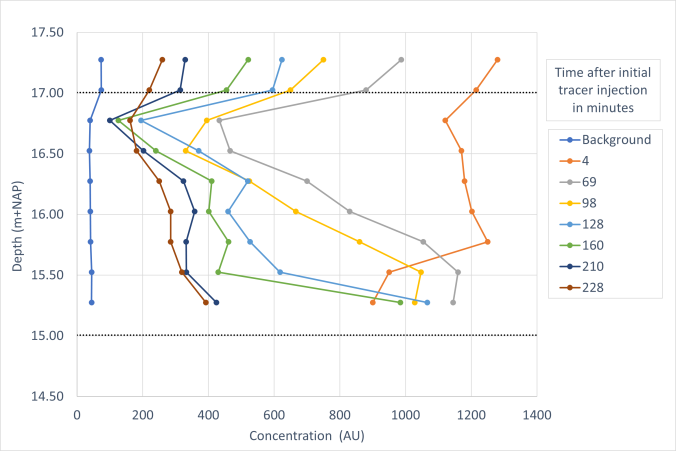

(a) Decline of Rhodamine water tracer concentration for test 5.13-3.

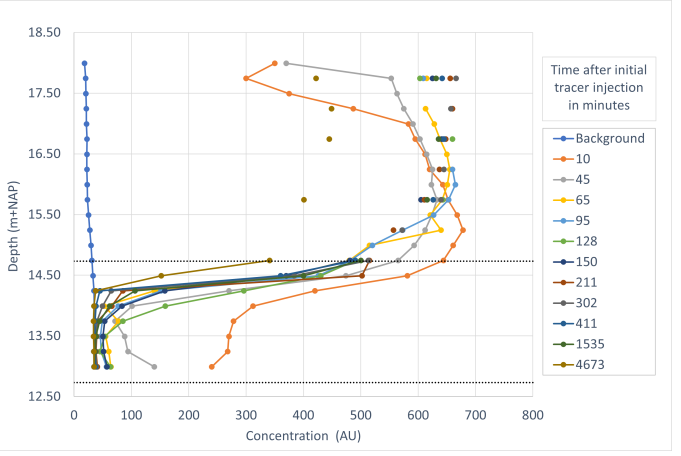

(b) Decline of Rhodamine water tracer concentration for test 5.15-1.

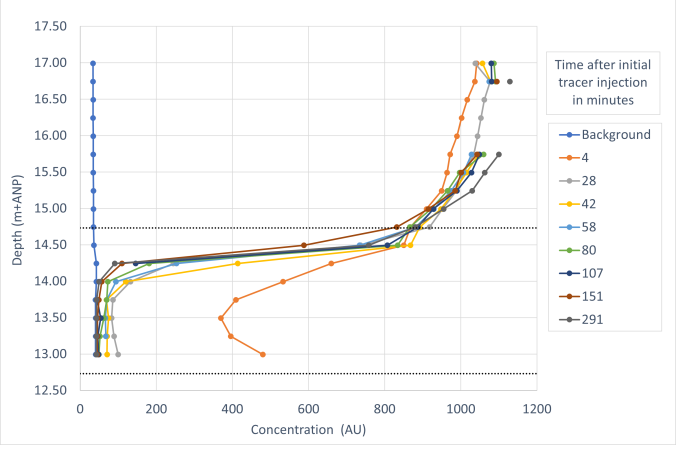

(c) Decline of Rhodamine water tracer concentration for test 5.15-2.

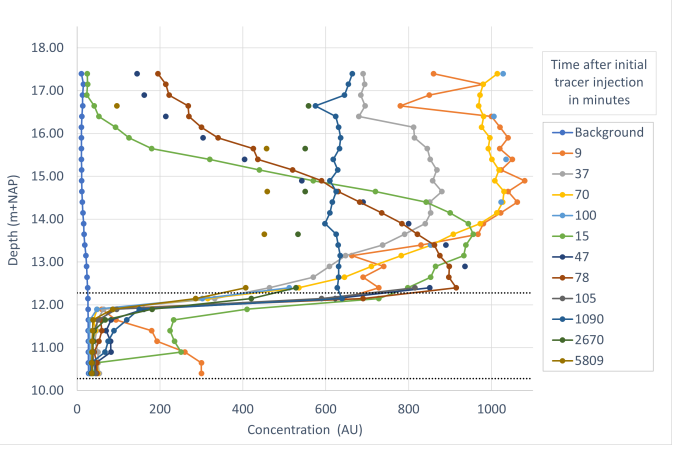

(d) Decline of Rhodamine water tracer concentration for test 5.18-1.

Figure H.3: Decline of Rhodamine water tracer concentration over depth for tests 5.13-3, 5.15-1, 5.15-2, and 5.18-1.

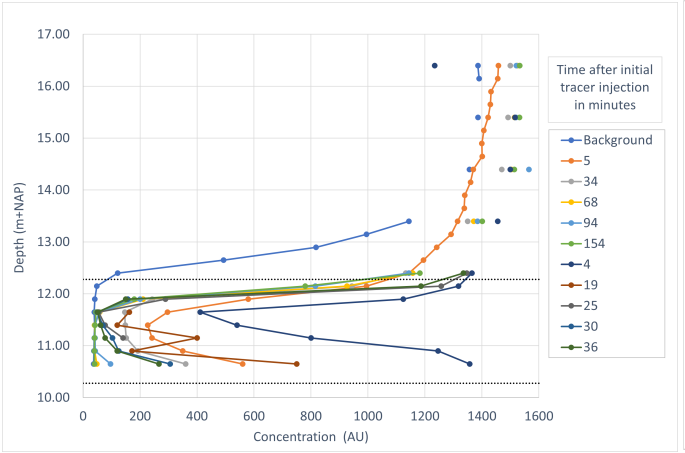

(a) Decline of Rhodamine water tracer concentration for test 5.18-2.

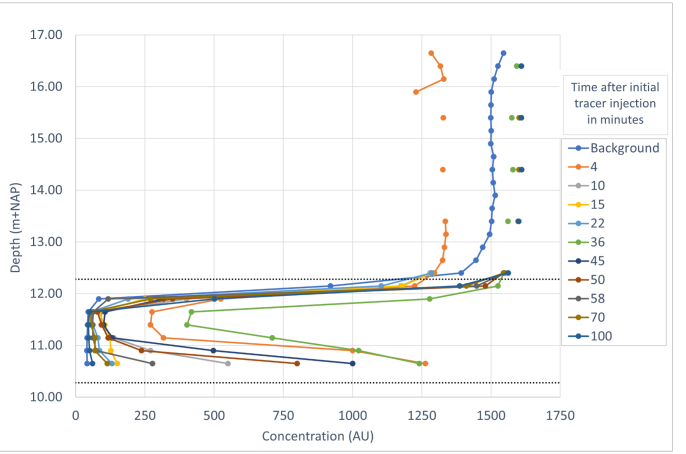

(b) Decline of Rhodamine water tracer concentration for test 5.18-3.

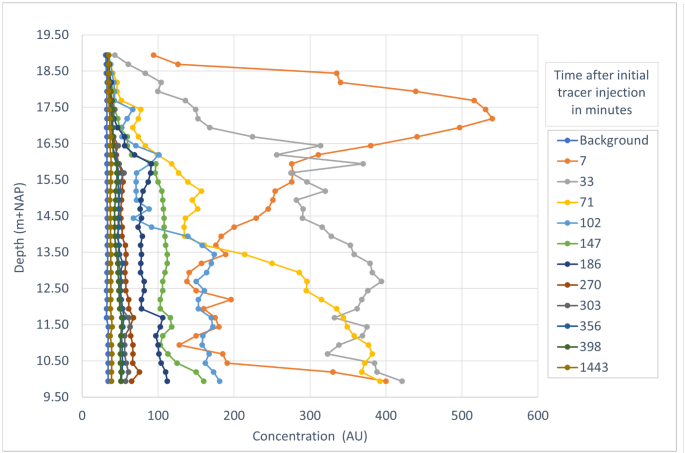

(c) Decline of Rhodamine water tracer concentration for test Z1-1.

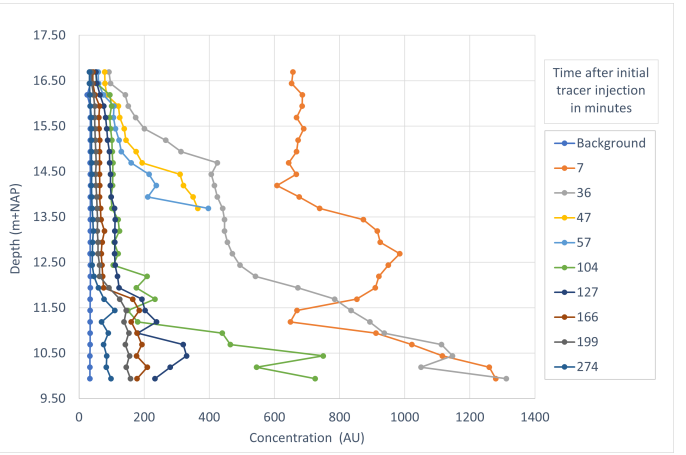

(d) Decline of Rhodamine water tracer concentration for test Z1-2.

Figure H.4: Decline of Rhodamine water tracer concentration over depth for tests 5,18-2, 5.18-3, Z1-1, and Z1-2.

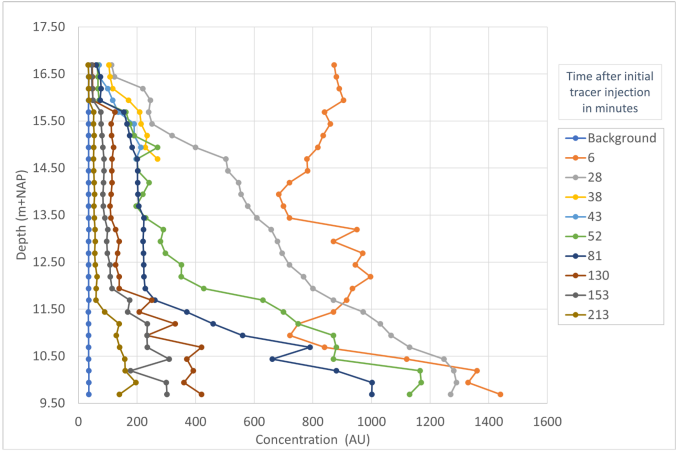

(a) Decline of Rhodamine water tracer concentration for test Z1-3.

Figure H.5: Decline of Rhodamine water tracer concentration over depth for test Z1-3.

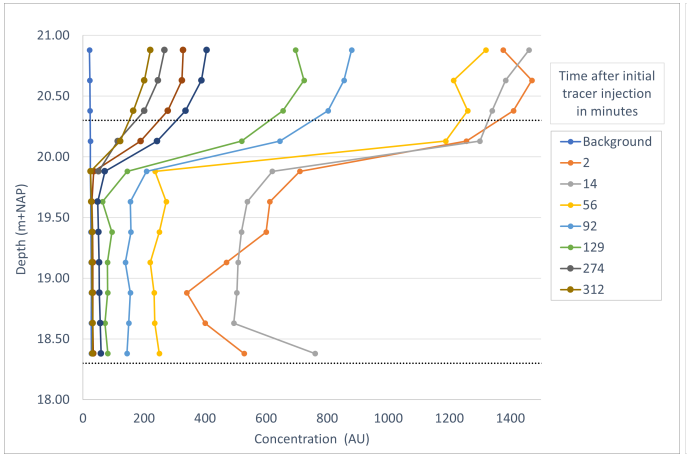

(a) Decline of Rhodamine water tracer concentration for test 6.11.

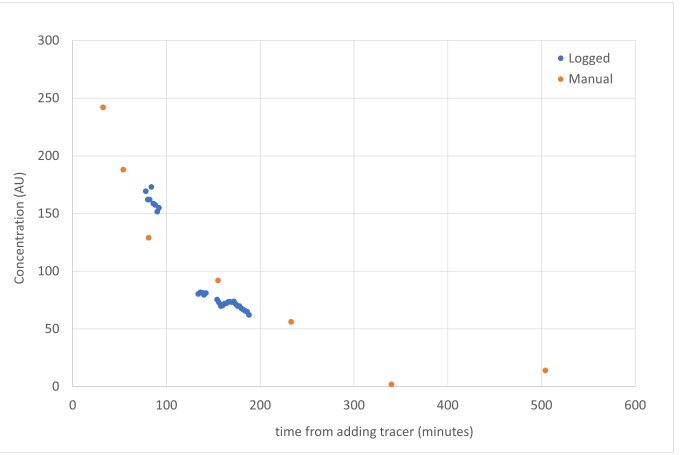

(b) Decline of Rhodamine water tracer concentration for logged for test 6.11.

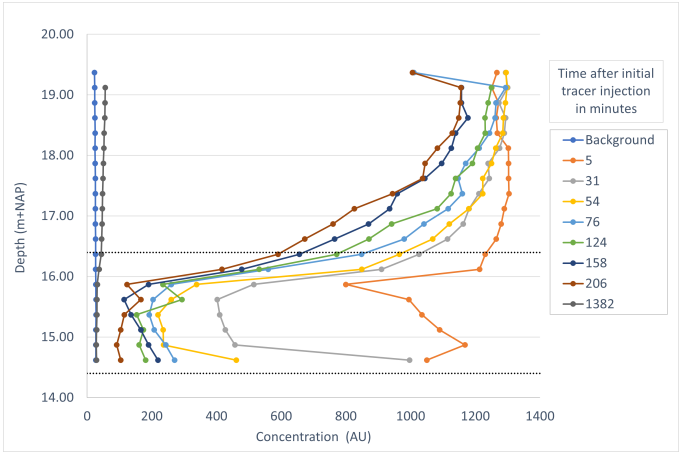

(c) Decline of Rhodamine water tracer concentration for test 6.14.

Figure H.6: Decline of Rhodamine water tracer concentration over depth for piezometer 6.11 and 6.14.

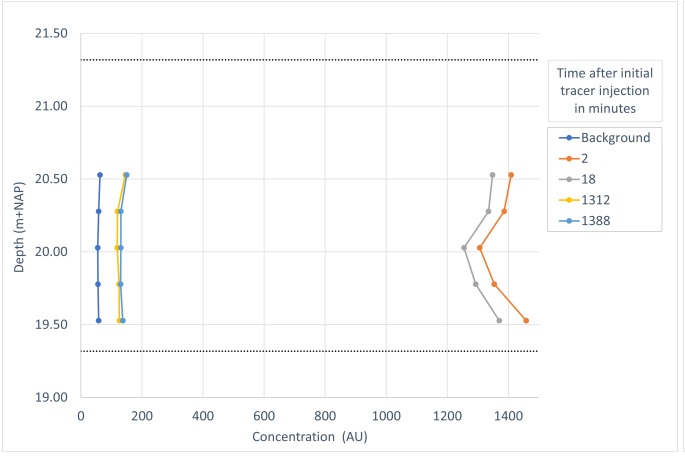

(a) Decline of Rhodamine water tracer concentration for test 7.9-1.

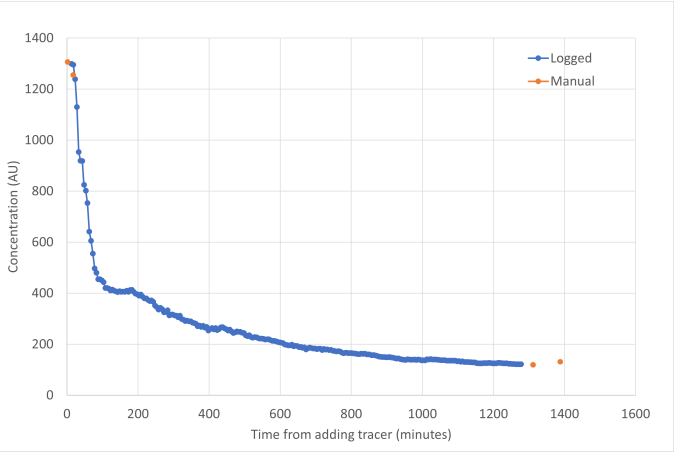

(b) Decline of Rhodamine water tracer concentration for logged overnight test 7.9-1.

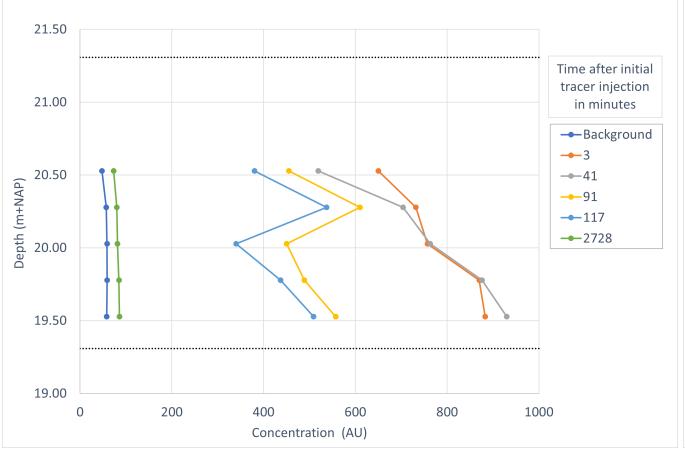

(c) Decline of Rhodamine water tracer concentration for test 7.9-2.

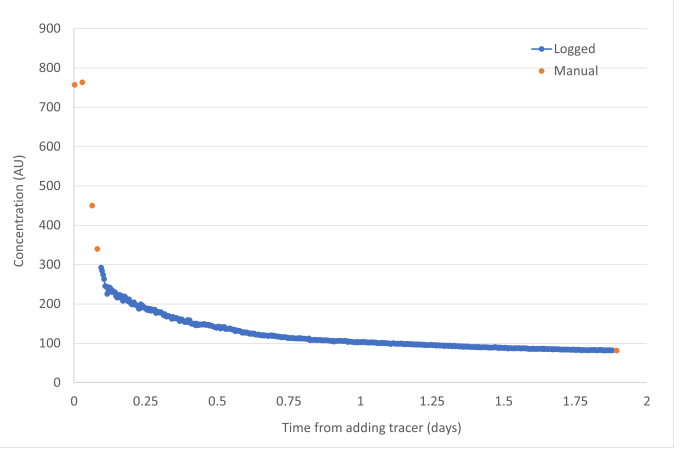

(d) Decline of Rhodamine water tracer concentration for overnight logged test 7.9-2.

Figure H.7: Decline of Rhodamine water tracer concentration over depth for piezometer 7.9.

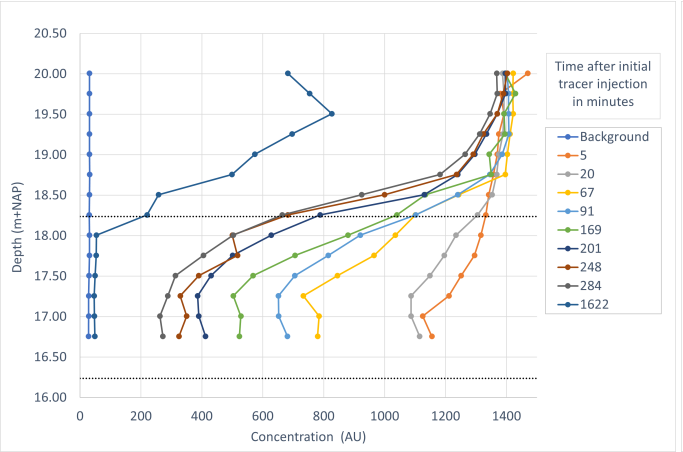

(a) Decline of Rhodamine water tracer concentration for test 7.12-1.

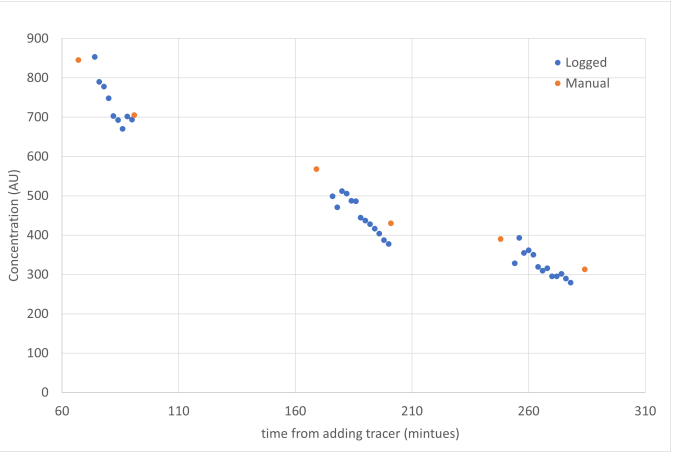

(b) Decline of Rhodamine water tracer concentration for logged overnight test 7.12-1.

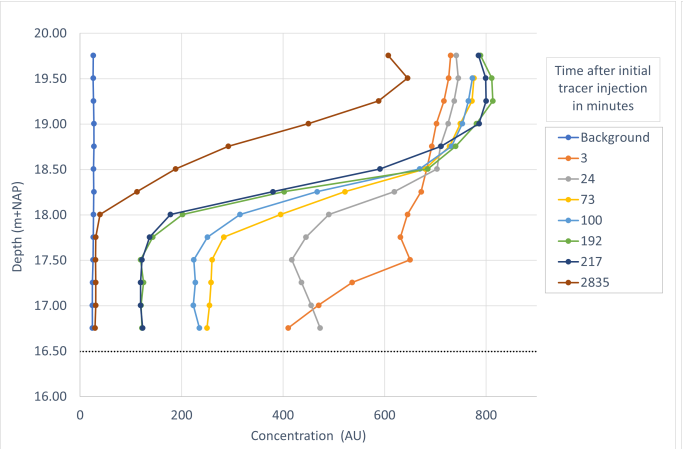

(c) Decline of Rhodamine water tracer concentration for test 7.12-2.

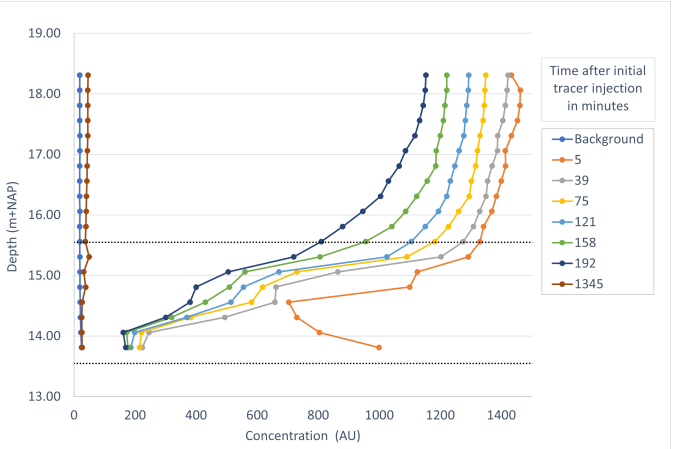

(d) Decline of Rhodamine water tracer concentration for test 7.15.

Figure H.8: Decline of Rhodamine water tracer concentration over depth for piezometers 7.12 and 7.15.

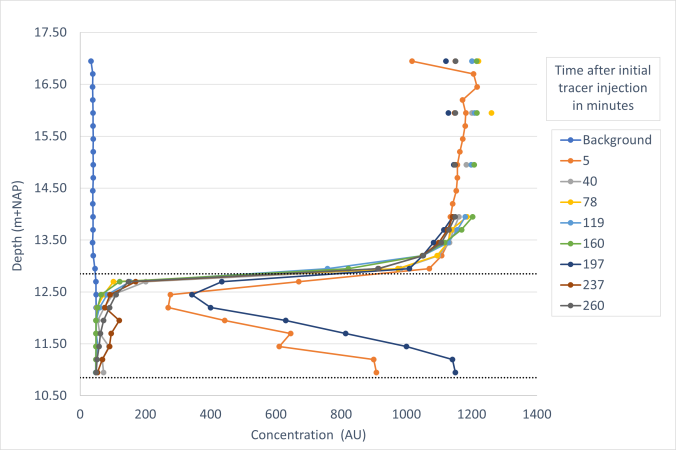

(a) Decline of Rhodamine water tracer concentration for test 7.18.

Figure H.9: Decline of Rhodamine water tracer concentration over depth for piezometer 7.18.

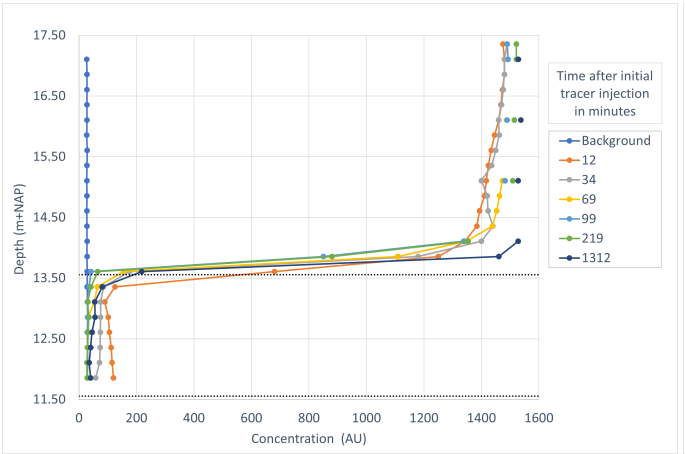

(a) Decline of Rhodamine water tracer concentration for test 8.18.

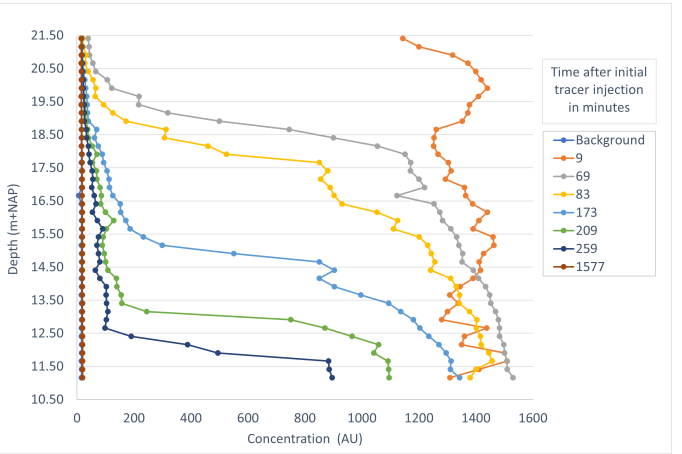

(b) Decline of Rhodamine water tracer concentration for for test Z2.

Figure H.10: Decline of Rhodamine water tracer concentration over depth for piezometer 8.18 and well Z2.

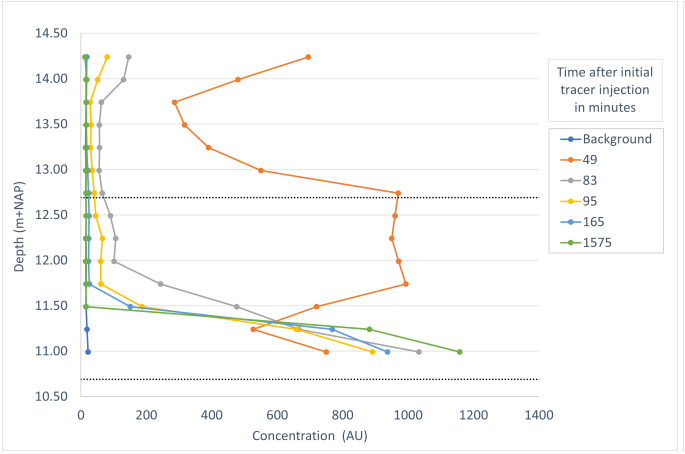

(a) Decline of Rhodamine water tracer concentration for test A1.1.

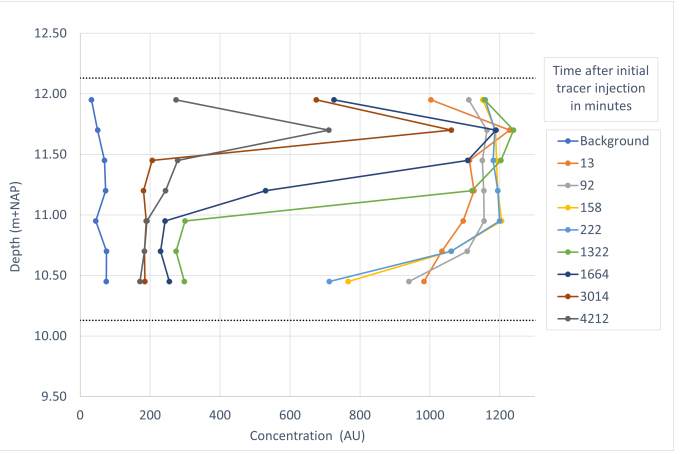

(b) Decline of Rhodamine water tracer concentration for for test A5.

Figure H.11: Decline of Rhodamine water tracer concentration over depth for wells A1.1 and A5.

I

POINT DILUTION TESTS

I.1. Z1-v-1

Dip to leachate before the test was 11.58 m-BTC. Tracer was injected at 11:27 on 07-05-2022. The fluorometer was inserted at 13.50 m-BTC, which was approximately 1.92 m below the leachate table, and 1.42 meter below the inserted slug of tracer. Dip to leachate after the test, at 17:30 was 13.56 mBTC, an increase of 6 cm. The infiltration timeline shows that drains 2 and 3 infiltrated between 09:00 and 10:00 prior to the start of the test.

Table I.1: Manual and logged measurements of the point dilution test Z1-v-1. The time is the time when tracer was first detected at the corresponding depth of the fluorometer.

Manual measurements			**Logged measurements**		
Time	**Fluorometer (mBTC)**	**Velocity (m/d)**	**Time**	**Fluorometer (mBTC)**	**Velocity (m/d)**
11:27	12.08		11:27	12.08	
11:39	13.50	170.4	11:39	13.50	170.4
11:46	15.00	308.6	11:48	15.00	240.0
11:52	16.00	240.0	11:57	16.00	160.0
12:08	17.00	90.0	12:05	17.00	180.0
12:22	18.00	102.9	12:18	18.00	110.8
12:31	18.75	120.0	12:31	18.75	83.1
	Average	172.3		Average	157.4
	St. dev	96.8		St. dev	55.2

I.2. Z2-v-1

Dip to leachate before the start of the test was 7.70 m-BTC. Tracer was injected at 14:10 on 07-05-2022. The fluorometer was inserted at 9.75 m-BTC, which was about 2.05 meters below the leachate table, and 1.55 meters below the inserted tracer slug. Figure I.1 shows the RWT concentration-depth profiles taken after the point dilution test had finished.

Table I.2: Manual and logged measurements of the point dilution test Z2-v-1. The time is the time when tracer was first detected at the corresponding depth of the fluorometer.

Manual measurements		
Time	**Fluorometer (mBTC)**	**Velocity (m/d)**
14:11	8.20	
14:32	9.75	106.3
14:46	10.75	102.9
14:57	11.75	130.9
15:18	12.75	68.6
15:37	14.75	151.6
15:51	15.75	102.9
16:16	16.75	57.6
16:34	17.75	80.0
	Average	100.1
	St. dev	31.3

I.3. Z2-v-2

Dip to leachate before the start of the test was 7.74 mBTC. Tracer was injected at 09:16 on 08-05-2022. The fluorometer was set at 9.75 m beneath the top of the well, which was about 2.01 m below the top of the leachate, and 1.51 m below the injected tracer of the slug. The test was repeated because the point dilution test from the day prior did not have any logged data. Figure I.2 shows the RWT concentration at 11:06 and 14:57 after test Z2-v-2 (grey and yellow). The measurement at 16:19 was a concentration-depth profile taken after test Z2-v-3.

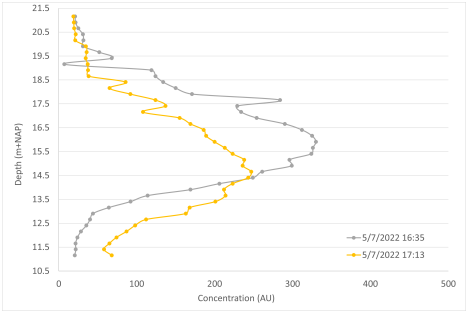

Figure I.1: Change of RWT (Rhodamine water tracer) concentration over depth for point dilution test Z2-v-1.

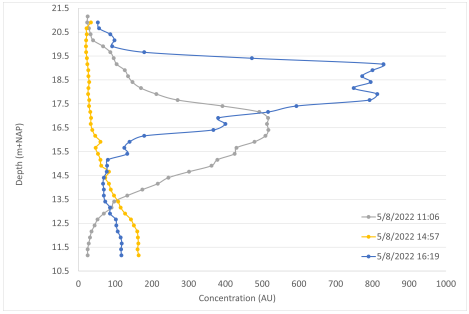

Figure I.2: Change of RWT (Rhodamine water tracer) concentration over depth for point dilution test Z2-v-2.

Table I.3: Manual and logged measurements of the point dilution test Z2-v-2. The time is the time when tracer was first detected at the corresponding depth of the fluorometer.

Manual measurements			**Logged measurements**		
Time	**Fluorometer (mBTC)**	**Velocity (m/d)**	**Time**	**Fluorometer (mBTC)**	**Velocity (m/d)**
09:16	8.24		09:16	8.24	
09:29	9.75	167.3	09:29	9.75	167.3
09:55	12.75	166.2	09:45	10.75	90.0
10:08	13.75	110.8	09:55	11.75	144.0
10:20	14.75	120.0	10:08	12.75	110.8
10:41	15.75	68.6	10:22	14.75	205.7
11:05	17	75.0	10:42	15.75	72.0
			11:06	17.00	75.0
	Average	118.0		Average	123.5
	St. dev	42.6		St. dev	50.6

I.4. Z2-v-3

Dip to leachate before the start of the test was 7.72 mBTC. Tracer was injected at 15:07 on 08-05-2022. The fluorometer was left at 9.75 mBTC, which was about 2.03 m below the leachate table and 1.53 m below injected tracer slug. The output of the fluorometer at the start of the test was 26.7 AU. A few moments after injection, the sensor was pulled up to 8.25 mBTC to get an estimation of the starting concentration, which was about 1600

AU. The blue graph in Figure I.2 shows the downward movement of the tracer slug 49 minutes after injection. At that point, the maximum RWT concentration was only 800 AU.

I.5. 5.13-V-1

Dip to leachate before the start of the test: 10.77 mBTC. Tracer was injected at 11:32. The fluorometer was attached at 13.00 mBTC, 0.27 m above the base of the piezometer, about 2.25 m below the leachate table, and 1.75 m below the injected tracer slug. This corresponds to about 15.75 m+NAP in the concentration-depth graph (Fig. 5.26)

J

INCREASED MIXING VOLUME

Figure 6.1 illustrates four possible scenarios for the installation of the new wells and piezometers: 1) Installation as designed, 2) No filter pack installed, 3) Some filter pack installed, but not uniformly, 4) No annulus. Table J.1 shows the calculation process behind the four scenarios, were the required mass of tracer for the filter section is calculated using the minimum and maximum mixing volume per scenario. These minimum and maximum masses were compared to the actual used tracer masses and initial tracer concentration (Table 6.2).

The Darcy velocities were calculated using the back-calculated diameters of piezometers 5.10 and 5.18 presented in section 6.2.1.1 (Fig. J.1 - J.6).

Table J.1: Four installation scenarios and the tracer mass needed to reach a certain target concentration, test 5.10-3 is used as example.

	1) As designed	**2) No filter pack**	**3) Some filter pack**	**4) No annulus**
Borehole diameter (mm)	150	150	150	50
Casing diameter ID (mm)	48	48	48	48
Well depth (m)	10.22	10.22	10.22	10.22
Dip to leachate (m)	9.09	9.09	9.09	9.09
Filter length (m)	1.13	1.13	1.13	1.13
Volume of filter section only (L)	2.04	2.04	2.04	2.04
Volume of borehole around filter (L)	17.92	17.92	17.92	0.00
Porosity of sand (%)	40	40	40	40
Pore volume of borehole (L)	7.2	7.2	7.2	0.0
Minimum mixing volume (L)	2.04	2.04	2.04	2.04
Maximum mixing volume (L)	9.21	19.97	19.97	2.04
Target tracer concentration (ppb)	1191	1191	1191	1191
(mg/L)	1.191	1.191	1.191	1.191
Mass tracer need for filter section				
For minimum mixing volume (mg tracer)	2.44	2.44	2.44	2.44
For maximum mixing volume (mg tracer)	10.97	23.78	23.78	2.44

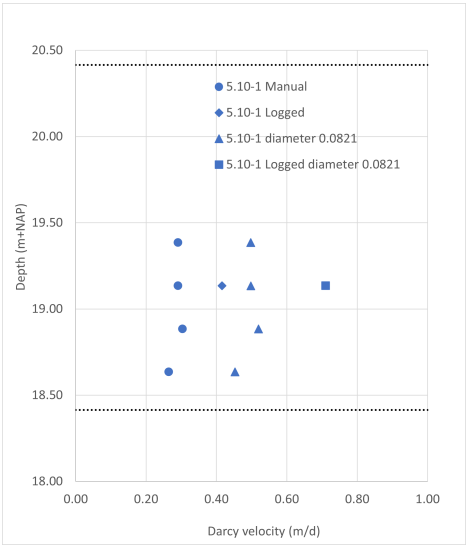

Figure J.1: Darcy velocity calculated for test 5.10-1, with diameter of 0.048 m and increased diameter of 0.0821 m.

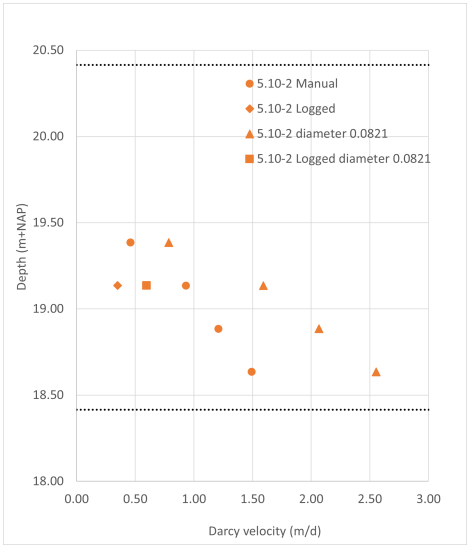

Figure J.2: Darcy velocity calculated for test 5.10-2, with diameter of 0.048 m and increased diameter of 0.0821 m.

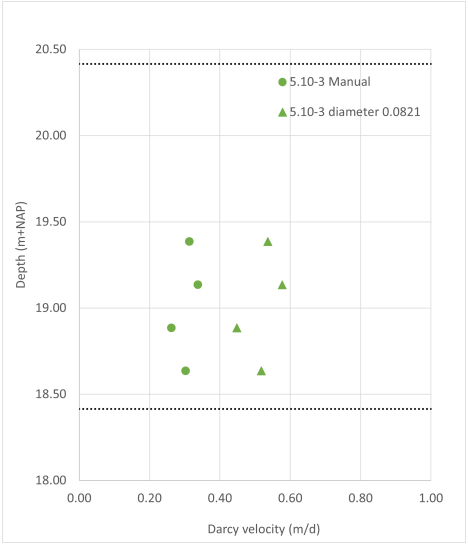

Figure J.3: Darcy velocity calculated for test 5.10-3, with diameter of 0.048 m and increased diameter of 0.0821 m.

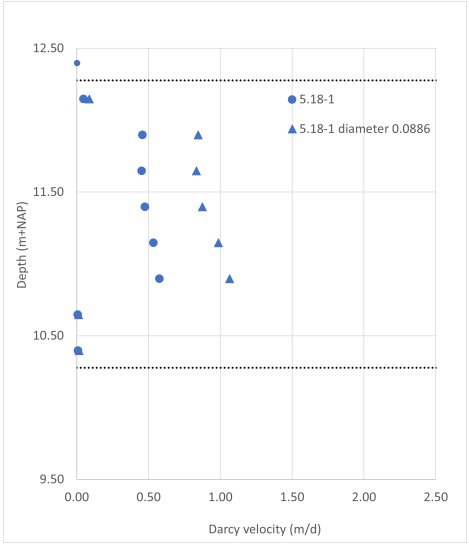

Figure J.4: Darcy velocity calculated for test 5.18-1, with diameter of 0.048 m and increased diameter of 0.0886 m.

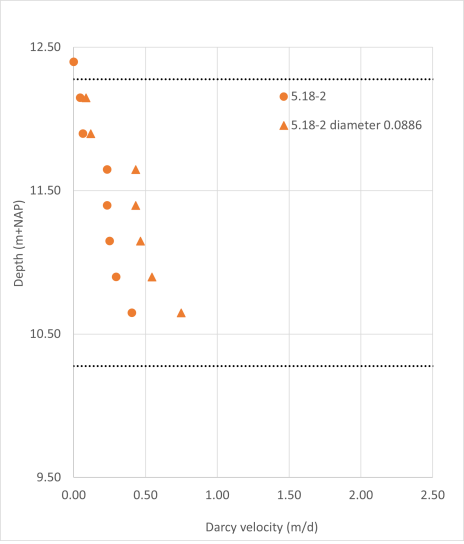

Figure J.5: Darcy velocity calculated for test 5.18-2, with diameter of 0.048 m and increased diameter of 0.0886 m

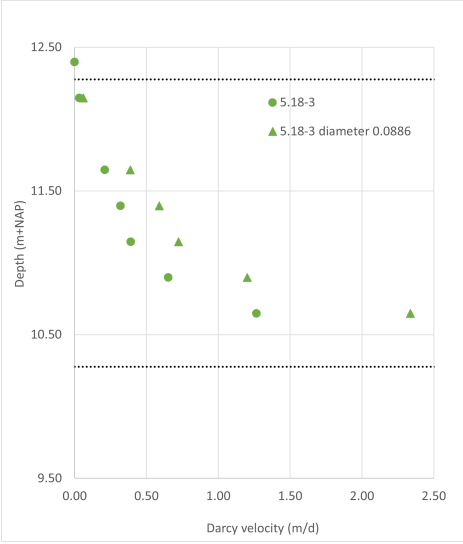

Figure J.6: Darcy velocity calculated for test 5.18-3, with diameter of 0.048 m and increased diameter of 0.0886 m.

K

Darcy velocity with error bars

The Darcy velocity calculated using the calculated range of borehole correction factors calculated in Table 6.4 are shown in Figures K.1 - K.18. The blue dot is the Darcy velocity calculated with a correction factor of 2, the error bars indicate the possible range of velocities based on an increased or decreased factor and the orange dot and error bars indicate a logged test result. An increase in Darcy velocity is the result of a lower borehole correction factor, and vice versa.

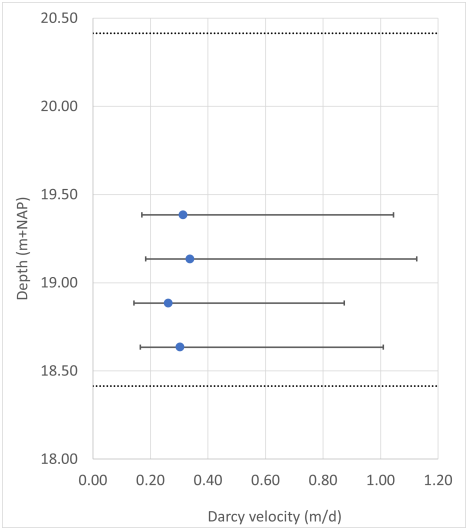

Figure K.1: Darcy velocities calculated for test 5.10-3, error bars indicate the range of velocities based on the estimated borehole correction factors.

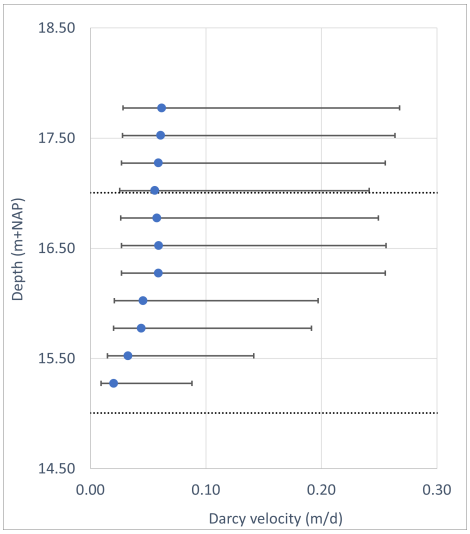

Figure K.2: Darcy velocities calculated for test 5.13-1, error bars indicate the range of velocities based on the estimated borehole correction factors.

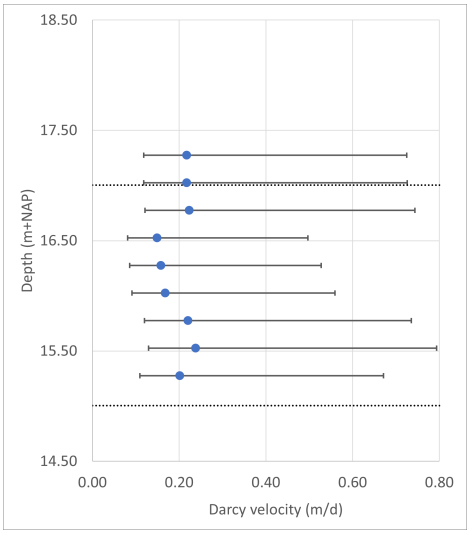

Figure K.3: Darcy velocities calculated for test 5.13-3, error bars indicate the range of velocities based on the estimated borehole correction factors.

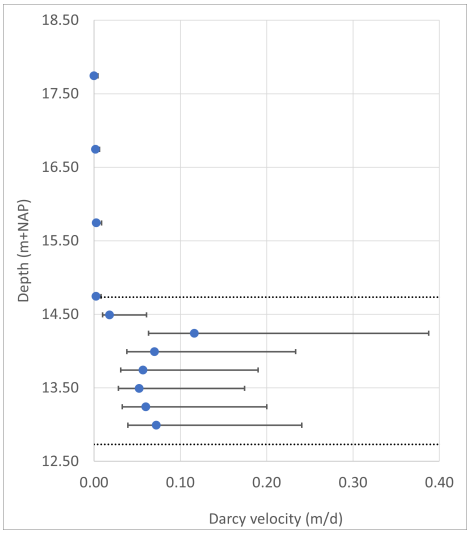

Figure K.4: Darcy velocities calculated for test 5.15-1, error bars indicate the range of velocities based on the estimated borehole correction factors.

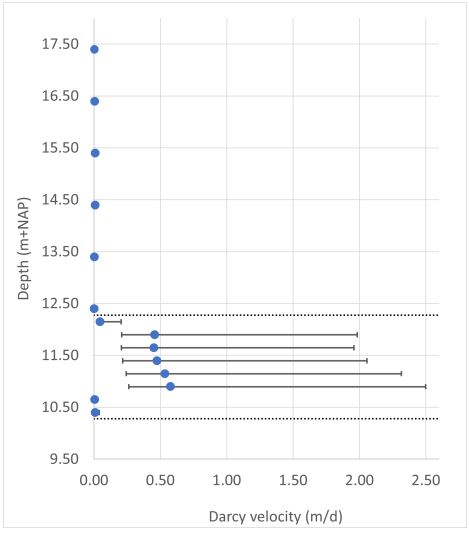

Figure K.5: Darcy velocities calculated for test 5.18-1, error bars indicate the range of velocities based on the estimated borehole correction factors.

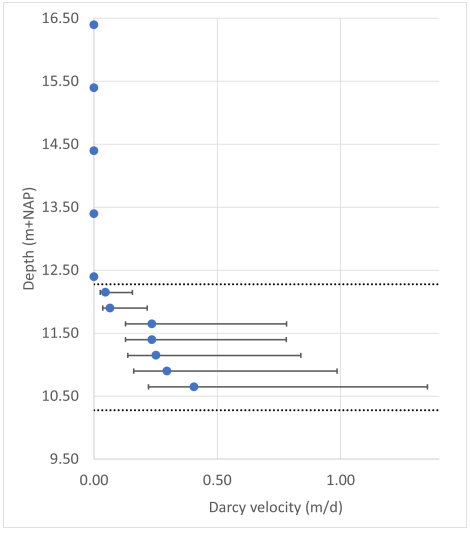

Figure K.6: Darcy velocities calculated for test 5.18-2, error bars indicate the range of velocities based on the estimated borehole correction factors.

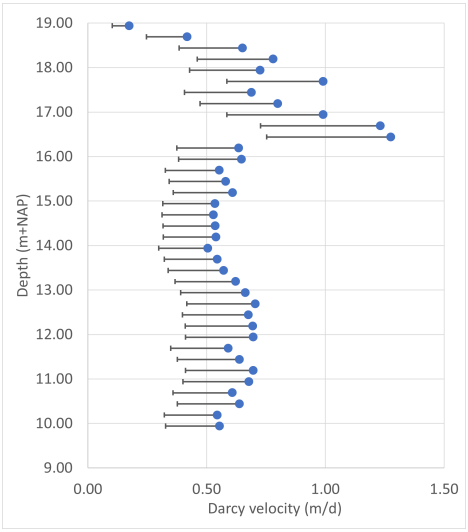

Figure K.7: Darcy velocities calculated for test Z1-1, error bars indicate the range of velocities based on the estimated borehole correction factors.

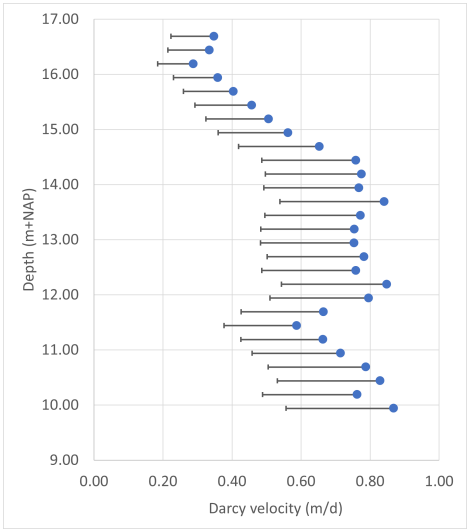

Figure K.8: Darcy velocities calculated for test Z1-2, error bars indicate the range of velocities based on the estimated borehole correction factors.

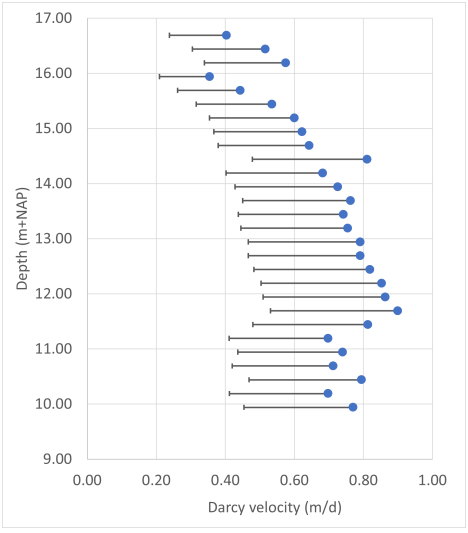

Figure K.9: Darcy velocities calculated for test Z1-3, error bars indicate the range of velocities based on the estimated borehole correction factors.

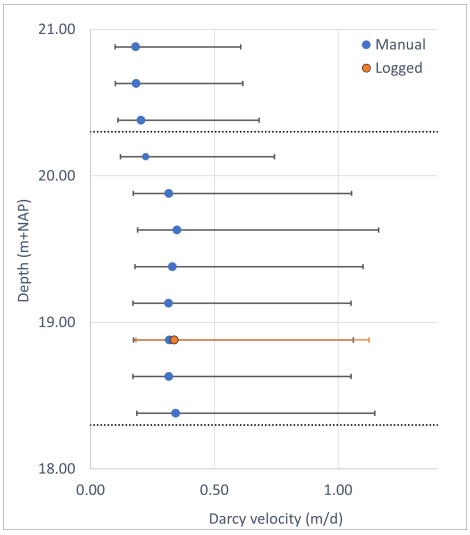

Figure K.10: Darcy velocities calculated for test 6.11, error bars indicate the range of velocities based on the estimated borehole correction factors.

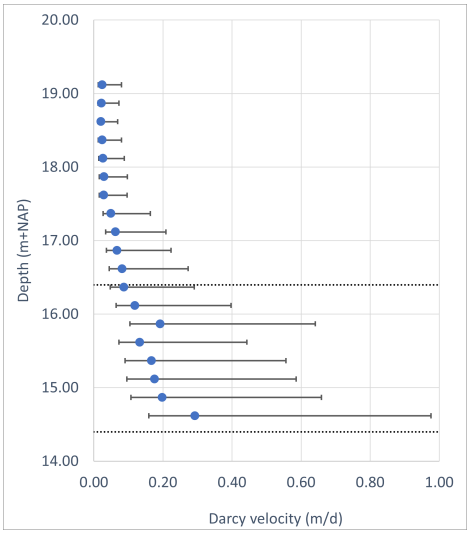

Figure K.11: Darcy velocities calculated for test 6.14, error bars indicate the range of velocities based on the estimated borehole correction factors.

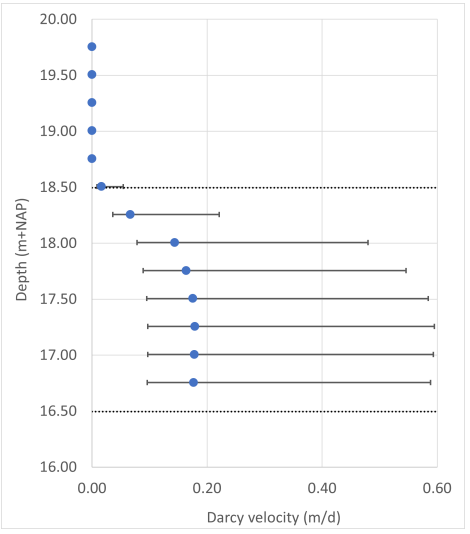

Figure K.12: Darcy velocities calculated for test 7.12-2, error bars indicate the range of velocities based on the estimated borehole correction factors.

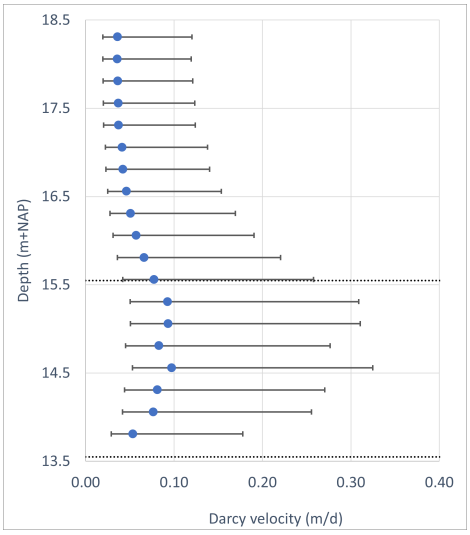

Figure K.13: Darcy velocities calculated for test 7.15, error bars indicate the range of velocities based on the estimated borehole correction factors.

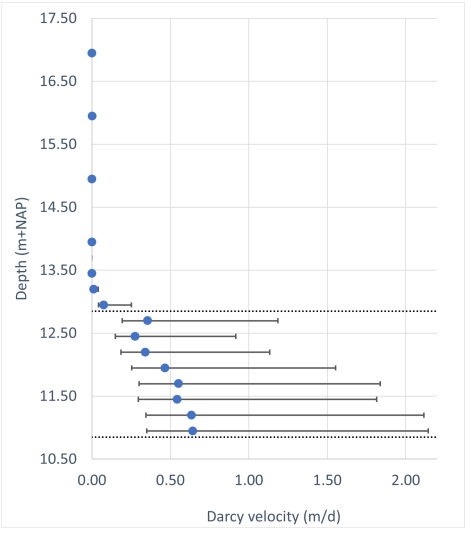

Figure K.14: Darcy velocities calculated for test 7.18, error bars indicate the range of velocities based on the estimated borehole correction factors.

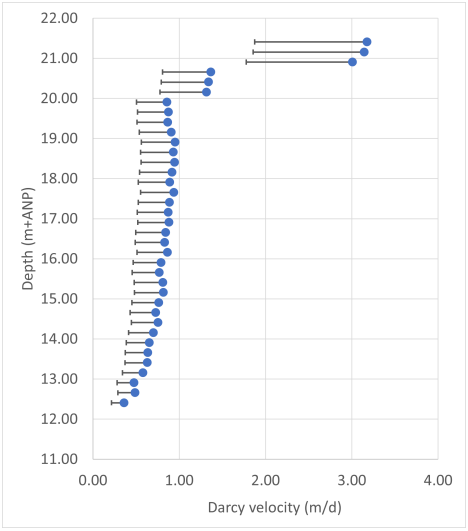

Figure K.15: Darcy velocities calculated for test Z2, error bars indicate the range of velocities based on the estimated borehole correction factors.

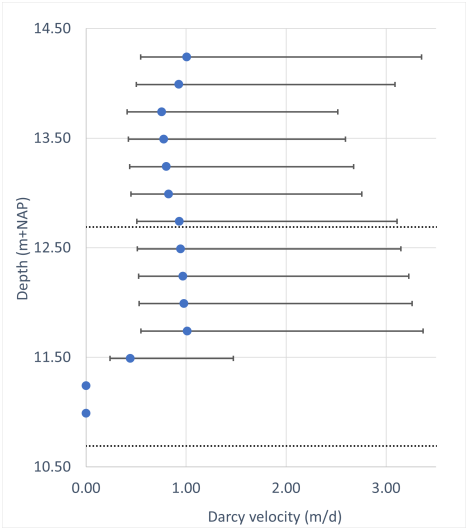

Figure K.16: Darcy velocities calculated for test A1.1, error bars indicate the range of velocities based on the estimated borehole correction factors.

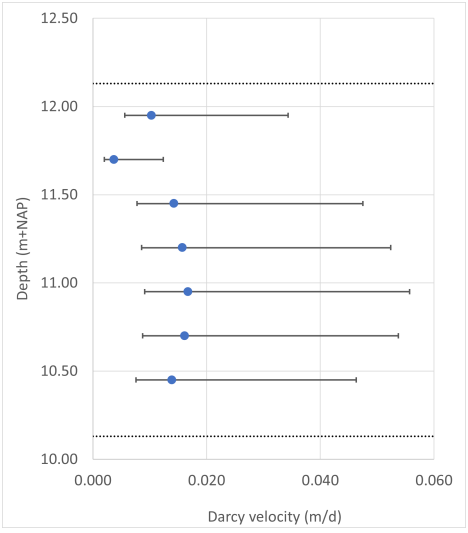

Figure K.17: Darcy velocities calculated for test A5, error bars indicate the range of velocities based on the estimated borehole correction factors.

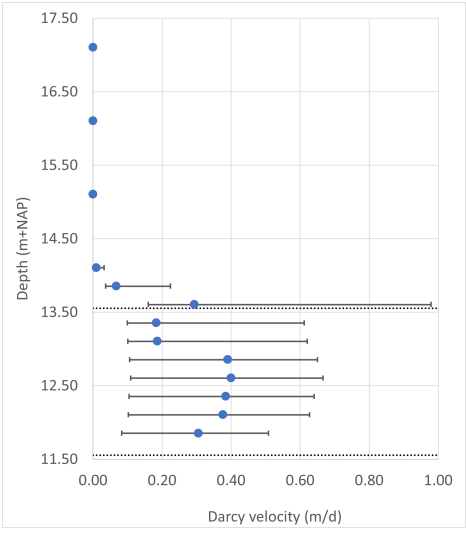

Figure K.18: Darcy velocities calculated for test 8.18, error bars indicate the range of velocities based on the estimated borehole correction factors.